

**THE POSTCRANIAL SKELETON OF THE EARLY
TRIASSIC NON-MAMMALIAN CYNODONT
GALESAURUS PLANICEPS: IMPLICATIONS FOR
BIOLOGY AND LIFESTYLE**

By

ELIZE BUTLER

Submitted in fulfillment of the requirements for the degree

MAGISTER SCIENTIAE (ZOOLOGY)

In the Faculty of Natural and Agricultural Sciences

Department of Zoology and Entomology

University of the Free State

Bloemfontein

Supervisor: Dr Jennifer Botha-Brink

December 2009

DECLARATION

I, the undersigned, hereby declare that the work contained in this dissertation is my own original work and that I have not previously in its entirety or in part submitted it at any university for a degree. I further more cede copyright of the dissertation in favour of the University of the Free State.

Signature:.....

Date:.....

ABSTRACT

Newly discovered skeletons of the Early Triassic basal cynodont, *Galesaurus planiceps*, has enabled a detailed morphological redescription of the postcrania of this genus. The examination of *Galesaurus* reveals two distinct morphs, namely a gracile and a robust morph. The primary differences between each morph lie in the pectoral and pelvic girdles with further subtle differences in the fore- and hind limbs. The morphological differences between the two morphs may be attributed to ontogeny, sexual dimorphism or the presence of two subspecies.

The morphology and high cortical thickness in the limb bones of *Galesaurus* indicates that it was a more robust animal compared to its closely related sister taxon *Thrinaxodon liorhinus*. *Galesaurus* was thus, capable of being an active burrower and may have used burrows to escape the harsh environmental conditions of the Early Triassic.

The bone microstructure of *Galesaurus* reveals uninterrupted fibro-lamellar bone, indicating fast continuous initial growth, with a change to lamellar-zonal bone, indicating a decrease in growth rate. The presence of annuli and LAGs in the peripheral lamellar-zonal bone indicates interrupted slow growth and suggests that *Galesaurus* may have been susceptible to environmental fluctuations. The growth patterns of *Galesaurus* and *Thrinaxodon* are similar, but can be distinguished from one another by the presence of lamellar-zonal bone in the former and parallel-fibred bone in the latter genus. Annuli and LAGs are absent in *Thrinaxodon*, implying that *Thrinaxodon* was less susceptible to environmental fluctuations than *Galesaurus*, as growth did not decrease or cease periodically.

Galesaurus, with a short biostratigraphic range from the Palingkloof Member, Balfour Formation and lowermost Katberg Formation of the *Lystrosaurus* Assemblage Zone, was previously known only from cranial and poorly preserved, isolated postcranial fragments. In contrast, extensive research has been conducted on the more abundant better-known *Thrinaxodon*, which has a biostratigraphic range that extends the entire *Lystrosaurus* Assemblage Zone. It was previously assumed that the postcranial skeletons of basal cynodonts were indistinguishable. However, this study has revealed morphological differences between *Galesaurus* and *Thrinaxodon*, allowing the taxa to be distinguished in the absence of cranial material. Examining postcranial material previously identified as *Thrinaxodon* and ensuring that collection material has been correctly identified can now test the short stratigraphic range of *Galesaurus*.

Key words

Galesaurus planiceps; basal cynodont; postcranial skeleton; bone histology; Early Triassic.

ACKNOWLEDGEMENTS

I thank my supervisor, Dr Jennifer Botha-Brink, for her guidance and advice during this study as well as the time and effort spent, it is much appreciated.

I am indebted to the following scientists and collection managers who made the study material available: Dr Roger Smith and Mrs Sheena Kaal (Iziko South African Museum, Cape Town); Prof Bruce Rubidge, Dr Mike Raath and Dr Bernard Zipfel (Bernard Price Institute for Palaeontological Research, University of the Witwatersrand, Johannesburg and Rubidge Collection, Graaff-Reinet); Dr Heidi Fourie and Stephanie Potze (Transvaal Museum, Pretoria) and Dr Jennifer Botha-Brink (National Museum, Bloemfontein).

I wish to thank the staff of the Palaeontology Department of the National Museum, Bloemfontein for the excellent preparation of material: John Nyaphuli, Joël Mohoi, Nthaopa Ntheri, Sam Stuurman and Sharon Ledibane. Annelise Crean of the Iziko South African Museum, Cape Town is also thanked for her excellent fossil preparation.

Prof Steve Fourie is especially thanked for his valuable advice and proof reading of the morphology chapter. Dr Rod Douglas and Dr Heidi Fourie are thanked for their advice and proof reading of several draft chapters. I am indebted to Liz Ranger-Craven, Elsa Kotze, Sudre Havenga, Trudie Peyper and Craig Barlow for technical assistance.

I am grateful to the Council and Director of the National Museum, Bloemfontein, for their support of this study as well as the National Research Foundation for funding.

Acknowledgements

I would in particular like to thank my Mom and Dad who always believed in me, my family for their support and finally, I wish to thank my husband, Hennie for advice and encouragement and my daughter, Liza for her moral support.

TABLE OF CONTENTS

Declaration	ii
Abstract	iii
Acknowledgements	v
Table of contents	vii
List of Figures	x
List of Tables	xiii

CHAPTER	PAGE
1. INTRODUCTION	1
1.1 Background	1
1.1.1 <i>Therapsida</i>	2
1.1.2 <i>Cynodontia</i>	3
1.1.3 <i>Epicynodontia</i>	6
1.1.4 <i>Galesaurus planiceps</i> (Owen, 1859)	7
1.2 Geological Setting	8
1.3 Rationale and Aim of Study	9
1.4 General Outline of Thesis	9
2. LITERATURE REVIEW	11
2.1 Synapsida	11
2.1.1 <i>Therapsida</i>	11
2.1.2 <i>Cynodontia</i>	12
2.1.3 <i>Epicynodontia</i>	12
2.2 Basal Cynodont Bone Morphology	13
2.2.1 <i>Cranium</i>	17
2.2.2 <i>Galesaurus planiceps</i>	18
2.2.3 <i>Postcranial Skeleton</i>	24

2. LITERATURE REVIEW	26
2.3 Early Research on <i>Galesaurus planiceps</i>	26
2.4 Bone histology	28
2.4.1 <i>Fossilization</i>	28
2.4.2 <i>Bone Histology</i>	28
2.4.3 <i>Implications of Bone Tissue Patterns</i>	33
3. MATERIAL AND METHODS	36
3.1 Material	36
3.2 Descriptive Techniques	47
3.2.1 Macro-measurements	47
3.3 Bone Histology	47
3.3.1 <i>Preparation of Fossil Bone for Histological Examination</i>	47
3.3.2 <i>Embedding Specimens</i>	47
3.3.3 <i>Cutting and Mounting of Specimens</i>	48
3.3.4 <i>Grinding and Polishing Specimens</i>	48
3.3.5 <i>Cross-sectional Geometry</i>	49
3.3.6 <i>Vascularization Quantification</i>	50
4. POSTCRANIAL DESCRIPTION	52
4.1 Preface	52
4.2 Axial Skeleton	54
4.2.1 <i>Vertebrae</i>	54
4.2.2 <i>Ribs</i>	66
4.3 Appendicular Skeleton	75
4.3.1 <i>Shoulder Girdle and Forelimb</i>	75
4.3.2 <i>Pelvic Girdle and Hind limb</i>	94
5. BONE HISTOLOGY	110
5.1 Ontogenetic status	110
5.2 Micro-analysis	110
5.2.1 <i>RC 845</i>	110
5.2.2 <i>NMQR 3678</i>	111
5.2.3 <i>NMQR 3542</i>	111
5.3 Interpretations	122
6. DISCUSSION	125

Table of Contents

7. CONCLUSIONS	140
REFERENCES	142
APPENDICES	
Appendix 1: Macro-measurements	

LIST OF FIGURES

CHAPTER		PAGE
1. INTRODUCTION		
Figure 1	Stratigraphic ranges of the major therapsid clades.	2
Figure 2	Distribution of non-mammalian cynodonts shown in time and space.	4
Figure 3	The biostratigraphy of the Karoo Basin, South Africa.	5
Figure 4	The abbreviated phylogeny of the Cynodontia.	6
2. LITERATURE REVIEW		
Figure 5	The biostratigraphic distribution of the basal cynodonts.	15
Figure 6	Skull of <i>Galesaurus planiceps</i> , in dorsal view.	19
Figure 7	Reconstruction of <i>Galesaurus planiceps</i> , skull NMQR 3542, in lateral view.	20
Figure 8	The skull of <i>Galesaurus planiceps</i> , in ventral view.	22
Figure 9	The skull of <i>Galesaurus planiceps</i> , NMQR 135, in occipital view.	23
3. MATERIAL AND METHODS		
Figure 10	<i>Galesaurus planiceps</i> , specimen SAM-PK-K10465, in dorsal view.	36
Figure 11	<i>Galesaurus planiceps</i> , specimen NMQR 3542, A) skull in right lateral view and disarticulated skeleton and B) pelvic girdle in medial view and associated hind limbs.	40
Figure 12	<i>Galesaurus planiceps</i> , specimen NMQR 3542, A) skull in left lateral view and disarticulated skeleton and B) pelvic girdle in lateral view and associated left hind limbs.	41
Figure 13	<i>Galesaurus planiceps</i> , specimen RC 845, in dorsal view.	42
Figure 14	<i>Galesaurus planiceps</i> , specimen RC 845, in ventral view.	43
Figure 15	<i>Galesaurus planiceps</i> , specimen, SAM-PK-K10468, A) dorsal and B) ventral view.	44
Figure 16	<i>Galesaurus planiceps</i> , specimen NMQR 3678, A) skull and anterior cervical vertebrae in right lateral view, B) right manus in ventral view, C) anterior axial skeleton and humeri in dorsal view and D) lumbar ribs and posterior axial skeleton in dorsal view.	45
		46

3. MATERIAL AND METHODS		36
Figure 17	Schematic representation of the relative bone wall thickness (RBT) measurements expressed as a percentage.	50
4. POSTCRANIAL DESCRIPTION OF <i>GALES SAURUS PLANICEPS</i>		52
Figure 18	The atlas of <i>Galesaurus planiceps</i> , A) RC 845, medial view of right half and B) NMQR 3542, lateral view of right half.	56
Figure 19	The right proatlas of <i>Galesaurus planiceps</i> , SAM-PK-K-10465, in dorsal view.	58
Figure 20	The axis of <i>Galesaurus planiceps</i> , NMQR 3678, in lateral view.	59
Figure 21	Thoracic vertebra of <i>Galesaurus planiceps</i> , SAM-PK-K1119, in A) anterior and B) lateral view.	64
Figure 22	Posterior cervical rib of <i>Galesaurus planiceps</i> , SAM-PK-K10465, in lateral view.	68
Figure 23	Three articulated posterior thoracic ribs of <i>Galesaurus planiceps</i> , SAM-PK-K10465, in lateral view.	70
Figure 24	The first two anterior lumbar ribs of <i>Galesaurus planiceps</i> , RC 845, in lateral view.	72
Figure 25	Caudal ribs of <i>Galesaurus planiceps</i> , RC 845, in lateral view A) the first right caudal rib with forked costal rib and B) fifth “rectangular” left caudal rib.	74
Figure 26	Left scapula of <i>Galesaurus planiceps</i> , in lateral view, A) photograph of specimen NMQR 3542 and B) specimen RC 845.	75
Figure 27	A reconstruction of the right scapulocoracoid of <i>Galesaurus planiceps</i> , in medial view.	77
Figure 28	The left clavicle of <i>Galesaurus planiceps</i> , SAM-PK-K10468, in dorsal view.	80
Figure 29	Interclavicle of <i>Galesaurus planiceps</i> , RC 845, in ventral view.	81
Figure 30	The right humerus of <i>Galesaurus planiceps</i> , in A) NMQR 3542, in anterolateral view and B) SAM-PK-10468, in ventral view.	83
Figure 31	The left radius of <i>Galesaurus planiceps</i> , NMQR 3542, in A) lateral and B) posterior view.	86
Figure 32	The left ulna of <i>Galesaurus planiceps</i> , SAM-PK-K10465, in lateral view.	87
Figure 33	The right manus of <i>Galesaurus planiceps</i> , SAM-PK-K10465, in dorsal view.	89
Figure 34	The left manus of <i>Galesaurus planiceps</i> , SAM-PK-K10468, in ventral view.	92

4. POSTCRANIAL DESCRIPTION OF *GALES SAURUS PLANICEPS*

Figure 35	The right ilium of <i>Galesaurus planiceps</i> , A) reconstruction of NMQR 3542 in medial view and B) RC 845 in lateral view.	95
Figure 36	The right pubis of <i>Galesaurus planiceps</i> , RC 845, in lateral view.	97
Figure 37	The right ischium of <i>Galesaurus planiceps</i> , RC 845, in lateral view.	99
Figure 38	The right femur of <i>Galesaurus planiceps</i> , NMQR 3542 in A) medial and B) ventral view.	101
Figure 39	The left tibia of <i>Galesaurus planiceps</i> , NMQR 3542, in anterior view.	104
Figure 40	The left fibula of <i>Galesaurus planiceps</i> , NMQR 3542, in posterior view.	106
Figure 41	The right pes of <i>Galesaurus planiceps</i> , BP/1/4506, in dorsal view.	107
5. BONE HISTOLOGY		
Figure 42	Transverse sections of <i>Galesaurus planiceps</i> , RC 845, tibia.	114
Figure 43	Transverse sections of <i>Galesaurus planiceps</i> , RC 845, fibula.	115
Figure 44	Transverse sections of <i>Galesaurus planiceps</i> , NMQR 3678, femur.	116
Figure 45	Transverse section of <i>Galesaurus planiceps</i> , NMQR 3542, humerus.	117
Figure 46	Transverse sections of <i>Galesaurus planiceps</i> , NMQR 3542, radius.	118
Figure 47	Transverse sections of <i>Galesaurus planiceps</i> , NMQR 3542, ulna.	119
Figure 48	Transverse sections of <i>Galesaurus planiceps</i> , NMQR 3542, femur.	120
Figure 49	Transverse sections of <i>Galesaurus planiceps</i> , NMQR 3542, tibia.	121

LIST OF TABLES

CHAPTER		PAGE
3. MATERIAL AND METHODS		36
Table 1	<i>Galesaurus planiceps</i> postcranial material examined in this study.	38
Table 2	<i>Thrinaxodon liorhinus</i> postcranial material examined in this study for comparative purposes.	39
4. POSTCRANIAL DESCRIPTION		52
Table 3	Grouping of the 12 <i>Galesaurus planiceps</i> specimens into gracile and robust morphs, based on skull length.	53
6. DISCUSSION		125
Table 4	Summary of differences between gracile and robust <i>Galesaurus planiceps</i> and <i>Thrinaxodon liorhinus</i> .	130
Table 5	Spatial distribution of <i>Galesaurus planiceps</i> and <i>Thrinaxodon liorhinus</i> in the <i>Lystrosaurus</i> Assemblage Zone of the Karoo Basin.	139

CHAPTER ONE

INTRODUCTION

1.1 Background

The non-mammalian synapsids (basal synapsids and Therapsida) are of particular interest as it is from this group that extant mammals are derived (Hopson and Crompton, 1969). The earliest members of the synapsids originated during the early part of the Late Carboniferous, approximately 300 million years ago (mya) (Kemp, 1982). They are distinguished from their diapsid contemporaries by the presence of a single lower lateral temporal fenestra; a temporal opening that is exhibited in all synapsids, including extant mammals. During the course of their history these animals radiated widely to become the dominant terrestrial fauna spanning approximately 40 million years (my), before finally becoming extinct during the Early Jurassic (Kemp, 1982).

The non-mammalian synapsid fossil record is relatively complete and one of the best-documented groups compared to other terrestrial fossil vertebrates (apart from perhaps Tertiary mammals; Kemp, 1982). Their evolution spans an extensive morphological progression, from early primitive forms with reptile-like features, to more derived forms, which are technically regarded as mammals.

1.1.1 Therapsida

The non-mammalian therapsids are divided into five major clades (Fig. 1) namely the Dinocephalia, Gorgonopsia, Anomodontia, Therocephalia and the Cynodontia (Kemp, 1982; Rubidge and Sidor, 2001.)

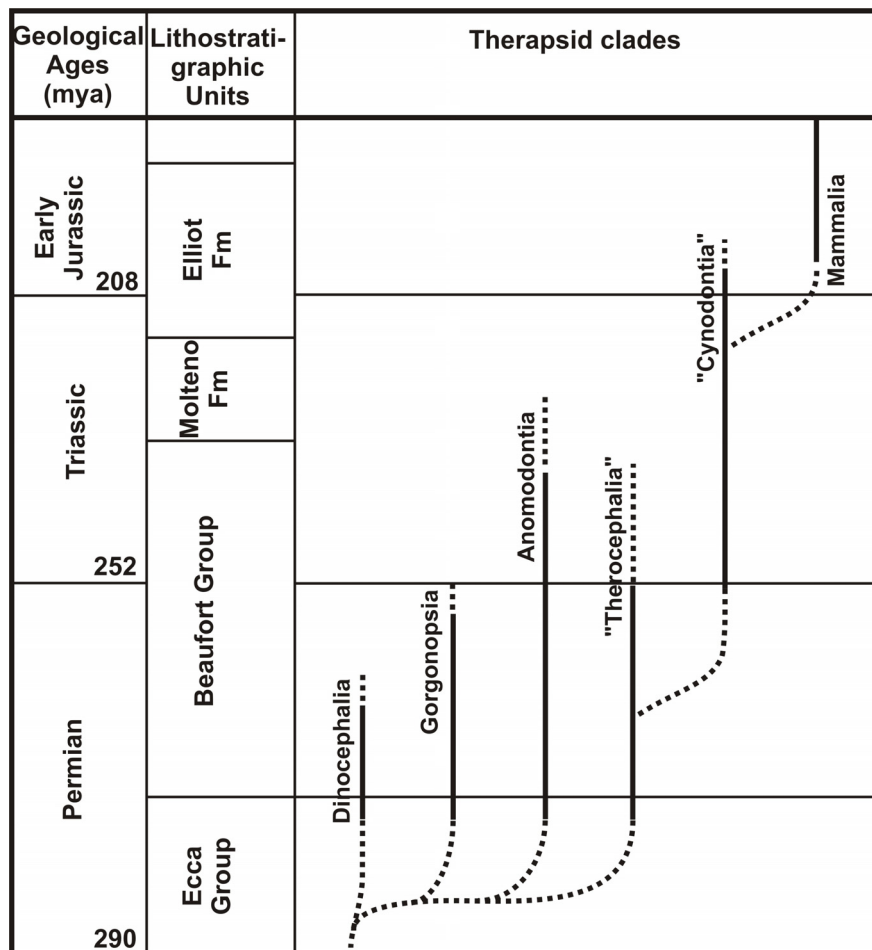


Figure 1. Stratigraphic ranges of the major therapsid clades (taken from Botha, 2002 and modified from Kemp, 1982; Mundil et al., 2004 and Carroll, 1988). "Mya" refers to millions of years ago and "Fm" refers to formation. Dotted lines indicate uncertain ranges.

The majority of basal non-mammalian synapsids are found in the Upper Carboniferous and Lower Permian strata of North America (Romer and Price, 1940; Kemp, 2005) (Fig. 2A), as well as a few isolated localities in various parts of Europe. The North American record ceases at the beginning of the Late Permian, followed by younger deposits in Russia (Fig. 2B). The Karoo Supergroup of South Africa is documented as one of the richest fossil records of therapsids from the middle Late Permian and Early Triassic (Fig. 3). Middle and Upper Triassic therapsids are also present in areas of the Karoo Basin, but are better represented in certain regions of South America (Kemp, 1982). The first true mammals evolved during the Late Triassic and the earliest members are abundantly found in deposits in Texas, India (Kielan-Jaworowska et al., 2004) and South Wales, with similar animals having been discovered in South Africa, China and the mainland of Western Europe (Kemp, 1982).

1.1.2 *Cynodontia*

The non-mammalian cynodonts are an extinct group of derived therapsids, which manifest many 'mammal-like' features. Features that represent the mammalian pattern include a double occipital condyle in the skull and an osseous secondary palate (Kemp, 1982). The non-mammalian cynodont postcanine dentition also became more complex and the dentary bone of the lower jaw (the unique, single bone that forms the entire lower jaw in mammals) became larger at the expense of the postdentary bones. This trend towards a single lower jaw bone in cynodonts strengthened the jaws for the attachment of powerful external abductor jaw muscles (Abdala and Damiani, 2004), implying an improvement in the strength and control of the mastication process and preparation of food in the oral cavity (Hopson, 1994).

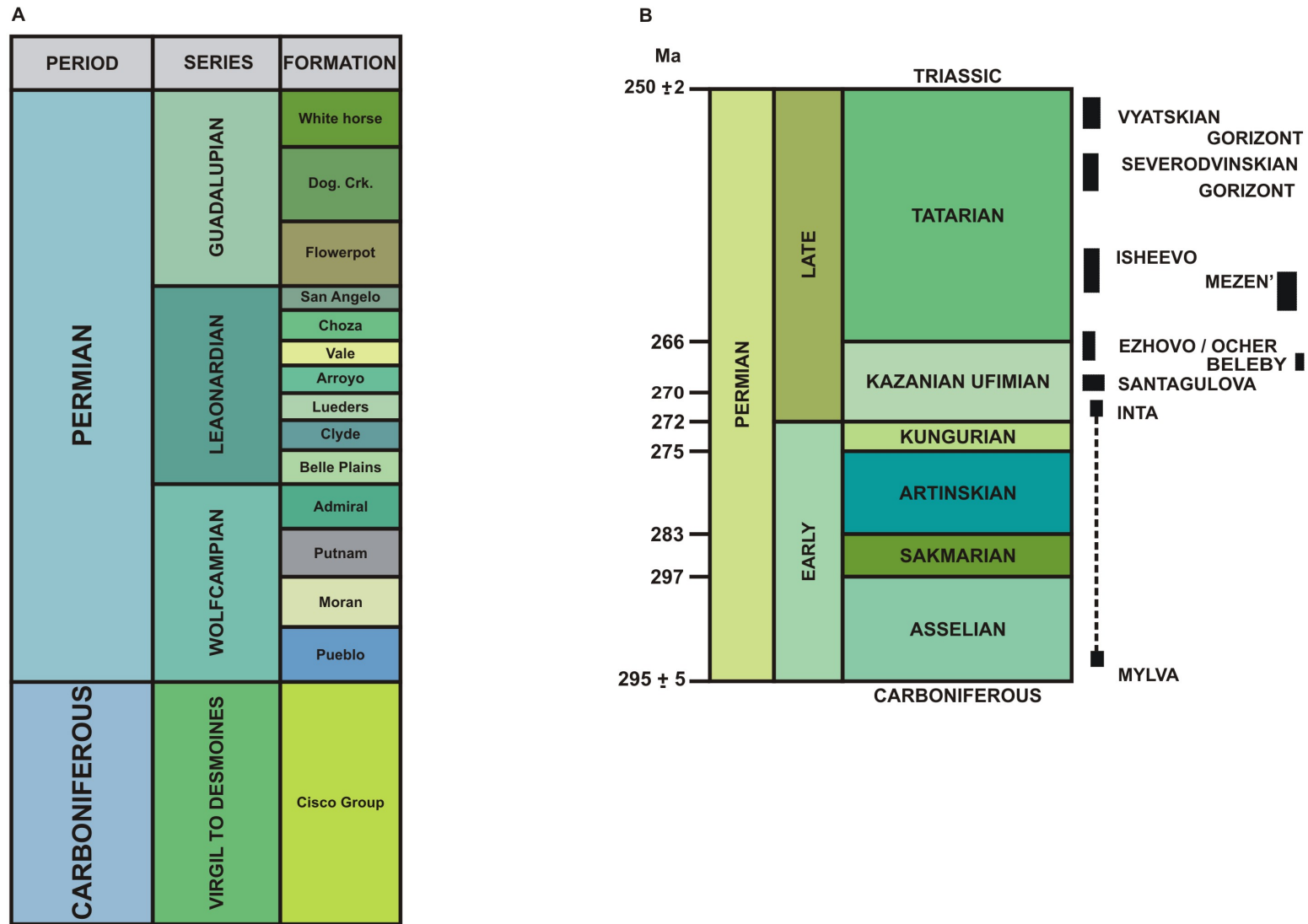


Figure 2. Distribution of non-mammalian cynodonts in time and space. A) The Permo-Carboniferous stratigraphic sequence of North America (modified from Kemp, 2005). B) The Permian stratigraphic sequence of Russia (after Modesto and Rybczynski 2000).

GEOLOGICAL PERIODS (MYA)	GROUP	FORMATION	MEMBER	ASSEMBLAGE ZONE
JURASSIC 199.6	STORMBERG	CLARENS		
		ELLIOT		<i>MASSOSPONDYLUS</i>
MOLTENO			<i>EUSKELOSAURUS</i>	
TRIASSIC 252	BEAUFORT	BURGERSDORP		<i>CYNOGNATHUS</i>
		KATBERG		<i>LYSTROSAURUS</i>
		BALFOUR	PALINGKLOOF	<i>DICYNODON</i>
			ELANDSBERG	
BARBERSKRANS				
DAGGABOERSNEK				
PERMIAN 299		ECCA	OUDEBERG	<i>CISTECEPHALUS</i>
			MIDDELTON	<i>TROPIDOSTOMA</i>
		DWYKA	KROONAP	<i>PRISTEROGNATHUS</i>
			WATERFORD/ FORT BROWN	<i>TAPINOCEPHALUS</i>
	<i>EODICYNODON</i>			
CARBONIFEROUS 359.2	DWYKA			

Figure 3. The biostratigraphy of the Karoo Basin, (east of 24°), South Africa. Material used in this study was recovered from the Lower Triassic *Lystrosaurus* Assemblage Zone of the Beaufort Group, Karoo Basin, (modified from Rubidge, 1995). Dates taken from Gradstein and Ogg (2004), and Mundil et al. (2004). (*Massospondylus* and *Euskelosaurus* are informal ranges and not formal assemblage zones).

1.1.3 *Epicynodontia*

The Epicynodontia is the most inclusive clade including Mammalia and excluding *Procynosuchus*, *Dvinia* and *Charassognathus*. The Epicynodontia clade thus includes *Cynosaurus*, *Galesaurus*, *Progalesaurus*, *Nanictosaurus*, *Thrinaxodon* and the Eucynodontia. The latter include cynodonts more derived than *Thrinaxodon* (Hopson and Kitching, 2001).

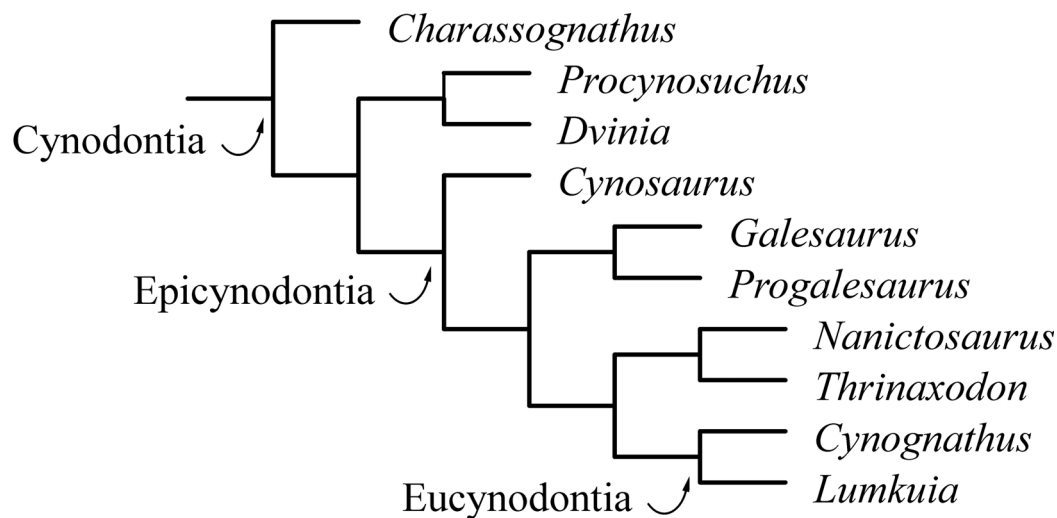


Figure 4. The abbreviated phylogeny of the Cynodontia (modified from Botha et al., 2007).

The epicynodonts thus include the family Galesauridae (Fig. 4). The family contains the genera *Progalesaurus lootsbergensis* (Sidor and Smith, 2004) and *Galesaurus planiceps* (Owen, 1859), both of which are characterized by the absence of a lingual cingula on the postcanine teeth and a triangular basisphenoid with an anterior projection in anterior view (Sidor and Smith, 2004). In the epicynodont cynodonts *Cynosaurus*, *Progalesaurus* and *Galesaurus*, the secondary bony palate extends medially from the maxilla and palatine and fails to contact medially. Due to the poor preservation of *Charassognathus*, the status of the secondary palate is unknown. However, in *Nanictosaurus* and *Thrinaxodon liorhinus*, the plates connect along the midline and thereby form a complete osseous secondary palate (Fourie, 1974). Kemp (1982; 1988) considers the Eucynodontia as all cynodonts more derived than

Thrinaxodon and characterizes the group as having features that produce an increasingly mammal-like skull and postcranial skeleton.

Studies on the postcranial skeleton of therapsids have not kept pace with the development of knowledge of the skull. In proportion to cranial remains, therapsid postcranial bones are under-represented in older collections, largely because they are more difficult to collect and are taxonomically less informative than the skull (Crompton and Jenkins, 1973).

The best-known basal non-mammalian cynodont is the relatively abundant *Thrinaxodon liorhinus*. Extensive research has been conducted by numerous authors on both the skull and skeleton (Broom, 1938; Brink, 1954; Van Heerden, 1972; Fourie, 1974). Jenkins (1971) described the postcrania of *Thrinaxodon* and the larger, more derived cynodonts *Diademodon* and *Cynognathus*, and made brief references to *Galesaurus planiceps*. Kemp (1982) also described the non-mammalian cynodonts, but again the basal members of the group were only briefly mentioned with particular emphasis on *Thrinaxodon liorhinus*. Jenkins (1971: 8) noted that "...the postcranial skeletons, insofar we know are remarkably alike. Thus it is possible to present a reasonably accurate portrayal of 'the cynodont' postcranial skeleton, despite the lack of a complete and well-preserved skeleton for any given genus." With the material available to Jenkins at the time he believed that "... no differences could be detected that might indicate species diversity." Since then however, new remarkably well-preserved postcranial material of *G. planiceps* has been recovered that can provide insight into the detailed morphology of this genus.

1.1.4 *Galesaurus planiceps* (Owen, 1859)

Galesaurus planiceps is known from the Early Triassic *Lystrosaurus* Assemblage Zone (AZ) of the Karoo Basin, South Africa. *Galesaurus* appeared very quickly after the End-Permian extinction event in the Karoo Basin, as its First Appearance Datum is approximately 22 m above the Permo-Triassic boundary (PTB) in the Palingkloof Member, Balfour Formation, of the Beaufort Group (Botha and Smith, 2006). However, the stratigraphic range of *Galesaurus* is relatively short, as no specimens

have been recovered from strata above the lower Katberg Formation, which overlies the Palingkloof Member (Fig. 3). The Last Appearance Datum (LAD) of *Galesaurus* is approximately 85 m above the PTB (Botha and Smith, 2006). The range is notably shorter than its closely related sister taxon *Thrinaxodon liorhinus*. Both these taxa appeared quickly after the End-Permian extinction event in the Karoo Basin and can be regarded as disaster taxa (taxa appearing in abundance immediately after an extinction), but the range of *Thrinaxodon* extends the entire *Lystrosaurus* AZ. The difference in their ranges is not fully understood and may be related to a difference in biology or lifestyle preference. Understanding the biology and lifestyle of *Galesaurus* and comparing this genus with that of *Thrinaxodon* may shed light on why *Thrinaxodon* was more abundant and consequently perceived to be more successful as a disaster taxon than *Galesaurus*. This information is relevant, because understanding the biology of all taxa originating after extinctions, is essential for understanding the dynamics of post-extinction recoveries.

1.2 Geological Setting

The sediments of the Lower Triassic consist primarily of red and olive-grey siltstone sediments interbedded with small thin sandstone sheets and sand-filled mud crack horizons. Large reddish brown weathered calcareous nodules are present, isolated along horizons, which incorporate red siltstone beds. The Permo-Triassic extinction event culminates at the top of a maroon laminate bed, approximately 9–15 m above the first occurrence of red mudrock and marks the base of the Palingkloof Member at the top of the Balfour Formation (Botha and Smith, 2006). The massive red siltstone sediments rapidly change into a more sandstone rich sequence consisting of light grey, fine-grained, sandstone separated by olive and dark-reddish brown mudrocks. These lower Katberg Formation sandstones consist of numerous disconformities lined with intraformational mud pebbles and characteristic conglomerates comprising nodules and concretions distinct from the sands (Botha and Smith, 2006).

The change in these sediments suggest that the river systems during the Late Permian altered from meandering, to slow flowing rivers with extensive seasonal floodplains to fast flowing rivers with almost no floodplains during the Early Triassic

(Smith, 1995) resulting in a severe loss of vegetation (Smith and Ward, 2001). A change in vegetation occurred as the *Glossopteris*-dominated flora disappeared and was replaced by the less diverse *Dicroidium*-dominated flora. The reddish sandstones are symptomatic of severe drought conditions (Kemp, 2005).

1.3 Rationale and Aim of Study

Descriptions of cynodont skulls were prioritized in the past and hence the under representation of cynodont postcranial skeletons in collections is explicable. A number of *Galesaurus* skulls were found in the past, but the associated postcrania consisted of isolated elements that were badly preserved and fragmentary. Until recently articulated skeletons of *Galesaurus* were unknown, but new specimens with associated, well-preserved postcrania, have now been recovered, allowing a detailed redescription of the postcranial skeleton to be completed.

The most extensive research on the cynodonts was done by Jenkins (1971) with his description of *Galesaurus*, *Thrinaxodon*, *Diademodon* and *Cynognathus*. The description in this study will thus be compared with that of Jenkins (1971).

The objective of this study is to use the morphological and bone histological information obtained to more fully understand the biology and lifestyle of *G. planiceps*. This taxon is important because of its appearance shortly after the End-Permian extinction event. It therefore forms part of the Early Triassic recovery fauna. Understanding the biology of these taxa is key to understanding the dynamics of post-extinction recovery phases.

1.4 General Outline of Thesis

Chapter two reviews the published literature on *Galesaurus planiceps*. Chapter three outlines the material used in this study and the localities from where they were recovered, as well as the methods, including the descriptive and bone histological analyses. Chapter four contains the morphological description of the postcranial skeleton of *Galesaurus* as well as a comparison with *Thrinaxodon*. Chapter five comprises the description of the bone histology of *Galesaurus planiceps*, which

Chapter 1: Introduction

provides information regarding the ontogeny, growth rate, and individual age and lifestyle habits of this species. The morphological and bone histology discussion will follow in chapter six and includes the implications for *Galesaurus* as an Early Triassic recovery taxon. Chapter seven presents the final conclusions.

CHAPTER TWO

LITERATURE REVIEW

2.1 Synapsida

The Synapsida is a clade that includes all taxa, extinct and extant, that share a closer relationship with mammals than they do with reptiles. The “Pelycosaurs” (paraphyletic clade) are the least derived of this group and retain many of the skeletal features of reptiles (Kemp, 1982). The division between synapsid and reptile lineages occurred approximately 300 Mya (Laurin and Reisz, 1995). The synapsids are characterized by a single lower temporal opening behind the eye, namely the lateral temporal fenestra. In the more basal genera, the fenestra was bound by the postorbital and squamosal, but as the synapsids became more derived during the Late Permian and Triassic, the temporal fenestra became larger to such an extent that the parietal bone became part of the upper border.

2.1.1 Therapsida

All synapsids more derived than the sphenacodontids (derived family of the “Pelycosaurs”) form the clade Therapsida (Laurin and Reisz, 1996). The Therapsida are particularly significant because it is from this group that extant mammals are derived (Hopson and Crompton, 1969). Their evolution spanned an extensive morphological progression from a basal synapsid grade to more derived forms, which can be regarded as mammals (reptiles or Reptilia in this study follows Modesto and Anderson, 2004, where ‘Reptilia’ is the most inclusive clade containing *Lacerta agilis* Linnaeus 1758 and *Crocodylus niloticus* Laurenti 1768, but not *Homo sapiens* Linnaeus 1758). Therapsid fossils are known from all continental regions, but are especially abundant in the Karoo sediments from southern Africa.

2.1.2 *Cynodontia*

The Cynodontia were the last major group of the Late Permian radiation of therapsids (Kemp, 2005) and include mammals as their extant subgroup (Rubidge and Sidor, 2001). Early cynodont evolution is particularly well documented in the rocks of the Beaufort Group (Karoo Supergroup) of South Africa, where they first appear in the middle Late Permian *Tropidostoma* AZ (Botha et al., 2007; Botha-Brink and Abdala, 2008). The Cynodonts survived the End-Permian extinction event and became particularly abundant in the lower and middle Triassic Katberg and Burgersdorp formations (*Lystrosaurus* and *Cynognathus* AZ respectively) of South Africa.

With time, the cynodont postcanine dentition became more complex. Instead of the upper teeth occluding with the lower teeth, they contacted the dorsal shelf of the dentary. The lower teeth contacted the secondary palate, internal to the upper teeth. The secondary palate was presumably covered by heavily keratinised epithelium, much like the dicynodonts (Kemp, 1982). The lack of occlusion between the postcanines in the basal cynodonts (Crompton, 1972) implies that they did not process their food extensively in the oral cavity, but probably caught, cut and swallowed the entire prey (i.e. insects and tiny vertebrates) without much chewing. The posteriorly curved main cusp of the postcanines was most likely used for preventing the escape of small prey from the oral cavity.

2.1.3 *Epicynodontia*

The monophyletic Epicynodontia includes the family Galesauridae, which consists of basal genera with an incomplete osseous secondary palate (*Cynosaurus*, *Progalesaurus* and *Galesaurus*) and slightly more derived taxa, with fully developed osseous secondary palates (*Thrinaxodon* and *Nanictosaurus*) (Kemp, 1982; 2005). A fleshy secondary palate probably completed the separation of the air passage from the mouth in the most basal forms. Unique to the galesaurids is a triangular basisphenoid with an anterior projection and the absence of a lingual cingula on the postcanine teeth (Sidor and Smith, 2004).

2.2 Basal Cynodont Bone Morphology

The phylogeny in this thesis is based on the most recent phylogeny of the basal cynodonts (Botha et al., 2007). Each genus will be mentioned briefly with an emphasis on *Thrinaxodon* as this genus consists of an adequate amount of well-preserved material that has been described by numerous authors. *Thrinaxodon* is also a closely related sister taxon of *Galesaurus*.

Botha et al. (2007) recovered the basal cynodont *Charassognathus* from the middle Late Permian *Tropidostoma* AZ of South Africa (Fig. 5). To date, only one specimen of this genus is known. It consists of the skull, mandible, a partially preserved axis and third cervical vertebra, and an articulated femur, tibia and fibula. This genus is distinguished from other cynodonts by the presence of a small notch on the base of the coronoid process, in a similar position to the base of the masseteric fossa in *Dvinia* and *Procynosuchus*. The angle of the dentary is also notably prominent and appears to be less developed than that of *Nanictosaurus*, but more developed than those of *Procynosuchus* and *Dvinia* (Botha et al., 2007).

Procynosuchus is a basal cynodont (Fig. 5) known from South Africa, Tanzania, Zambia, Germany and Russia (Kemp, 1979; Rubidge, 1995). It is known from the uppermost portion of the middle Late Permian *Tropidostoma* AZ to Late Permian *Dicynodon* AZ and coeval beds in East Africa and Europe (Botha-Brink and Abdala, 2008). Numerous authors have described the skull and postcranial skeleton of *Procynosuchus* (Broom, 1948; Kemp, 1979, 1980; Brink, 1951). The genus has undergone little change beyond the basic postcranial therapsid condition (Kemp, 2005), although the dentition illustrates an incipient evolution of more complex molars and several skull and lower jaw features indicate an elaboration of the jaw musculature as well as the development of an incomplete secondary palate. This basal cynodont lacks expanded costal plates and accessory zygapophyses, which are present in the later cynodonts such as *Galesaurus* and *Thrinaxodon* (Kemp, 1980). The hind limb was capable of an erect and sprawling gait. This dual-gait mechanism was functionally intermediate between a primitive sprawling gait and the erect gait of the more derived, later cynodonts. The vertebrae differentiate into clear

cervical, thoracic and lumbar regions. Kemp (1980) suggested that the girdles illustrate specializations indicating a semi-aquatic, otter-like mode of life.

The basal cynodont *Dvinia* as described by Tatarinov (1968) is similar to *Procynosuchus* and thus far, is only known from the Late Permian of Russia (Fig. 5). The material of this genus is fragmentary and consists of incomplete distorted skulls with associated postcrania.

Unfortunately, all the unequivocal *Cynosaurus* specimens are distorted. This genus has been recovered from the Late Permian *Dicynodon* AZ of South Africa (Van Heerden, 1976; Van Heerden and Rubidge, 1990) (Fig. 5). *Cynosaurus* has teeth similar to that of *Thrinaxodon*, but without a cingulum (Van Heerden, 1976).

To date, only one specimen of *Progalesaurus lootsbergensis* has been found (Fig. 5). This specimen was recovered near the top of the Palingkloof Member, Balfour Formation of the *Lystrosaurus* AZ of South Africa (Sidor and Smith, 2004). Autapomorphies of *Progalesaurus* include numerous mesial and distal accessory cusps flanked by a recurved main cusp, a posttemporal fenestra bordered by the squamosal ventrally and a large external naris (Sidor and Smith, 2004).

Nanictosaurus closely resembles *Thrinaxodon*, but differs from the latter by the presence of longer postcanines and the absence of tooth occlusion (Van Heerden, 1976). This genus is known from the *Dicynodon* Assemblage Zone of South Africa (Fig. 5).

Thrinaxodon is the best-known of all the epicynodonts. Both the skull and postcranial skeleton have been studied in detail. *Thrinaxodon* has been recovered from the *Lystrosaurus* AZ of South Africa and the contemporaneous Fremouw Formation of Antarctica (Colbert and Kitching, 1977) (Fig. 5). A specimen of a complete *Thrinaxodon* skeleton has also been found in a burrow cast suggesting that this genus was fossorial (Damiani et al., 2003).

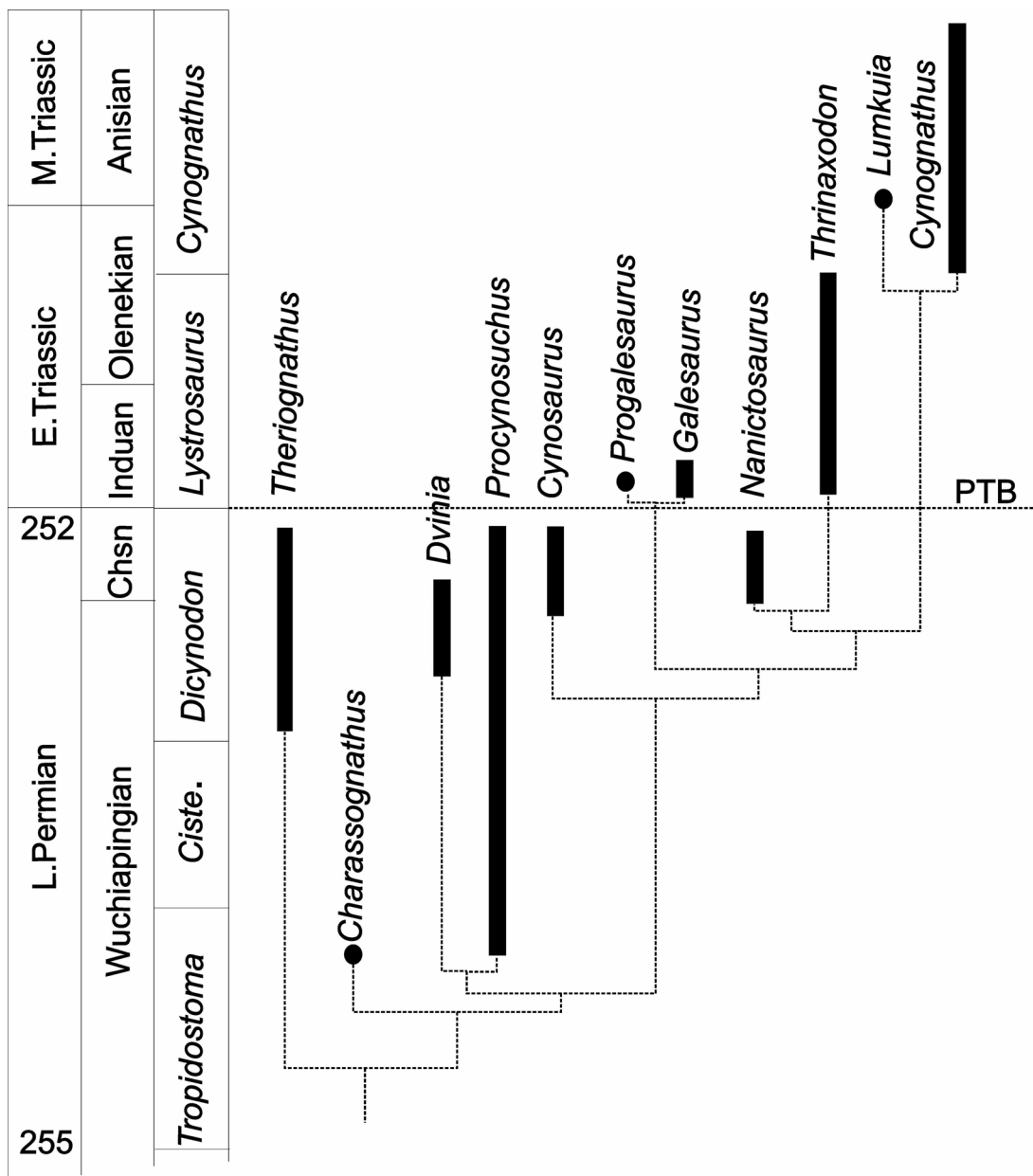


Figure 5. The biostratigraphic ranges of the basal cynodonts (modified from Botha-Brink and Abdala, 2008). The vertical bars and solid circles indicate taxon ranges and single specimen occurrences, respectively. Ape is in million of years. *Theriognathus* is the sister group of the Cynodontia. Stratigraphic chart follows Mundil et al. (2004) and Catuneanu et al. (2005). Abbreviations: **Chsn**, Changhsingian; **Cist.**, *Cistecephalus* Assemblage Zone; **PTB**, Permo-Triassic boundary.

Thrinaxodon was a lightly built, active carnivore and reached approximately 50 cm in length (Carroll, 1988). This species is more derived than the most basal cynodonts due to the formation of a solid bony secondary palate, with sutural attachment of the

maxillae and the palatine at the midline beneath the nasal passage. The pterygoids contact medially and the interpterygoid vacuity is closed by the pterygoids in the adults. The dentition is mammal-like (Carroll, 1988) and consists of four upper and three lower incisors, similar to most of the more derived cynodonts. A single canine in the upper and lower jaw and seven to nine postcanine teeth are present, whereas the precanines are lost in *Thrinaxodon* and *Galesaurus* (Kemp, 1982). The crowns are laterally compressed and a series of linearly arranged cusps are present. Tooth replacement was still frequent. The lower jaw consists of the dentary, with a coronoid process that extends dorsally above the zygomatic arch. The masseteric fossa reaches the base of the dentary. The postdentary bones are not greatly reduced and are in sutural contact with the dentary. The relatively large reflected lamina of the angular extends laterally from the bone surface. The articular forms the entire surface for the articulation with the skull. The reduced quadrate and quadratojugal fit loosely into adjacent sockets of the squamosal base (Kemp, 1982).

Dorsoventral flexion occurs in an arc up to 90° between the occipital condyle and the atlas. The greater mobility between the head and trunk was achieved due to the division of the originally single occipital condyle as in reptiles, to the formation of a double occipital condyle on either side of the foramen magnum (more derived cynodonts and later mammals). The specialization of the atlas-axis complex relieved the restriction of the rotation between the head and the atlas (Carroll, 1988).

There is a clear distinction between the thoracic and lumbar regions of the trunk in *Thrinaxodon*. The vertebral column consists of seven cervical vertebrae, 13 thoracic, seven lumbar and five sacral vertebrae. The most striking feature of the postcranial skeleton is the expansion of the proximal portion of the ribs into broad costal plates. The thoracic and lumbar ribs possess plate-like expansions (Hopson and Kitching, 1972) whereas the ribs in the lumbar region consist of the costal plate without a distal shaft. Kemp (1980) suggested that the costal plates are associated with establishing greater rigidity of the vertebral column and increased locomotory thrust from the hindlimb. Kemp (1982), then later suggested a reduction in lateral movement of the vertebral column.

Most of the weight of *Thrinaxodon* was carried by the scapula portion of the glenoid, which faces ventrally and laterally (Carroll, 1988). The heavy humeral head reflected dorsally so that the humerus moved closer to the body. The articulating surfaces of the tibia and fibula were modified to accommodate their vertical position. All of these modifications resulted in a more erect posture (Carroll, 1988).

2.2.1 Cranium

The temporal fenestra in basal cynodonts is greatly enlarged and expands laterally and posteriorly producing a narrow intertemporal or sagittal crest in the parietal bone. By expanding posteriorly, the temporal fenestra caused the development of a posteriorly reflected squamosal and produced a bowed lower temporal bar or lower zygomatic arch laterally, which bows upward above the level of the jaw hinge. A groove in the squamosal accommodates the quadratojugal and quadrate. The orbital margin excludes the frontal, whereas the reduced postorbital bone is restricted to the anterior part of the fenestra. The nasal bones expand posteriorly and meet the lacrimals (Kemp 1982).

A characteristic of the lower jaw is a relatively large dentary with a broad coronoid process, which rises above the zygomatic arch (Benton, 1990). A depression on the lateral surface of the coronoid indicates that the adductor musculature had invaded the lateral surface of the jaw. Even in the earliest taxa, the reflected lamina of the angular is reduced to a small, thin bone (Kemp, 1982). The quadrate and articular bones, forming the jaw articulation, are reduced in size.

The cynodont dentition is unique and differentiated into unserrated incisors and serrated/unserrated canines followed by complex multi-cusped postcanine teeth. The prominent angle of the dentary is a notable characteristic of the Cynodontia as well as the reflected lamina of the angular, which has small lateral crests. A bony secondary palate is partially complete in the basal forms, which is formed by the palatal extension of the premaxillae, maxillae and palatines. In the more derived forms, a fully developed secondary palate is present. The generally fused vomers form a median bone (Kemp, 1982).

The supraoccipital is very narrow and the tabulars are broad and surround the posttemporal fenestra. A double occipital condyle is present. The floor of the braincase is thin and the basisphenoidal tubera, present in other therapsids, is lost in the cynodonts. The epipterygoid is broadly expanded and forms a large, thin sheet of bone lateral to the sidewall of the braincase (Kemp, 1982).

2.2.2 *Galesaurus planiceps*

In dorsal view, the general outline of the skull is wide and low, being widest in the region of the zygomatic arches (Fig. 6). The skull has a blunt broad snout and a greatly sloping occiput (Parrington, 1934).

The nasal bones are unusually large, constricted in the middle and extend over the nostrils anteriorly (Rigney, 1938). The septomaxilla forms a sheet of bone that lines the floor of the naris and extends backwards and upwards between the nasal and maxilla. A septomaxillary foramen is present. The maxilla is perforated by foramina, particularly in the area of the canine. The maxilla forms a large portion of the lateral wall of the snout and contacts the lacrimal and jugal posteriorly. Two large foramina, above the fifth and sixth postcanines, are present (Parrington, 1934). The ascending process of the premaxilla overlaps the nasal dorsally. The anterior premaxillary foramen is a small opening located anteriorly on the base of the ascending process (Abdala, 2007).

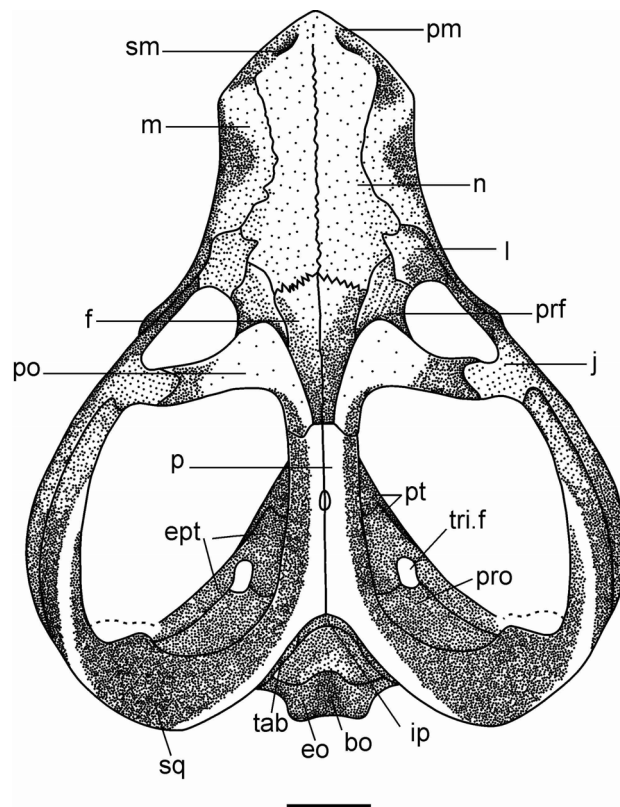


Figure 6. The skull of *Glochinodontoides gracilis*, junior synonym of *Galesaurus planiceps*, (Romer, 1966), in dorsal view (redrawn and modified from Boonstra, 1935). Scale bar represents 1 cm. Abbreviations: **bo**, basioccipital; **eo**, exoccipital; **ept**, epipterygoid; **f**, frontal; **ip**, interparietal; **j**, jugal; **l**, lacrimal; **m**, maxilla; **n**, nasal; **p**, parietal; **po**, postorbital; **pm**, premaxilla; **prf**, prefrontal; **pro**, prootic; **pt**, pterygoid; **sm**, septomaxilla; **sq**, squamosal; **tab**, tabular; **tri f**, trigeminal foramen.

The large, pentagonally-shaped lacrimals have a flat outer surface (Rigney, 1938). A fossa is present medial to the crista lacimalis. Two canals, one above the other, lead anteriorly from this fossa to meet the lacrimonasal canal that opens into the nasal cavity. The prefrontals extend from halfway along the border of the lacrimals to the middle of the upper border of the orbits where they meet the postorbitals to form the upper orbital margin (Fig. 6). The frontal is excluded from the orbital margin by the prefrontal and postorbital, as in other cynodonts. The relatively small and narrow frontals extend anteriorly between the nasals and posteriorly, almost to the parietal foramen, but do not form part of the orbital border (Broom, 1932a).

The parietals extend anteriorly along the lateral walls of the brain case where they contact the postorbitals (Fig. 6). The postorbitals extend posteriorly and terminate a short distance anterior to the pineal foramen. The parietals form a wide intertemporal crest and surround a large pineal foramen. Posteriorly, the parietals are separated from the interparietal by a wedge and, by extending posteriorly; they separate the tabulars from the squamosals (Parrington, 1934).

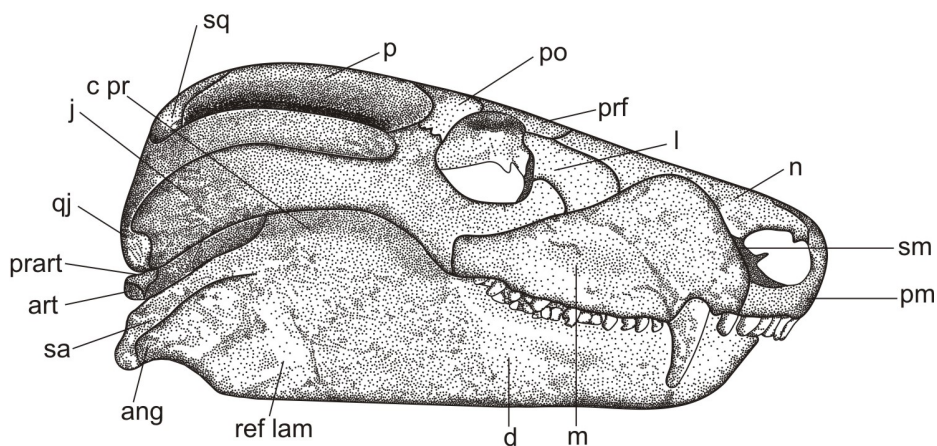


Figure 7. Reconstruction of *Galesaurus planiceps* skull, NMQR 3542, in right lateral view. Scale bar represents 1 cm. Abbreviations: **ang**, angular; **art**, articular; **c pr**, coronoid process; **d**, dentary; **j**, jugal; **l**, lacrimal; **m**, maxilla; **n**, nasal; **p**, parietal; **pm**, premaxilla; **po**, postorbital; **prart**, prearticular; **prf**, prefrontal; **qj**, quadratojugal; **ref lam**, reflected lamina; **sa**, surangular; **sm**, septomaxilla; **sq**, squamosal.

The large jugals form the ventral border of the orbit (Fig. 7). The large posterior extensions of the jugals almost reach the area where the quadratojugal meets the squamosal. The squamosal forms the upper half of the zygomatic arch and articulates with the paroccipital process of the opisthotic. It extends medially to contact the parietals from where it tapers anteriorly. The quadrate has a large vertically ascending process and fits into a depression on the anterior face of the squamosal. The quadratojugal consists of a cylindrical base and a dorsal extension,

which extends to the squamosal. This projection is on a medial plane and leans slightly inwards (Parrington, 1934).

The first postcanine has only one cusp, while the rest of the postcanine teeth are flattened with two curved cusps. The second tooth has a long anterior cusp and a short posterior cusp (Broom, 1932a). The incisors have a wide base, whereas the crown tapers to a point. The canines and postcanines are located near the outer rim of the maxilla, thus allowing room for the lower teeth, which lie medially to the upper set when the jaw is closed. Postcanine tooth replacement is thought to have occurred throughout life (Parrington, 1934). Palatal teeth are absent. The dental formula is as follows: $i^4/3$; $c^1/1$; $Pc^{12}/12$.

The dentary is the largest element in the jaw (Fig. 7). Foramina in the dentary served as openings for blood vessels and nerves traveling to the teeth. The angular, which consists of a trough-like body, covers most of the surangular, and has a large reflected lamina (Parrington, 1934). The angular passes along the dentary and meets the splenial, which rests on a shallow ventral flange of the dentary. The surangular consists of a flattened bone. The angular supports the prearticular on its inner side and expands posteriorly to clasp the articular. The articular is an oval swelling of bone that sits beneath the prearticular (Parrington, 1934).

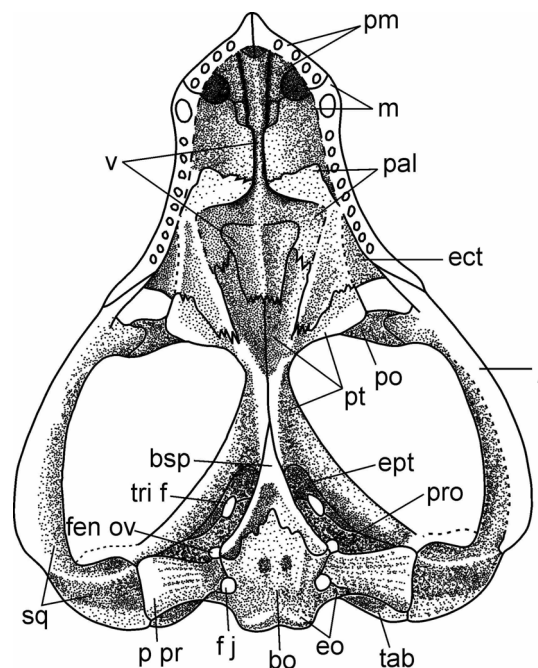


Figure 8. The skull of *Glochinodontoides gracilis*, junior synonym for *Galesaurus planiceps*, (Romer, 1966), in ventral view (redrawn and modified from Boonstra, 1935). Scale bar represents 1 cm. Abbreviations: **bo**, basioccipital; **bsp**, basisphenoid; **ect**, ectopterygoid; **eo**, exoccipital; **ept**, eipterygoid; **fen ov**, fenestra ovalis; **f j**, jugular foramen; **j**, jugal; **m**, maxilla; **pal**, palatine; **pm**, premaxilla; **po**, postorbital; **p pr**, paroccipital process of the opisthotic; **pro**, prootic; **pt**, pterygoid; **sq**, squamosal; **tab**, tabular; **tri f**, trigeminal foramen; **v**, vomer.

The palate is only slightly developed posteriorly (Fig. 8) (Rigney, 1938). In ventral view, it lies almost entirely beneath the rami of the lower jaw. The nasopharyngeal passages are formed from stout pterygoid ridges, which become shallower and diverge from one another in the palatine region. The fused vomers overlie the pterygoids. The palatines have transverse rami, which curve vertically on the inside of the lower jaw. The vomer consists of a long medial blade and a transverse process on either side. The posterior part of the vomer contacts the pterygoid and extends anteriorly to the posterior edge of the secondary palate. The transverse process extends ventrally from its dorsal border to meet the palatine. The anterior portion of the transverse process forms part of the medial septum of the nasal cavity and a hanging support for the secondary palate (Rigney, 1938).

The basicranial axis is formed by the fused parasphenoid, basisphenoid and basioccipital. The medial basisphenoid is a thick flat bone that broadens posteriorly. The fenestra ovalis is a large foramen situated in the prootic and forms part of the ear region. The jugular foramen lies anterior to the exoccipital (Fig. 8) (Rigney, 1938).

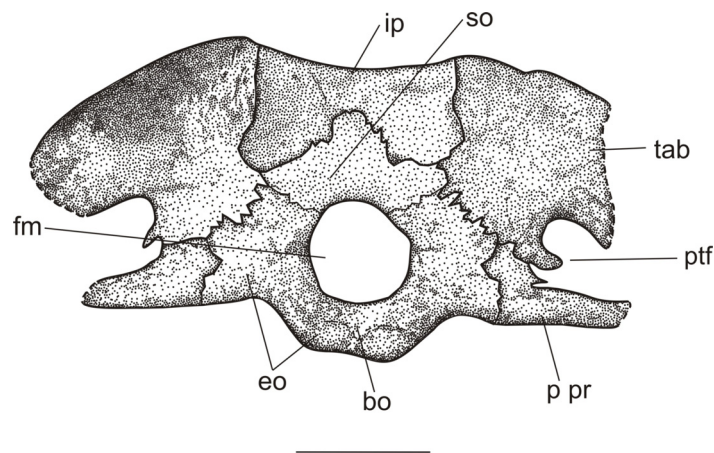


Figure 9. The skull of *Galesaurus planiceps*, NMQR 135, in occipital view. Scale bar represents 1 cm. Abbreviations: **bo**, basioccipital; **eo**, exoccipitals; **fm**, foramen magnum; **ip**, interparietal; **ptf**, posttemporal fossa, **p pr**, paroccipital process of the opisthotic; **so**, supraoccipital; **tab**, tabular. Dashed lines represent uncertain edges.

The interparietal protrudes anteriorly between the parietals as a stout wedge and extends along the upper occipital crest on either side, from which point the lateral margins extend ventrally. A wide process of the supraoccipital extends upwards to contact the interparietal immediately above it (Fig. 9). It is slightly raised medially, with depressions on either side. The supraoccipital is bound on either side by the tabulars and forms the dorsal border of the foramen magnum. The exoccipitals extend from the ventrolateral surface to the supraoccipital and surround the foramen magnum (Parrington, 1934). The tabulars meet the parietals and squamosals and extend ventrally to surround the posttemporal fossa and meet the paroccipital process of the opisthotic. The tabular contacts the squamosal to form a ridge (Rigney, 1938).

The occipital condyles are formed by the exoccipital. A small opisthotic wedge is visible between the paraoccipital and the lower portion of the tabulars. The paraoccipital process is formed by the opisthotics, which in turn fuse with the prootic anteriorly. The opisthotic bone forms the posterior bony structure of the inner and middle ear (Rigney, 1938). The prootic extends from the opisthotics along the length of the epipterygoids to the anterior region of the basicranial. The epipterygoid extends dorsal from the middle of the pterygoid bar and posteriorly to the quadrate. It expands upward to meet the parietal and anteriorly to meet the prootic in lateral view (Fig. 8). The inner borders of the prootic are supported by the basisphenoid (Parrington, 1934).

2.2.3 Postcranial Skeleton

Axial skeleton

Relatively few therapsid genera are known from complete, well-preserved axial material. Judging from the little available cynodont axial material known, a small amount of differentiation can be seen. Jenkins (1971) doubted whether cynodonts could have had the same dorsoventral movement as extant mammals because cervical, thoracic and lumbar spinous processes are not differentiated to the same extent as living mammals.

Seven cervical vertebrae is a feature of all synapsids (Crompton and Jenkins, 1973). Cynodonts had freely articulating ribs on every cervical vertebra. Changes in the axial skeleton of basal cynodonts include a reduction of the atlas centrum and its fusion to the axis vertebra and retention of the cervical intercentra in *Galesaurus*, *Thrinaxodon* and *Cynognathus* (Parrington 1977; Jenkins, 1971). These modifications promoted a greater flexibility and thus head movement, compared to reptiles.

The characteristically expanded proximal ends of cynodont ribs have been studied by numerous palaeontologists. Crompton and Jenkins (1973) suggested that the imbrications (overlapping) of costal plates and the widespread fusion of plate-bearing ribs to the vertebrae added mechanical stability to the vertebral column. The structure of the ribs and the extent to which imbrication was developed differs between genera.

The rib structure is the most variable of all cynodont postcranial features. Crompton and Jenkins (1973) also suggested that the variation may indicate an adaptive experiment, possibly in association with a more mammalian postural and locomotor behaviour.

Appendicular Skeleton

The cynodont pectoral girdle is similar to that of other therapsids in that both the coracoids and interclavicles are retained, although the coracoid lacks a supraspinous fossa (Jenkins, 1971). The pectoral girdle represents a generalized pattern from which the definitive mammalian structure possibly evolved.

In the typical basal synapsid, the ilium projects directly upward, the pubis projects anteroventrally, and the obturator fenestra is absent. Jenkins (1971) found that the cynodont ilium varied from the typical synapsid pattern. In the galesaurids, the iliac blade is spoon-shaped with a long posterior process and resembles that of extant mammals. Using the limited material that was available at the time Crompton and Jenkins (1973) suggested that the pelvis might have achieved a characteristic mammalian form before the pectoral girdle did.

Originally the limb bones of the cynodonts were less derived and resembled that of basal synapsids. The heavy, complex humerus moved mainly in a horizontal plane. Over time the opening of the glenoid changed and with the development of a more distinct humeral head, the humerus was able to move closer to the body, thus becoming more mammalian.

Muscles on the femur indicate that this bone also moved in a horizontal plane. In Early and middle Triassic cynodonts the femoral head angled more dorsally and anteriorly to the shaft and moved more effectively in a dorsoventral arc (Carroll, 1988).

Only a few cynodont manus and pes elements are known (Jenkins, 1971). *Thrinaxodon* has ten carpals (excluding the pisiform) and a phalangeal count of 2-3-

4-4-3. More derived cynodonts approach the mammalian condition by reducing the number of carpals and reaching the mammalian phalangeal count of 2-3-3-3-3.

2.3 Early Research on *Galesaurus planiceps*

The first known skulls of fossil “reptiles” with a mammal-like tooth arrangement were sent to the British Museum in 1853 by the South African based Andrew Bain (Broom, 1911). Owen later described a skull that was remarkably mammal-like, as *Galesaurus planiceps*, in a paper read before the Geological Society in 1859. In Owen’s famous classification of the fossil “reptiles”, he formed the order Anomodontia for the South African reptiles of the *Dicynodon* type, but omitted the specimens with a mammal-like dentition. In 1861, Owen published his “Palaeontology” where he made *G. planiceps* the type of a “family” of the Anomodontia, and named it the Cynodontia (Broom, 1911). He still defined the Anomodontia, as reptiles with teeth limited to a single maxillary pair and thus, did not regard *Galesaurus* as a true anomodont. In 1876, Owen issued his “Catalogue of the South African Fossil Reptiles” and placed specimens with a mammal-like dentition into the new order, Theriodontia. In 1903, Broom concluded that this order was not a natural group and divided it into a primitive group, the Therocephalia and a higher group the Cynodontia. This name is also the name first applied to animals of the *Galesaurus* type.

Although *Galesaurus planiceps* was the first discovered cynodont, the type specimen is considerably crushed and the teeth poorly preserved. As a result, the type has never been fully described and this has led to a considerable amount of confusion. Owen first described the holotype, housed in the British Museum of Natural History (Cat. No 36220) in 1859. According to the museum catalogue the specimen was recovered from the “Rhenosterberg” and possibly from the *Lystrosaurus* AZ. In 1876 a more complete description with figures was provided in the British Museum Catalogue.

In 1876, Owen described a small imperfect cynodont skull under the name of *Nyctosaurus larvatus*, collected at Commissee Drift, Caledon River of the Upper

Beaufort Group. Broom examined the types of *G. planiceps* and *N. larvatus* in the British Museum and concluded that they were separate taxa (Broom, 1905).

Originally, the type of *Thrinaxodon liorhinus* was identified as a second specimen of *Galesaurus* by various authors, but Seely (1894) finally noted the differences and described it as a new genus and species. In 1916, Van Hoepen gave the name *Glochinodon detinens* to a badly preserved cynodont skull, mandible and cervical vertebra from Harrismith in the Free State. This specimen has unusual postcanines in which a large anterior cusp curves over a smaller, anteriorly curved, posterior cusp. This type of tooth morphology was previously unknown and Van Hoepen concluded that it was a new genus. In 1924, Haughton redescribed the *Glochinodon detinens* skull and added figures. Broom (1932a) considered this genus to be a synonym of *Galesaurus planiceps* and briefly described the two specimens with some postcranial elements. The genus *Glochinodontoides gracilis* (TM 83) consisting of a skull, mandible and isolated postcranial elements from Harrismith, South Africa was then described by Haughton in 1924.

However, Romer (1966) considered the genera "*Glochinodon*" and "*Glochinodontoides*" as junior synonyms of *Galesaurus*, but he did not indicate whether he regarded them as distinct or one species (Van Heerden, 1972). Consequently small, immature specimens were referred to the genus *Galesaurus* and large, mature specimens to *Glochinodontoides* (Hopson and Kitching, 1972).

Broom described *Notictosaurus luckhoffi* in 1936. Brink and Kitching described *Notictosaurus trigonocephalus* in 1951 but considered it to be a synonym of *G. planiceps*.

Junior Synonyms of *Galesaurus planiceps* 1859

- *Glochinodon detinens* Van Hoepen, 1916 (c.f. Hopson and Kitching, 1972).
- *Glochinodontoides gracilis* Haughton, 1924 (c.f. Hopson and Kitching, 1972).
- *Notictosaurus luckhoffi* Broom, 1936 (PARS).

- *Notictosaurus trigonocephalus* Brink and Kitching, 1951.

For the decades following Owen's original description, studies on *Galesaurus* (such as Watson, 1920; Rigney, 1938; Broom, 1936; Parrington, 1934) were devoted primarily to describing morphological aspects of the cranium and thus little attention was given to the postcranial skeleton.

2.4 Bone histology

2.4.1 Fossilization

During the fossilization process, bone is subjected to a variety of diagenetic processes, which changes the bone composition. With the death of an animal the organic components, including cells and blood vessels, decompose, whereas the mineralized component becomes fossilized (Chinsamy and Dodson, 1995), thus preserving the structural organization of the bone. Even after millions of years of burial, the histological structure of fossil bone is mostly preserved intact. Thus a fossilized skeleton provides information about the morphology of an animal, but by studying the bone microstructure, information about the growth rate, ontogeny and biomechanics may also be obtained.

2.4.2 Bone Histology

A layer of specialized dense connective tissue, the periosteum, generally covers the surface of most bones (except articulation surfaces and regions of tendon and ligament attachment). The endosteum lines the bone surfaces of the medullary cavity (Francillon-Vieillot et al., 1990). Bone may be periosteal (resulting from periosteal ossification) or endosteal (resulting from endosteal ossification), depending on whether it is formed on external or internal surfaces, covered by the periosteum or the endosteum respectively (Reid, 1996).

Two types of bone can be distinguished according to the overall porosity namely cancellous (spongy) bone and compact (dense) bone. Both types of bone have the same histological elements and are usually present in every bone, but the amount and distribution of each type varies. Compact bone usually forms the outer regions of

bone and is laid down centrifugally, normally by periosteal deposition. Cancellous bone consists of slender, irregular trabeculae which form a meshwork and the intercommunicating spaces are filled with bone marrow (Leeson and Leeson, 1981).

The elements of a skeleton consist of three types of bones: long, short and flat bones. Typical long bones consist of an elongated cylindrical shaft (diaphysis) a medullary cavity (bone marrow cavity), and the epiphyses on either end. A transitional area between the epiphysis and diaphysis is known as the metaphysis. The diaphysis is formed mainly from compact bone and the epiphysis consists of spongy bone covered by a thin layer of compact bone. The cavities of spongy bone are continuous with the diaphysis bone marrow cavity. Short bones are robust and irregular in shape and consist of spongy bone covered by a thin layer of compact bone. Flat bones show a noticeable preferential development in a single plane or curved surface and the bones of the two plates enclose a middle layer of spongy bone. Each bone type grows differently and transitions between all three bone types may occur (e.g. ribs) (Leeson and Leeson, 1981).

A characteristic of bone is the arrangement of the mineralized bone matrix into layers or lamellae. The inner circumferential lamellae are less developed and are present on the inner surface, just beneath the endosteum. Small oval lacunae are placed uniformly, both within and between the lamellae and each lacuna is occupied by a single bone cell or osteocyte. Radiating from each lacuna are slender tubular passages, the canaliculi, which penetrate the lamellae and join with the canaliculi of adjacent lacunae. The lacunae are thus interconnected by an extensive system of fine canals.

During the development of bone, collagenous fibres of the periosteum become trapped within the circumferential lamellae as Sharpey's fibres, which anchor the periosteum to the underlying bone and are particularly numerous at points of insertion of ligaments and tendons (Cormack, 1987; Leeson and Leeson, 1981).

Bone is usually classified according to several factors including a) fibrillar organization, b) vascular arrangement (arrangement of the blood vessels), c) bone type and d) cortical stratification.

Fibrillar Organization

Collagen fibres are usually grouped into bundles and are distinguished by their orientation (e.g. regular, irregular or radial). There are three types of matrix organizations namely woven, lamellar and parallel-fibred bone matrix (Reid, 1996).

- ***Woven Bone Matrix***

This matrix consists of coarse and loosely packed collagen fibres, which vary in size and are irregularly distributed. The osteocyte lacunae are normally globular to round and are not very well organized. The lacunae are sometimes more abundant and closely packed than in other tissues (Francillon-Vieillot et al., 1990; Reid, 1996).

- ***Lamellar Bone Matrix***

This matrix corresponds to the highest level of spatial bone organization and consists of succeeding thin lamellae (Francillon-Vieillot et al., 1990; Reid, 1996). The closely packed collagen fibres run parallel to one another in each lamella, but the direction can change from one lamella to the next. A lamella may contain a few linear rows of flattened osteocytes with a few canaliculi (Ricqlès, 1991).

Parallel-fibred Bone Matrix

This type of bone matrix consists of closely packed collagen fibers lying approximately parallel to each other. The degree of organization of this type of matrix is between that of woven and lamellar bone matrices and is functionally linked to the variations in the growth rate which they record (Francillon-Vieillot et al., 1990; Ricqlès, 1991; Reid, 1996). These cells are flattened and more or less randomly distributed.

Vascular Arrangement

Channels present in bone contain nerves, lymph and vascular canals that run through the bone tissue. Nutrients are distributed to the bone tissue via these channels and the quantity and organization of the channels affect the efficiency of the nutrient distribution. Primary osteons are formed when these vascular canals become surrounded by centripetally deposited lamellae during periosteal growth. These vascular canals may occur in various patterns and some nomenclature is based on the way in which the vascular canals are arranged (Reid, 1996).

Haversian bone is compact bone constructed from secondary osteons or Haversian systems that replace primary bone through the process of Haversian reconstruction. Normally reconstruction starts in the oldest primary bone and may, but not always, spread outward. The primary bone around vascular canals enlarges by bone resorption and produces resorption spaces. Layers of lamellar bone are then deposited and grow inward to form cylindrical secondary osteons with single vascular canals. At first, the interstitial bone is still primary bone and surrounds these osteons, but with more secondary osteons deposited, the primary bone is replaced through secondary reconstruction. Resorption spaces may start to invade on older secondary osteons, resulting in a tissue formed completely from the last-formed secondary osteons and the interstitial remnants of partly resorbed older ones, comprising fully developed or dense Haversian bone. Secondary osteons have a characteristic cement line or reversal line which marks the furthest extent of bone removal (Reid, 1996).

Types of Bone Tissue

Woven-fibred Bone Tissue

This bone tissue consists of a woven bone matrix. Bone formation is rapid and the matrix is randomly organized. Fine cancellous bone tissue is formed during rapid bone formation. Fibro-lamellar bone is formed by woven bone that includes primary osteons (Francillon-Vieillot et al., 1990; Reid, 1996). Fibro-lamellar bone is characterized according to vascular canal arrangement.

Lamellar Bone Tissue

This type of bone tissue is characterized by lamellar bone matrix. When bone deposition is slow, lamellar bone results (Amprino, 1967). This type of bone tissue is usually poorly vascularized and associated with zonal bone tissue although it may also occur in azonal bone tissue.

- ***Zonal Bone***

Zonal bone occurs when growth is sporadically interrupted by a series of concentric growth rings in periosteal bone tissue (Reid, 1996). The bone tissue consists of regions that correspond to periods of fast growth alternating with annuli or LAGs (Lines of Arrested Growth) which are thin regions that correspond to periods of slow growth or growth cessation respectively. The simplest zonal bone tissue consists of avascular bone. Zones of more complex bone tissue contain vascularized parallel-fibred or fibro-lamellar bone with globular osteocytes and canaliculi. Annuli are thin, avascular or poorly vascularized regions, commonly consisting of lamellar bone or occasionally parallel-fibred bone. Osteocytes in annuli are flattened and canaliculi are absent or poorly developed (Francillon-Vieillot et al., 1990; Reid, 1996).

Azonal Bone

This bone tissue type does not have cyclically developed growth rings.

Parallel-fibred Bone Tissue

This bone type is created from a parallel-fibred matrix and is vascularized by primary osteons and/or simple vascular canals. Parallel-fibred bone tissue is usually more vascularized than lamellar bone tissue (Francillon-Vieillot et al., 1990; Reid, 1996).

Accretionary Bone

Some animals grow throughout their lives and never reach a maximum size. Others stop growing after they reach a maximum size. In these animals a slight thickening of the periosteal bone surface may still occur throughout life. This accretionary bone is usually poorly vascularised and represents a decrease in growth rate. Peripheral rest

lines are rest lines present in this slow forming tissue (Francillon-Vieillot et al., 1990; Reid, 1996).

Cortical Stratification

Bone usually shows structural discontinuities or apposition lines. An interruption or rest line occurs when the deposition of bone is interrupted and then restarted. External or internal resorption of bone produces a resorption surface and when new bone deposition takes place on this surface the junction between the new and old bone is known as a reversal line (Reid, 1996). Resorption and deposition take place in opposite directions.

Bone Remodeling

Bone is a dynamic tissue which is constantly being renewed and reformed throughout life. As bone grows its internal structure is continually reconstructed and remodeled. Remodeling is the result of resorption of bone in certain areas and the deposition of new bone elsewhere (Reid, 1996). Internal remodeling occurs as well as remodeling at the bone periphery and is normally related to the fetal development of an animal, but can also be associated with mechanical and physiological changes during life (Amprino, 1967). Both primary and secondary bone can be affected by bone remodeling.

2.4.3 Implications of Bone Tissue Patterns

Skeletochronology

The age of an individual can be determined using LAG or annulus counts and is called skeletochronology. Research using fluorochrome dyes has shown that the pattern of bone deposition is seasonally related to zones forming during the warmer months and annuli forming during colder/drier months. It has thus been accepted that one annulus corresponds to one year in an extinct animal, so allowing the age of an individual to be estimated (Castanet and Smirina, 1990). In older individuals the earlier growth rings near the medullary cavity may be removed by resorption. The age of the animal may be estimated using the width of the initial zones of the smallest and

apparently the youngest individual to obtain an estimation of the number of resorbed growth rings and adding that to the total count (Chinsamy, 1993).

Sexual Maturity

Research on many extant animals has shown that a reduction in width between consecutive growth rings may occur when sexual maturity is reached and it is thus possible to determine when the onset of sexual maturity in fossil animals occurred. Although the change in pattern reflects a decrease in diametric growth rate, it may not indicate that the animal has reached maximum size, but that sexual maturity has been reached (Sander, 2000).

Deductions from Bone Histology

The growth rate at which an animal grows is directly reflected to the rate of bone deposition and nature of the fibrillar matrix. When bone formation is rapid the matrix is randomly organized, with poorly organized osteocyte lacunae and a woven bone tissue results. When bone deposition is slow, the matrix is ordered and lamellar bone tissue forms. Fibro-lamellar bone is common in mammals and birds and is formed during rapid bone deposition (Amprino, 1967; Reid, 1990). This type of bone frequently occurs in dinosaur bones and it has been concluded that dinosaurs were endothermic, but this bone type also occurs in juvenile crocodiles (Buffrènil, 1981). The occurrence of fibro-lamellar bone is thus not proof of an endothermic physiology. The general structure of the primary compact bone presents a direct evaluation of whether the bone deposition was continuous or interrupted. Cyclical bone deposition occurs when compact bone is stratified into distinct growth rings. This bone type is known as lamellar-zonal bone and comprises zones and annuli or LAGs. The zones are more vascularized and represent periods of fast growth, whereas the annuli are poorly vascularized and represent periods of slow growth. If bone growth ceases completely LAGs result. Uninterrupted bone formation results in the absence of zonation in the compact bone.

The bone microstructure of juveniles is generally more porous than adults and exhibits randomly arranged primary osteons in a woven bone matrix. The vascular

canals move progressively closer together until lamellation and zonation become impossible to differentiate (Reid, 1996). With increasing age, the rapidly formed bone tissue changes to a more slowly deposited bone tissue. The bone microstructure thus reflects the ontogenetic status of an individual since juvenile and adult bones differ.

The specific lifestyle of an animal is reflected in the structural design of its bones. Thick and relatively short limb bones are an advantage for fossorial animals (animals that dig holes/burrows) (Casinos et al., 1993). Magwene (1993) established that therapsids and extant mammals had relatively thinner bone walls and probably had lighter bones than crocodiles and lizards. Wall (1983) found that the bone wall of aquatic and semi-aquatic mammals exceeds 30% of the average bone diameter. The lifestyle of an extinct animal may thus be assessed using bone histology; for example, an increase in the thickness of the compact bone wall may reflect an aquatic, semi-aquatic or fossorial lifestyle (Wall, 1983, Botha, 2003).

The study of bone microstructure thus provides important information on the growth, ontogeny, biomechanics and lifestyle of an animal. Although the physiology of an extinct animal cannot be directly determined, using information obtained from bone tissue patterns, other aspects of its biology such as growth, ontogeny and lifestyle can be assessed.

CHAPTER THREE

MATERIAL AND METHODS

3.1 Material

Positively identified *Galesaurus planiceps* cranial and associated postcranial material was selected from various collections in South Africa for study. *Galesaurus* is a relatively rare taxon and thus, only a few specimens were available. The study material includes 12 specimens from the collections of the Transvaal Museum (TM) of the Northern Flagship, Pretoria; Iziko South African Museum (SAM-PK-K), Cape Town; Bernard Price Institute for Palaeontological Research (BP/1), University of the Witwatersrand, Johannesburg; Rubidge Collection of Wellwood (RC), Graaff-Reinet and the National Museum, Bloemfontein (NMQR) (Table 1).

Due to their excellent preservation, some of the study specimens deserve special mention:

BP/1/4506 was found *in situ* by J. W. Kitching from the farm Fairydale, Bethulie District in 1974. The well preserved, articulated skull and partial skeleton consists of the right humerus, radius, ulna, manus, pes and a few caudal vertebrae.

RC 845 was also collected by J. W. Kitching from the farm Fairydale, Bethulie District in 1977. This beautifully preserved fossil consists of a complete skull and articulated skeleton in aggregation with the procolophonoid, *Owenetta kitchingorum* and a diplopod millipede (Abdala et al., 2006). Due to the *in situ* state of these specimens and the preservation of delicate skeletal elements in articulation, Abdala et al. (2006) suggested that these animals died and were buried quickly in a place protected from both biological (e.g. scavengers and trampling) and physical (e.g. flooding and wind) agents of bone dispersal.

Chapter 3: Material and Methods

Specimens SAM-PK-K10465 and NMQR 3542 were collected during a joint expedition between the Iziko South African Museum and the National Museum to the farm Fairydale, Bethulie District in 2005. Specimen SAM-PK-K10465 was collected by Roger Smith and is a complete fully articulated skull and skeleton, with just a few caudal vertebrae displaced out of their natural position. NMQR 3542 was collected by John Nyaphuli and consists of a skull and several disarticulated postcranial elements (Table 1). Both specimens were found *in situ*.

Specimen NMQR 3678 was collected by Sam Stuurman from the farm Fairydale, Bethulie District in 2008. The specimen consists of at least three skulls and associated postcrania, while all skull roofs are absent. All three specimens were found *in situ*. One specimen has been prepared, and includes a particularly well preserved right manus.

Table 1. *Galesaurus planiceps* postcranial material examined in this study. All study material was recovered from the Lower Triassic *Lystrosaurus* AZ, Katberg Formation of the Beaufort Group, Karoo Basin.

Galesaurus planiceps

Accession no.	Material	Farm, District
NMQR 135	A fully preserved skull and a partial skull and fragmentary postcrania, including a disarticulated scapulocoracoid	Oviston area, Venterstad
NMQR 3340	Skull and partial limb bone	Rietpoort, Dewetsdorp
NMQR 3542	Skull and disarticulated left scapula, vertebrae, ribs, femora, humeri, radii, left ulna, left tibia and fibula, part of pelvis and portions of the manus or pes (Fig. 11 and 12)	Fairydale, Bethulie
NMQR 3678	Three skulls of which skull roofs are absent, atlas, axis, proatlas and articulated vertebrae, partially prepared postcrania in articulation, including right manus (Fig.16)	Fairydale, Bethulie
TM 83	Skull and disarticulated scapulae, vertebrae, rib fragments, femora, humeri, right radius, ulnae, tibiae and fibulae	James' Donga, Harrismith
RC 845	Skull and almost complete articulated postcranial skeleton; excluding the radii, ulnae, left femur, left tibia, left fibula, manus and pes (Fig. 13 and 14)	Fairydale, Bethulie
BP/1/4506	Skull and articulated left humerus, radius, ulna, manus and scapula, vertebrae, ribs, parts of the pelvic girdle, femora, tibiae, fibulae, and left and right pes	Fairydale, Bethulie
BP/1/5064	Skull and several postcranial fragments, including vertebrae, portions of manus or pes	Fairydale, Bethulie
BP/1/4714	Skull and several postcranial fragments including right scapula, coracoid fragment, interclavicle, vertebrae, ribs and partial left humerus	Draycot, Escourt
SAM-PK-K10465	Skull and complete articulated postcranial skeleton with dislodged caudal vertebrae (Fig. 10)	Fairydale, Bethulie
SAM-PK-K10468	Skull and disarticulated postcranial skeleton, including scapulae, complete right and partial left humeri, vertebrae, clavicles, partial interclavicle, complete right radius and partial right ulna and left manus (Fig. 15)	Fairydale, Bethulie
SAM-PK-K1119	Complete skull and disarticulated postcranial elements, thoracic vertebrae, left scapula, partial left humerus, radii and ulnae	Harrismith District

Table 2. *Thrinaxodon liorhinus* postcranial material studied for comparative purposes. All material was recovered from the Lower Triassic *Lystrosaurus* AZ of the Beaufort Group in the Karoo Basin.

Thrinaxodon liorhinus

Accession no.	Material	Farm, District
BP/1/1730	Skull and almost complete articulated skeleton, including vertebrae, scapulae, right humerus, radius, ulna, right partial manus, partial left manus, ribs, right femur, tibia, fibula and partial right pes	Newcastle
SAM-PK-K1395	Disarticulated skeletons without skulls, including thoracic ribs, coracoid, procoracoid, scapulae, clavicles, humeri, radius, ulna, femur, tibia, fibula and manus	Unknown

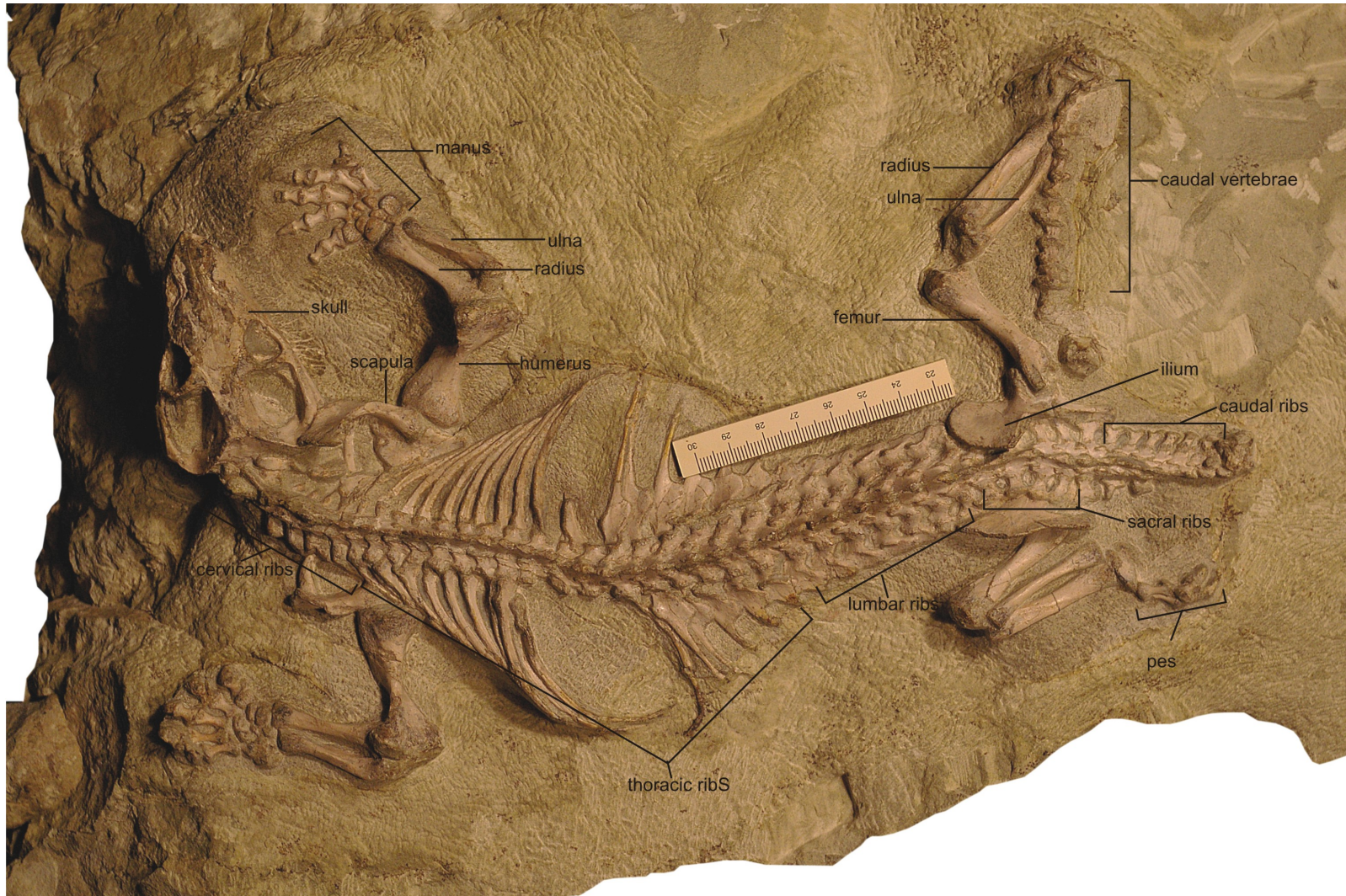


Figure 10. *Galesaurus planiceps*, specimen SAM-PK-K10465, in dorsal view. Scale bar represents 7 cm.

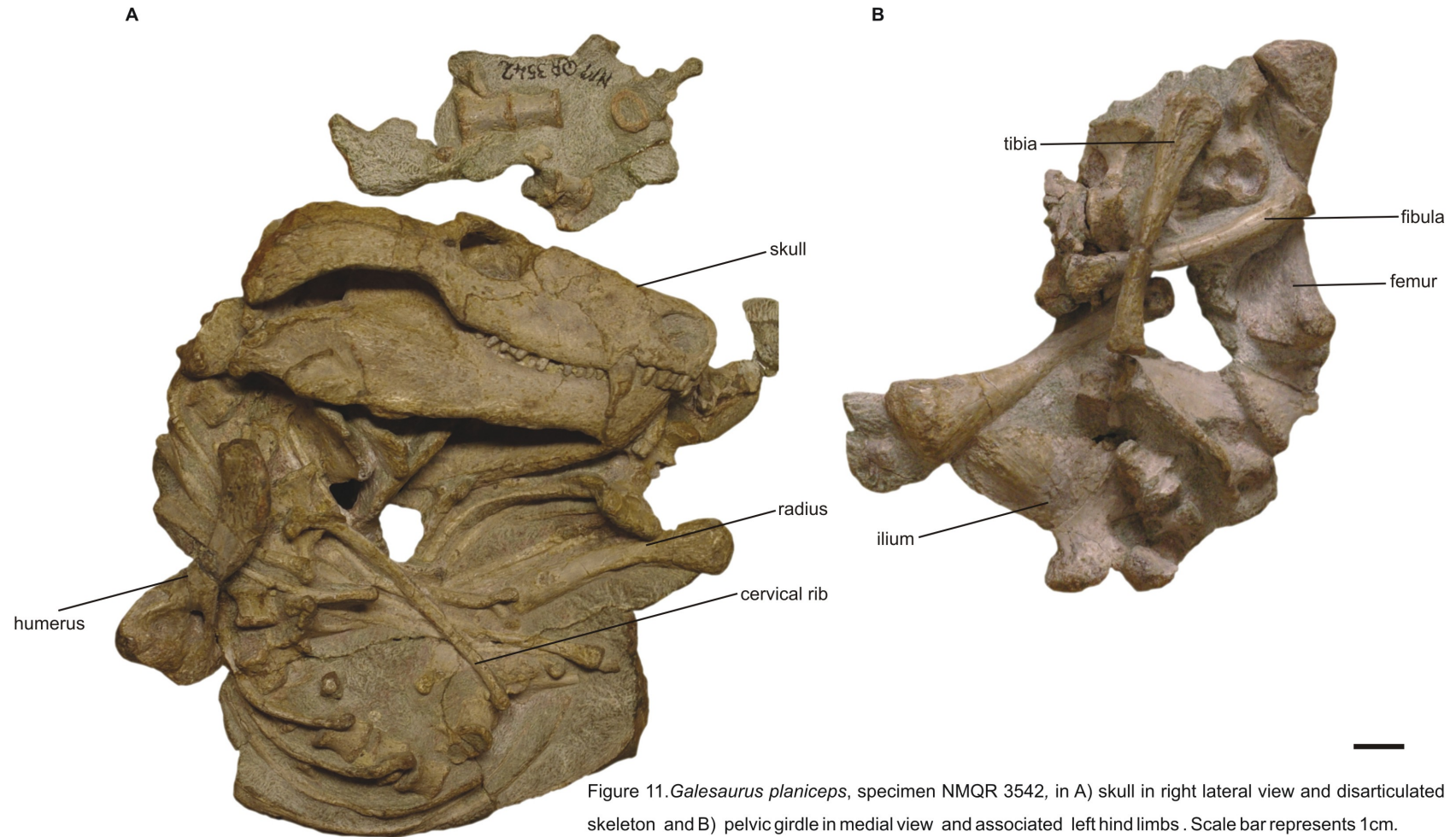
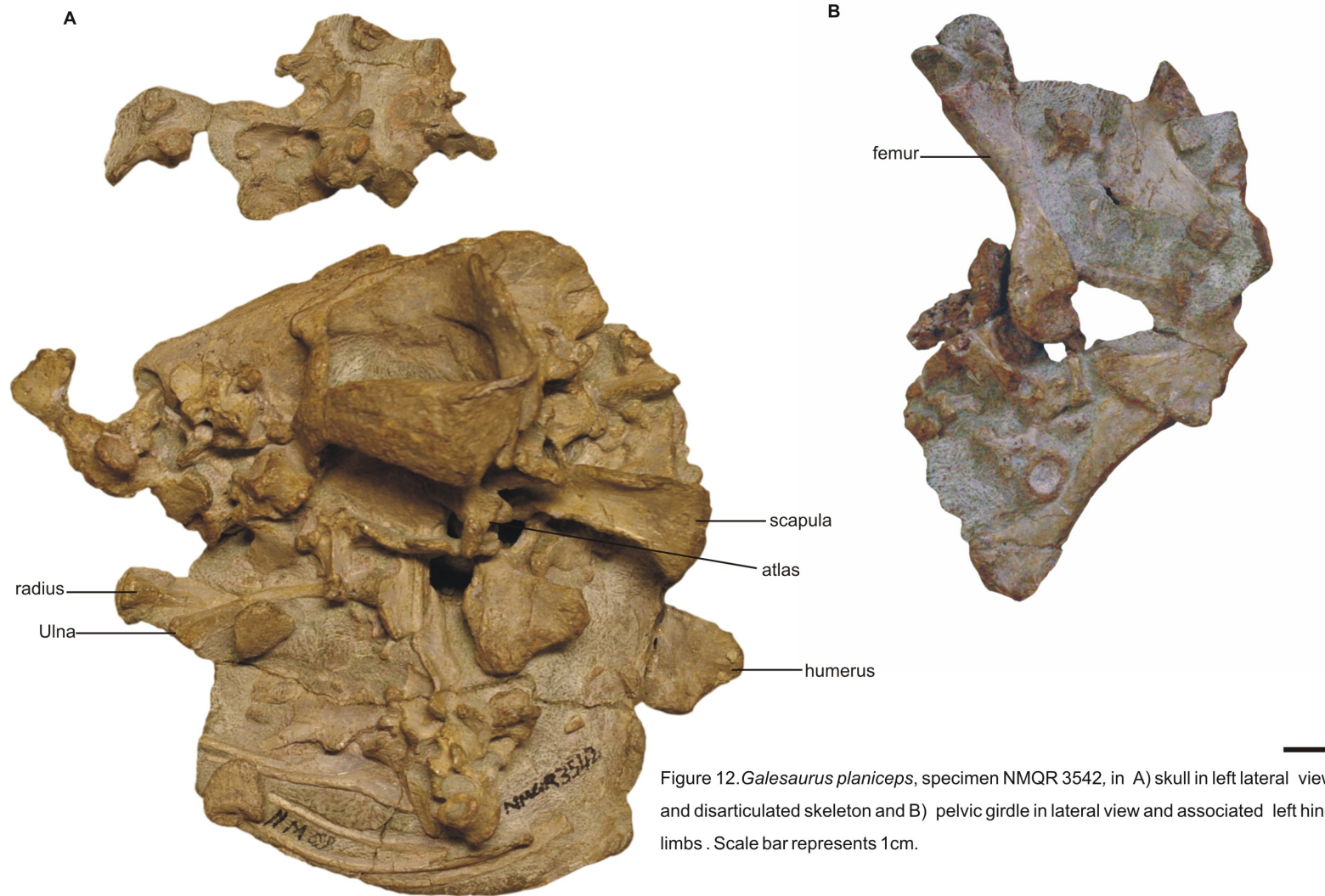


Figure 11. *Galesaurus planiceps*, specimen NMQR 3542, in A) skull in right lateral view and disarticulated skeleton and B) pelvic girdle in medial view and associated left hind limbs. Scale bar represents 1cm.



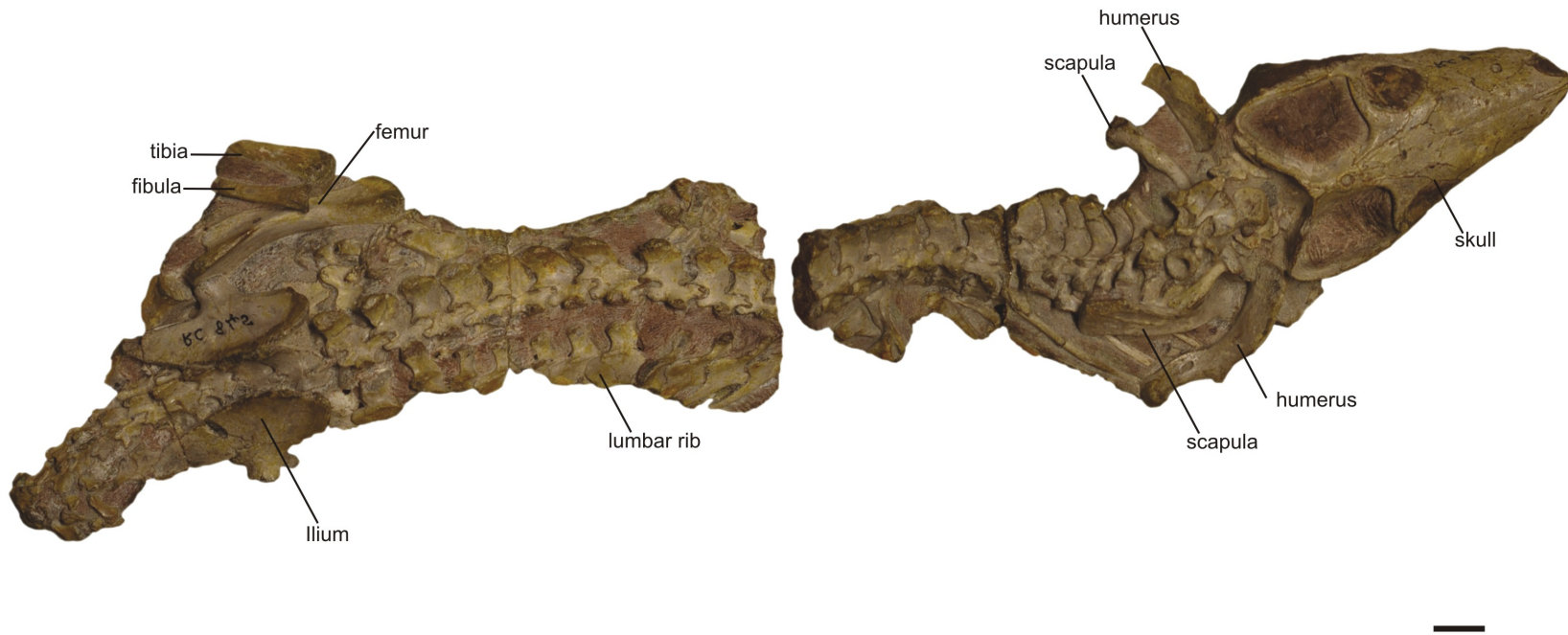


Figure 13. *Galesaurus planiceps*, specimen RC 845, in dorsal view . Scale bar represents 1 cm.

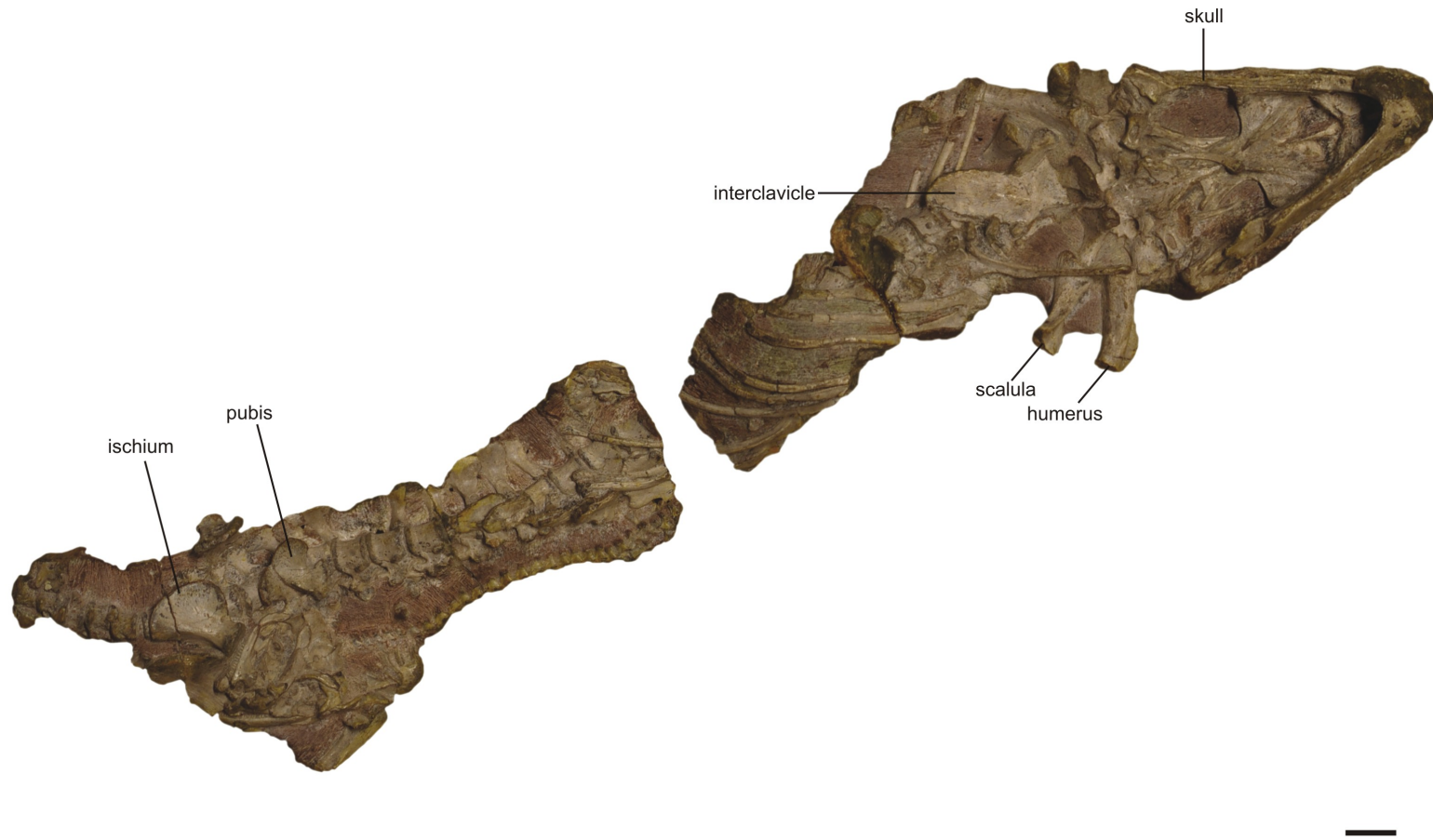


Figure 14. *Galesaurus planiceps*, specimen RC 845, in ventral view. Scale bar represents 1 cm.

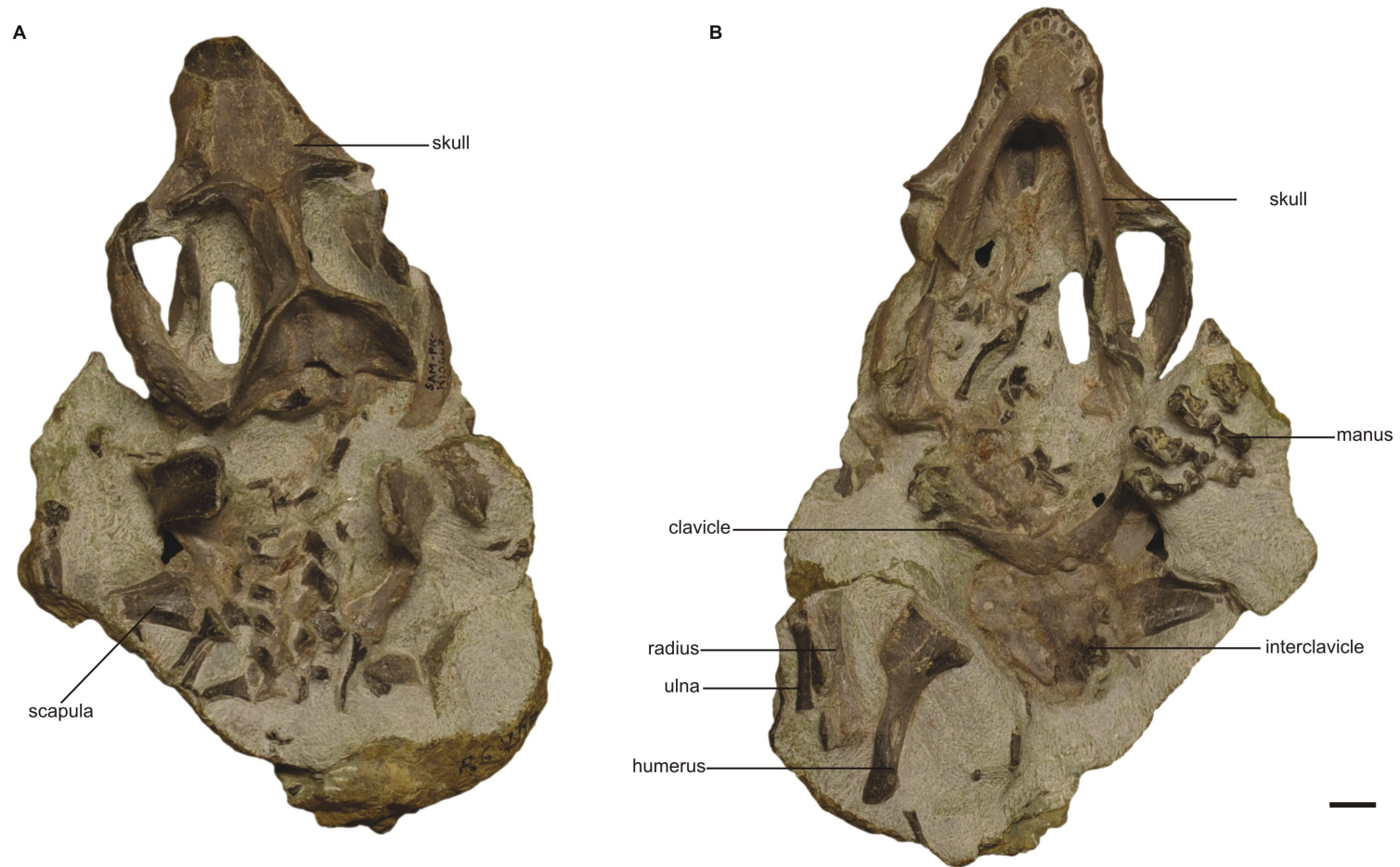


Figure 15. *Galesaurus planiceps*, specimen SAM-PK-K 10468, in A) dorsal and B) ventral view. Scale bar represents 1 cm.

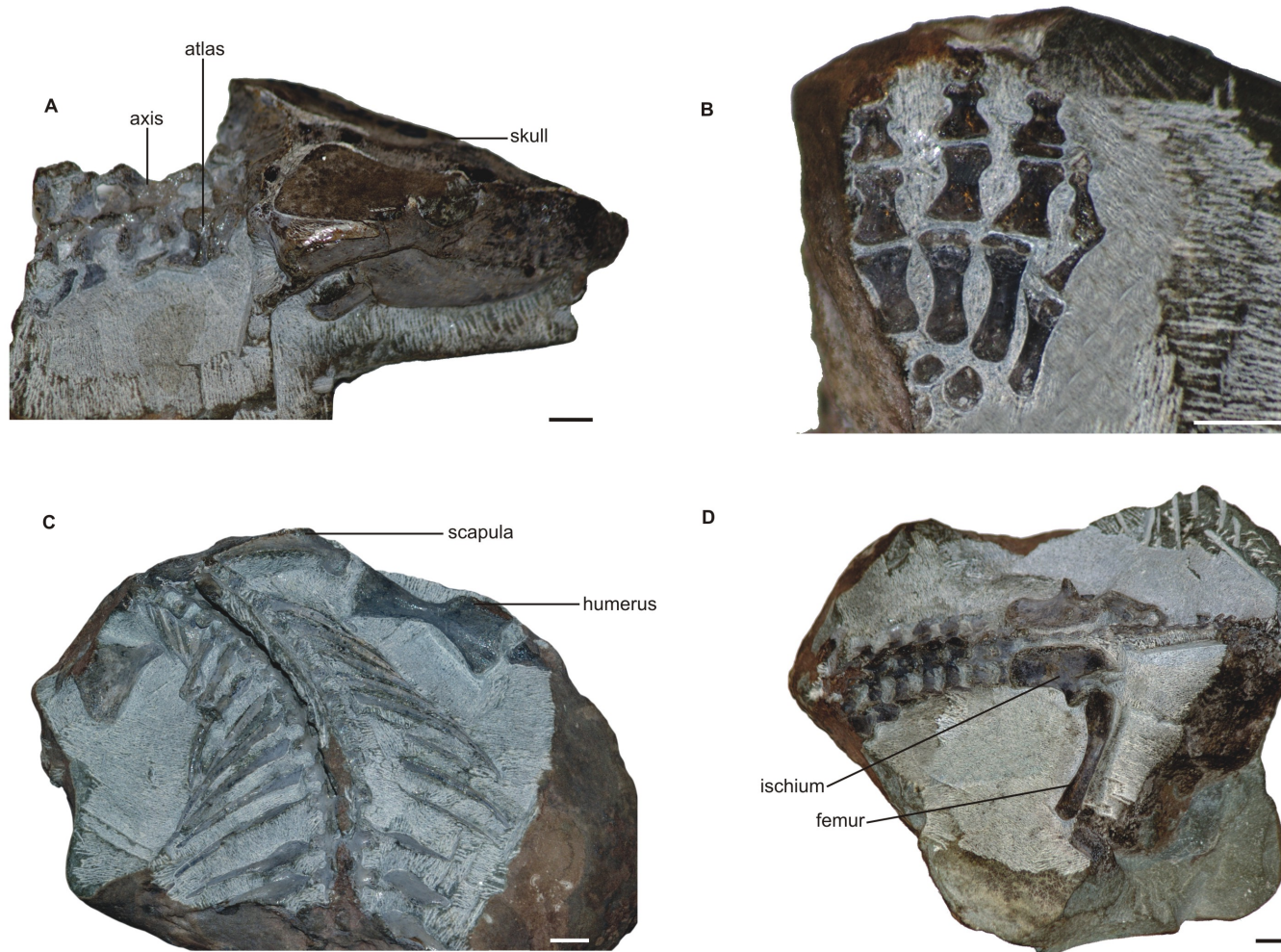


Figure 16. *Galesaurus planiceps*, specimen NMQR 3678, in A) skull and anterior cervical vertebrae in right lateral view, B) right manus in ventral view, C) anterior axial skeleton and humeri in dorsal view and, D) lumbar ribs and posterior axial skeleton (pelvis and femur) in dorsal view. Scale bars represents 1 cm

3.2 Descriptive Techniques

The study material was mechanically prepared using VPX-2 air engravers. The fossil preparators of the Bernard Price Institute, Iziko South African Museum and National Museum manually prepared the specimens. Glyptol and Paraloid were used to glue broken specimens back together. Specimen SAM-PK-K1119 was prepared by acid-preparation by preparators of the Iziko South African Museum. A Pentax 100K and a Nikon Coolpix 5400 digital camera were used to photograph specimens.

3.2.1 Macro-measurements

Where available, the total lengths, midshaft diameter, proximal and distal widths of all specimens were measured.

3.3 Bone Histology

Measurements, photographs and illustrations were completed of the specific bone elements described. Casts were made of the limb bones thin sectioned for bone histology.

3.3.1 Preparation of Fossil Bone for Histological Examination

The method for preparation of fossil bone follows that of Botha (2002) with modifications. Wherever possible, sections were taken from the midshaft as the midshaft undergoes less secondary remodeling than other bone elements and thus the primary bone tissue can be better examined.

3.3.2 Embedding Specimens

Fossil bones are brittle and were thus embedded in a mounting medium, which prevented disintegration during the sectioning and grinding processes. When specimens were embedded the following procedure was followed:

A specimen was placed in a soft, plastic container which was lined with Vaseline (petroleum jelly) to prevent the resin from sticking to the container after setting.

Epofix Resin and catalyst were used to embed the specimens. The amount of resin and catalyst were determined using a Shimadzu EL 1200 weighing balance. The resin and catalyst were mixed in a ratio of 0.158 and placed in a Struers Epovac vacuum chamber for approximately five minutes to remove all bubbles. A bed of resin, covering the bottom of the container was allowed to dry for 24 hours.

Newly prepared resin and catalyst were used to imbed the specimens. These specimens, immersed in resin, were placed in the vacuum chamber and left for three to five minutes while the bubbles were removed. The specimen was removed from the vacuum chamber and left to set for 24 hours.

3.3.3 Cutting and Mounting of Specimens

Once the resin was set, the specimen was removed from the plastic container and the resin block was cut into smaller sections using a diamond cutting blade on an Accutom-50 thin sectioning machine. The position where the bone was sectioned was documented to allow comparative analysis between bones as bone structure differs between individual bones and different regions of the same bone. The smaller blocks were polished and mounted on a frosted glass slide using the glue, Specifix Resin with the Specifix curing agent and left overnight to set. Frosted glass slides were used for enhancing the resolution and adhesion for the mounting medium. The slides were clearly marked by permanent markers.

3.3.4 Grinding and Polishing Specimens

The specimen on the glass slide was placed in the Accutom-50 and cut into thinner sections. These thinner sections were then ground to a thinness of approximately 200µm. The thin sections were examined under a microscope at intervals to check the thickness of the fossil bone.

The slides were viewed and analysed using a Nikon DS-FI1 polarizing petrographic microscope, which allows viewing under polarized light. Photographs were taken using the computer program, NIS-Elements D 3.0.

3.3.5 Cross-sectional Geometry

The thickness of the compact bone wall or relative bone wall thickness (RBT) (Chinsamy, 1991; Botha, 2002) of each bone was measured using an eyepiece micrometer in the Nikon DS-FI1 polarizing petrographic microscope. Four measurements were taken to calculate the RBT. The vertical (d_1) and horizontal diameter (d_2) of the bone was measured using sections from the midshaft of each bone. The diameters were added and divided by two to obtain the mean diameter (D).

$$D = (d_1 + d_2) / 2$$

The bone wall thickness was determined by measuring the thickness of the compact bone at four consecutive places around the bone (Fig. 17). The bone wall thickness (T) was determined by adding these measurements ($t_1 + t_2 + t_3 + t_4$) and dividing the sum by four.

$$T = (t_1 + t_2 + t_3 + t_4) / 4$$

The final relative bone wall thickness was calculated by the following formula:

$$RBT = (T/D) \times 100$$

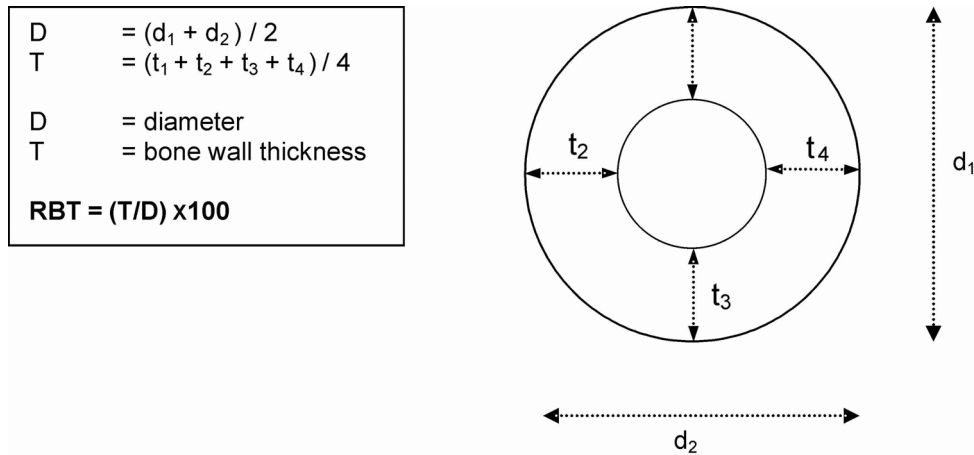


Figure 17. Schematic representation of the relative bone wall thickness (RBT) measurements, expressed as a percentage (taken from Botha, 2002).

The transition between the medullary cavity and the cortex is not always distinct due to the presence of bony trabeculae in the medullary cavity. The RBT measurements thus refer to the minimum thickness of the compact bone.

3.3.6 Vascularization Quantification

The channel area in each bone was calculated to quantify the amount of vascularization in the bone. This quantification does not give an absolute channel area, but the maximum possible area occupied by channels. In life, these channels would have included lymph and nerves as well as vascular canals. Thus, the vascular canals do not always occupy the entire channel area and the results obtained in this study are consequently a representative of the maximum amount of vascularization in the midshaft of each bone (Stark and Chinsamy, 2002).

Measurements were taken from the midshaft in the mid-cortical region of each bone. An image capturing computer program, NIS-Elements D 3.0 was used to capture images at 10X magnification from the Nikon DS-FI1 polarizing petrographic microscope.

A field of view was randomly selected in the mid-cortex and thereafter every third field of view was examined. The surface area of each channel was calculated (in microns) by tracing the perimeter of the channel and then calculating the surface area of each encircled area. The sum of the surface area of all channels in each view was calculated and converted into a percentage.

CHAPTER FOUR

POSTCRANIAL DESCRIPTION

4.1 Preface

The axial skeleton of *Galesaurus* has been described by several authors (Haughton, 1924; Parrington, 1934; Kemp, 1969). Jenkins (1971) conducted extensive research on the cynodonts *Thrinaxodon* and the more derived *Cynognathus* and *Diademodon*, but only briefly mentioned *Galesaurus*. As some of the postcranial morphology in the studied specimens is not fully preserved or accessible, the description provided here for *Galesaurus* is supplemented from the literature.

The skull length of each specimen available for study was measured to determine the largest specimen, which was then regarded as the maximum size for the genus (Table 3). All study specimens including the largest specimen, which is regarded as 100% adult size, have clearly open neurocentral sutures on the vertebrae. Basal skull lengths range from 63 to 102 mm (Table 3). Skulls less than 63 mm in length were not available for study. Based on the gross morphology of the 12 study skulls and associated postcrania two distinct morphs were recognised; a small, gracile form and a large robust form (see description). The study material comprises six robust morphs and six gracile morphs. The current study provides the possibility that small juvenile (0%-30%) *Galesaurus* may be recovered in future. Sub-adults were allocated to 31-79% adult size and adults 80-100%.

Table 3. Grouping of the 12 *Galesaurus planiceps* specimens into gracile and robust morphs, based on skull length. Examinations were based on gross morphology of the skull and skeleton (all gross measurements are provided in Appendix 1).

<i>Accession no</i>	<i>Skull length (mm)</i>	<i>% Adult</i>	<i>Ontogenetic status</i>	<i>Gracile</i>	<i>Robust</i>
RC 845	63	62	Sub-adult	X	
SAM-PK-K10465	65	64	Sub-adult	X	
SAM-PK-K1119	70	69	Sub-adult	X	
NMQR 3678	72	71	Sub-adult	X	
BP/1/4714	79	78	Sub-adult	X	
BP/1/4506	81	79	Sub-adult	X	
NMQR 135	92	90	Adult		X
NMQR 3340	101	99	Adult		X
BP/1/5064	101	99	Adult		X
NMQR 3542	102	100	Adult		X
TM 83	102	100	Adult		X
SAM-PK-K10468	102	100	Adult		X

4.2 Axial Skeleton

4.2.1 Vertebrae

The axial skeleton of *Galesaurus* is differentiated into five regions with seven cervical (including the atlas, paired pro-atlas and axis), 13 thoracic, seven lumbar, five sacral and 25 caudal vertebrae. As in *Thrinaxodon*, the total vertebral count of *Galesaurus* is 32, excluding the caudal vertebrae.

Cervical

Atlas

The cynodont atlas consists of four separate ossifications, a centrum, two halves of the neural arch and the first intercentrum. The neural spine and anapophyses on the atlas are characteristically absent.

The anterior surface of the atlas is not visible in any of the studied specimens and is thus described from the literature. A large convex articular facet is divided into four regions (Jenkins, 1971). Two dorsolateral wings of the facet extend posteriorly on either side almost reaching the basis of the axis neural arch. These wings also face anteriorly and articulate with the concave articulation facet on each half of the atlas neural arch. The facet for the atlas intercentrum projects anteroventrally and articulates with a broad, but shallow, concave surface of the first intercentrum. Above this concave facet is a broad transversely convex area that faces mostly anteriorly. Jenkins (1971) noted that in some *Thrinaxodon* and *Galesaurus* specimens a faint medial swelling is present adjacent to the dorsal rim, thus incompletely dividing the atlanto-occipital joint into separate areas for the occipital condyles.

The atlas neural arch consists of one lamina (l) that does not co-ossify with the lamina of the opposite neural arch. Two articulation facets are present on the medial surface of the atlas arch (Fig. 18); one for the atlas centrum (f a c) and the other for the occipital condyles (f o c) (Fig. 18A). Jenkins (1971) noted that the facet for the occipital condyles (f o c) is anteroposteriorly longer in *Galesaurus* than the facet for the atlas centrum. This was found to be the case in gracile *Galesaurus* and it thus agrees with the findings of Jenkins (1971). This differs from the condition in *Thrinaxodon* in which the facets are

equal in length. The articulation facet of specimen RC 845 agrees with the description in the literature in that the facet for the occipital condyle is slightly longer than the facet for the atlas centrum (Fig. 18A) (Jenkins, 1971) and is concave and almost crescent in outline. These facets cannot be seen in specimen NMQR 3542, but this could be due to incomplete preservation. Laterally, facets for the articulation with the proatlas (f pra) and atlantal rib (f at r) are present (Fig. 18B). A short robust neck separates the medial articulation facets from the rest of the atlas (RC 845) and is thus thicker than the rest of the bone.

The lateral part of the lamina of the neural arch is a relatively flat bony structure and extends ventrally to become the transverse process (tr p). Although the medial part of the lamina is particularly thin and usually incomplete, it does not extend medially beyond the atlas centrum and occipital facet. The laminae lie almost vertically above the neural canal and they do not make contact. Dorsally, the neural canal was probably completed by cartilage or ligaments during life (Jenkins, 1971). In each study specimen where the atlas was preserved (NMQR 3542; NMQR 3678; and RC 845) a prominent triangular bone protrusion (b p) is present at the junction between the neck and the base of the transverse process, probably serving as muscle attachment. This bone protrusion has not been described in *Thrinaxodon* or the more derived cynodonts *Diademodon* and *Cynognathus*.

Extending into the dorsal part of the *Galesaurus* atlas lamina is a shallow groove (gr) that broadens ventrally (Fig. 18B). The shallow groove is positioned slightly more dorsally than described by Jenkins (1971) as a broad dorsolateral groove in *Thrinaxodon* and *Galesaurus*. Jenkins (1971) also noted that in larger cynodonts, a small tuberosity, probably serving as muscle attachment, is present on the posterior edge of this groove. This tuberosity is present in NMQR 3542, but it is not particularly prominent.

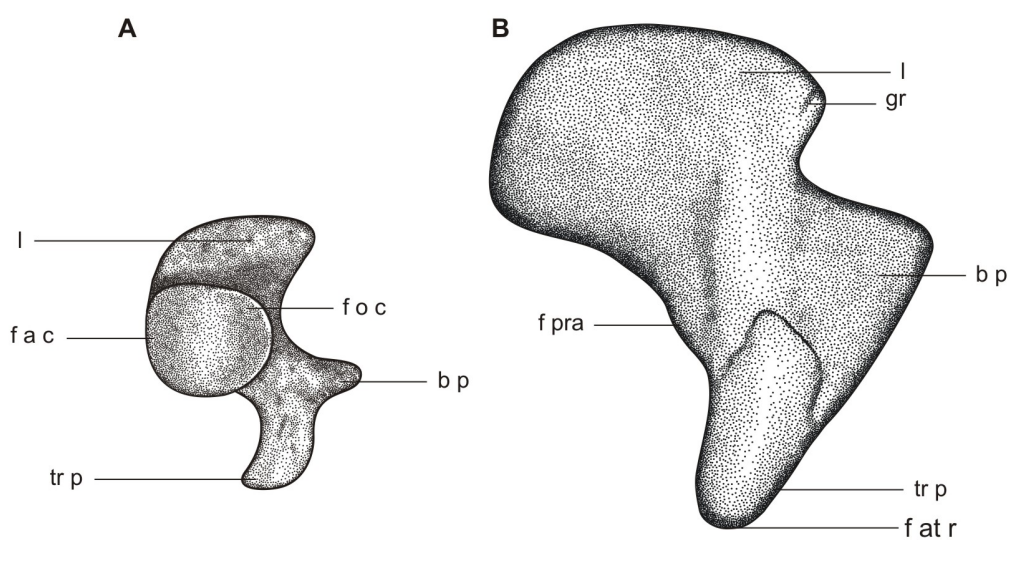


Figure 18. The atlas of *Galesaurus planiceps*, A) RC 845, medial view of right half and B) NMQR 3542, lateral view of right half. Scale bar represents 1 cm. Abbreviations: **b p**, bone protrusion; **f a c**, facet for atlas centrum; **f at r**, facet for the atlantal rib; **f o c**, facet for occipital condyle; **f pra**, facet for the proatlas; **gr**, groove; **l**, lamina; **tr p**, transverse process.

Jenkins (1971) described a rounded sulcus between the anterior edge of the atlas lamina and the anterior rim of the occipital facet in *Thrinaxodon* and *Galesaurus*. This rounded sulcus is only partially visible in medial view in RC 845 and is therefore described from the literature. The proatlas covers the sulcus dorsally, forming a short canal that passes posteriorly through a notch between the lateral portion of the facets for the atlas centrum and occipital condyle, and the transverse process. It disappears on the posteroventral aspect of the transverse process (Jenkins, 1971). The slightly convex facet for the proatlas (**f pra**) lies between the base of the transverse process and the atlas lamina. Jenkins (1971) noted that this facet completely covers the sulcus by contacting the anterior rim of the atlantal occipital facet in the more derived cynodonts *Cynognathus* and *Diademodon*, whereas in *Thrinaxodon* it overhangs the sulcus.

The slightly tapering transverse process (**tr p**) of *Galesaurus* projects posterolaterally and slightly ventrally. The process has a slim, elongated, posterolaterally and slightly

ventrally oriented facet for articulation with the atlantal rib (f at r) at its distal end (Fig. 18B) whereas the transverse process of *Thrinaxodon* is more rectangular in shape.

A bone, resembling the atlas centrum in posterodorsal view, may be present in NMQR 3542, but due to poor preservation this cannot be confirmed. The atlas centrum of RC 845 can be seen in posterior view, and measures 4 mm in length. The postaxial cervicals are approximately 6 mm in length and thus the atlas centrum is somewhat shorter than the rest of the cervical series. This may have allowed for more manoeuvrability between the skull and neck. Jenkins (1971) described the dorsal surface of the atlas centrum as fairly flat. It bears a broad, oval concavity perforated by nutrient foramina. He found that the atlantal centrum in *Galesaurus* is partially fused to the axis centrum with incomplete closure of the joining suture, and that fusion of the axis centrum with the atlantal centrum is variable, and may be dependent on the age of the animal. This articulation of the atlas centrum and axis has not been confirmed in this study due to the position in which they are preserved.

The atlas intercentrum of *Galesaurus* is known, but not preserved in any specimen seen in the current study. It has a variable outline in cynodonts when viewed from above or below (Jenkins, 1971). In *Galesaurus* it is a narrow rectangular bone except for a protruding lip that articulates with the atlas centrum. The ventral surfaces of all intercentra are broadly convex. An anterior facet for the occipital condyles and a posterior facet for the atlas centrum are present on the dorsal surface of the first intercentrum. The dorsal surface of the oval atlas centrum is concave and confluent with part of the posterior border of the occipital facets. These intercentral facets for the occipital condyles face anterodorsally and slightly medially. A rounded notch in the middle of the anterior border of the intercentrum partially separates the two occipital facets. Jenkins (1971) found this notch to be more deeply incised in *Thrinaxodon*, *Cynognathus*, and *Diademodon* than in *Galesaurus*. A posterolaterally directed parapophysis is present on each of the posterolateral corners of the intercentrum. An oval facet is present on the apex of the parapophysis for the capitulum of the atlantal rib. A distinct protrusion projects posteriorly from under the atlas centrum facet and most likely functioned as attachment of a ligament to the atlas centrum.

Proatlas

The paired proatlas (pra) are supported posteriorly by the anterior process of the atlas (Haughton, 1924). Parrington (1934) described the proatlas ossicles as rhomboidal, whereas Jenkins (1971) described them as trapezoidal (Fig. 19), the latter description were confirmed in this study. The ventral margin of the proatlas is horizontally oriented, slightly concave and also the thickest part of the plate (Jenkins, 1971).

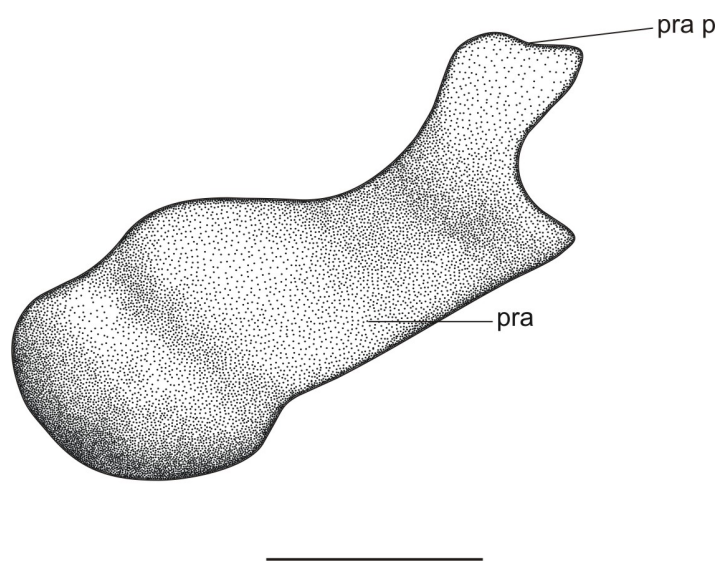


Figure 19. The right proatlas of *Galesaurus planiceps*, SAM-PK-K10465, in dorsal view. Scale bar represents 1 cm. Abbreviations: **pra**, proatlas; **pra p**, proatlas process.

The ventral border of the proatlas appears to thicken anteroposteriorly. The anterior and posterior margins are almost parallel to one another and incline anteriorly at about 20° from the ventral margin. The plate appears to be curved and slightly twisted so that the lateral half faces dorsolaterally and the medial half posterodorsally (Jenkins, 1971). The proatlas process (pra p) halfway along the ventral margin, on the lateral surface, but is incomplete in all the study specimens as well as those studied by Jenkins (1971). However, this process was described by Haughton (1924) as a strong blunt process near the outer end that stands almost at right angles to the main body of the bone. The outline of the proatlas of *Thrinaxodon* is similar to that of *Galesaurus*, but it is more gracile and slightly more elongated.

Axis

The neural spine of the axis is a broad, hatchet-shaped blade (n s) (Fig. 20). In dorsal view, the neural spine is particularly thin in the middle. It expands towards its anterior and posterior ends and terminates anteriorly in a tuberosity (NMQR 3678; SAM-PK-K10465). The thin, concave neural spine of *Galesaurus* was incompletely preserved in the specimens Jenkins (1971) studied, and he suggested that in both *Thrinaxodon* and *Galesaurus*, the axis blade was straight or even possibly convex. However, this differs from Brink's (1954) findings on *Thrinaxodon* as well as the present study on *Galesaurus* where the blade was found to be concave. The neural spines of NMQR 3678 and SAM-PK-K10465 differ from that of gracile RC 845, which is more rounded than the former two. A fossa representing the origin of an unknown muscle is present above the base of the prezygapophyses and another lies almost in the centre of the blade surface on either side of the neural spine (Jenkins, 1971).

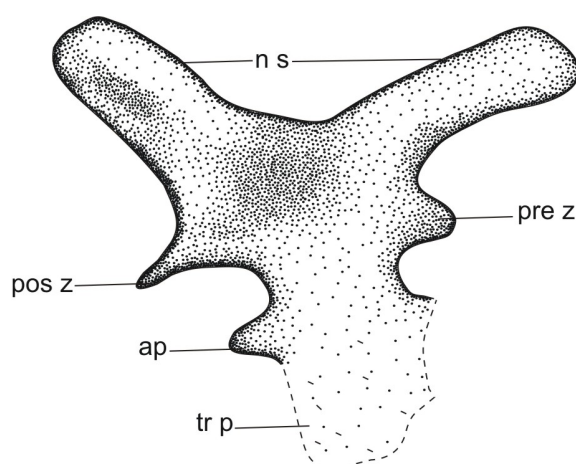


Figure 20. The axis of *Galesaurus planiceps*, NMQR 3678, in lateral view. Scale bar represents 1 cm. Abbreviations: **ap**, anapophysis; **n s**, neural spine; **pos z**, postzygapophysis; **pre z**, prezygapophysis; **tr p**, transverse process. Dashed lines represent uncertain edges.

The right transverse process of the axis (SAM-PK-K10465) is rectangular and robust, with a lateral and somewhat posteroventrally oriented projection. The transverse process is slightly more horizontally oriented than the rest of the cervical vertebrae. Jenkins (1971) noted an oval articulation facet for the tuberculum of the axial rib on the ends of the transverse process.

Jenkins (1971) did not have access to the anterior face of the axis, but speculated that the centrum was probably amphicoelous, similar to all the postaxial cynodont cervical vertebrae. The axis centrum is not accessible in any of the available specimens in this study and is thus described from the literature. Anteroposteriorly, the lateral sides of the axis centrum are concave and meet along the midline to form a keel (Jenkins, 1971). There are nutrient foramina on the lateral sides of the centra. The dorsal part of the centrum has three angled surfaces, namely two dorsolateral ones that join with the neural arch and a third between the two to form a groove in the floor of the neural canal. In the centre of this canal is a fossa of unknown function (Jenkins, 1971). The axial neural arch meets the centrum along almost its entire length, but not posteriorly where the centrum rim is continuous along the whole articular surface. The anterior quarter of the neural arch extends beyond the anterior part of the centrum and articulates at an angle with the posterior corners of the atlas centrum. Jenkins (1971) suggested that these articulations were formed from cartilage. The articulations between the axis and atlas centrum, and the axis neural arch are fused. The prezygapophysis (pre z) is notably thin and terminates in a blunt point in both *Galesaurus* and *Thrinaxodon* (Jenkins, 1971). This size reduction of the axis prezygapophyses is thought to have improved the flexibility of the atlanto-axial rotation and therefore agrees with the findings of Kemp (1969). In contrast, the postzygapophyses (post z) are robust and the ventrolaterally oriented facet has an incline of approximately 45°. The anapophysis (ap) is situated below the postzygapophyses and is in line with the apex of the transverse processes (tr p) (Fig. 20).

The axial intercentrum is not accessible or preserved in the study specimens. The element is known from previously described articulated *Galesaurus* specimens, but due to their articulated position, the morphology of the articular surfaces is not known. Jenkins (1971) noted that the intercentrum of *Galesaurus* has a curved plate structure.

Remaining Cervicals

Jenkins (1971) noted that in both *Thrinaxodon* and *Galesaurus* the height of the neural spines of the fifth and sixth cervical vertebrae differ, whereas the seventh is slightly taller than any preceding spine. The cervical neural spines taper anteroposteriorly at the apex and are curved posteriorly whereas the spine of the third cervical is sharply curved, thus providing space for the posteriorly projecting axis blade. This indicates that the neck curved upwards to elevate the head above the level of the shoulder girdle (Kemp, 1969). Jenkins (1971) noted, and the present study confirmed, that the neural spines of the third, fourth and fifth cervicals in *Galesaurus* are fusiform (spindle-shaped) in cross-section and differ from the elliptical cross-section of the cervicals in *Thrinaxodon*. The posterior edge of the neural spine of the seventh cervical in *Galesaurus* is swollen. The neural spines of the cervical vertebrae of *Galesaurus* BP/1/4506 are slightly more vertical and less curved compared to other study specimens.

The intercentra of the study specimens are not visible. Jenkins (1971) noted that the intercentra in *Thrinaxodon* were approximately one half the width of the adjacent pleurocentra. They are positioned between each of the first five cervical centra and possibly between the last cervical and first thoracic, but are absent caudally from the first thoracic vertebra.

The pleurocentra of the disarticulated *Galesaurus* specimen NMQR 3542 are circular in cross-section, prominently amphicoelous and somewhat constricted laterally and ventrally around the centre. The rib facets between the adjacent centra are clefts, and are formed by two adjacent facets on the dorsolateral edge of each centrum rim. The neural arch forms a protruding lip, which overhangs each centrum rim. Notches on the anterior and posterior surfaces are present for articulation with the respective indentations of the neural arch. The notch on the anterior surface is more deeply incised than the posterior notch. Jenkins (1971) suggested that these notches may have functioned to inhibit the dorsal displacement of two successive vertebrae. The intervertebral foramen is bordered dorsally by a posteriorly directed anapophysis received by a lateral depression of the next posterior neural arch. Anapophyses, as

seen in the articulated specimens NMQR 3678, SAM-PK-K10465, and BP/1/4506, arise ventrolaterally to the postzygapophyses and form extended, blunt protrusions. These anapophyses are smoothly convex laterally to fit the lateral depression of the next neural arch. Jenkins (1971) found that the anapophyses are absent on the atlas, but from the axis, they progressively increase in size and agrees with the findings in this study. Stout transverse processes (tr p), extend from the neural arch and are directed posterolaterally and ventrally on the axis and all remaining cervical vertebrae of SAM-PK-K10465. The transverse process of the seventh cervical vertebra is slender and projects laterally and anterolaterally on the first thoracic vertebra. Jenkins (1971) noted that the axial tuberculum facet is elongated and oval in shape but, posteriorly on the cervicals, the tuberculum facet shortens with the long axis becoming more vertically oriented. The capitulum facet is almost cylindrical and has a small ventral projection onto the anteroventral corner of the seventh cervical vertebra. This projection becomes progressively more developed in the thoracic series until the tuberculum and capitulum facets become continuous and form synapophyses.

The very slight ridge Jenkins (1971) described in *Thrinaxodon* that runs anteroposteriorly across the dorsal surface of the laminae of the third to seventh cervical vertebrae was not observed in the specimens in this study, but the possibility that this is due to incomplete preservation cannot be ruled out.

Jenkins (1971) noted that the cervical intercentra of at least three cynodont genera namely *Galesaurus* (although not visible in this study), *Thrinaxodon* and *Cynognathus* were retained. The intercentra in early tetrapods allowed the vertebral column to be more flexible by forming an additional centrum with the pleurocentrum across two body segments, thus allowing the vertebral column to bend and the neck region to be more flexible (Parrington, 1967, 1977).

Thoracic

Thirteen thoracic vertebrae are present in *Galesaurus*. The neural spines of the thoracic vertebrae do not taper to the apex as they do in the cervicals (Parrington, 1934). The thoracic series are distinguished from the cervical series by their low anteroposteriorly wide neural spines that are almost triangular in cross-section (SAM-PK-K10465; BP/1/4506; NMQR 3678) which may have provided a larger surface area for muscle attachment.

Jenkins (1971) described the thoracic acid prepared vertebrae in *Galesaurus* SAM-PK-K1119 and this specimen was re-examined in the present study. The tuberculum facet on the transverse process usually faces laterally. Anteriorly, the capitular fovea is formed by two separate demifacets on adjacent rims of successive thoracics. Thus the wedge-shaped fovea is located on the dorsolateral edge of the rim below the neurocentral suture. On the base of the neural arch, projecting anteriorly past the rim of the centrum, a caudal demifacet is partially formed. As the demifacet becomes larger in the more posterior thoracics, it forces the fovea to a more caudal position. The facet becomes less crescentic and more fusiform posteriorly as the size of the anterior capitular demifacet increases and the facets for the tuberculum and capitulum almost merge (Jenkins, 1971).

An anteroventral extension of the transverse process almost reaches the neurocentral suture and a posteroventral extension reaches the base of the anapophysis. In all the study specimens, a pronounced neurocentral suture on all the vertebrae is distinct, even in the largest specimen NMQR 3542.

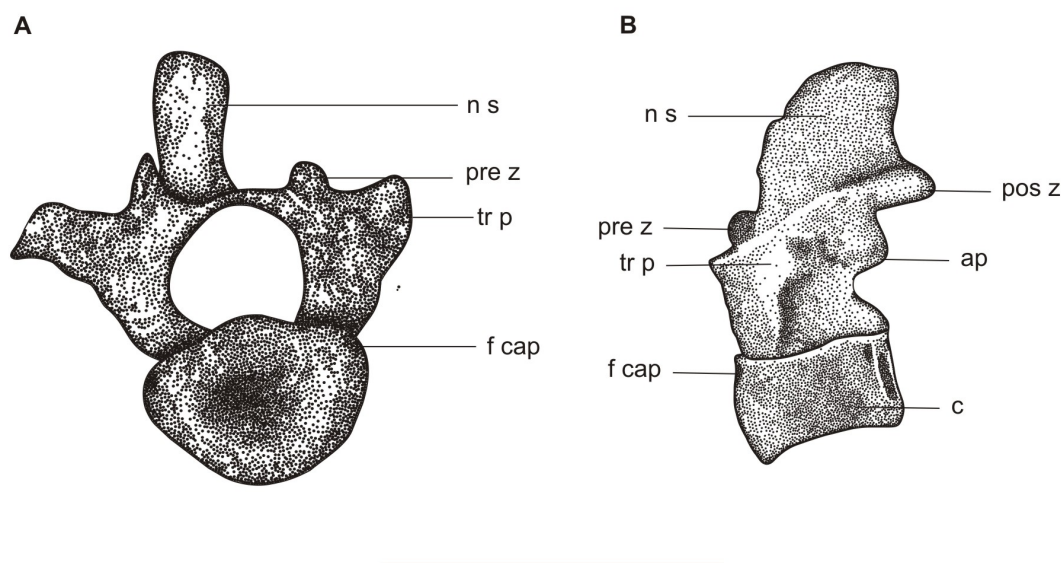


Figure 21. Thoracic vertebra of *Galesaurus planiceps*, SAM-PK-K1119, in A) anterior and B) lateral view. Scale bar represents 1 cm. Abbreviations: **ap**, anapophysis; **c**, centrum; **n s**, neural spine; **pre z**, prezygapophysis; **pos z**, postzygapophysis; **f cap**, facet for the capitulum; **tr p**, transverse process.

Jenkins (1971) noted that the anterior thoracic neural spines are the highest and decrease in height posteriorly and this condition was also found in this study (SAM-PK-K10465; NMQR 3678). This is in contrast to *Thrinaxodon*, where this kind of differentiation is absent (Jenkins, 1971). In both *Galesaurus* and *Thrinaxodon* each neural spine base is wider anteriorly in the series. The transverse processes (tr p) in both taxa are also directed laterally and slightly anteriorly. When viewed from above there is a progressive increase in the series in their anteroposterior breadth (Jenkins, 1971). Anteriorly, each transverse process is crescentic in cross-section. The transverse processes of the thoracic vertebrae of NMQR 3542 are twice as wide as their centra and are thus notably longer than any of those in *Thrinaxodon*, where the centra and transverse process are similar in width.

The articulation facets of the prezygapophyses (pre z) are cuplike (U-form) depressions (Fig. 21), and consist of a nearly vertical wall laterally and a horizontal wall medially (Jenkins, 1971). A horizontally oriented ridge, which is an anterior continuation of the

neural spine, separates the horizontal sectors medially. A portion of the articular facet is recessed within the neural lamina.

Posteriorly, the postzygapophyses (pos z) are distinct processes protruding from the base of the neural spine and are separated by a groove, which receives the anterior basal part of the spine of the following vertebra. The postzygapophyses extend past the rim of the centrum and articulate with the prezygapophyses. As in *Thrinaxodon*, the vertical aspect of the zygapophyseal facets changes posteriorly towards a more horizontal plane (Jenkins, 1971). Anteroposteriorly, there is an increase in the length in the laminae as measured between the tips of the zygapophyses.

Lumbar

Galesaurus has seven lumbar vertebrae. The first lumbar vertebra is the first dorsal vertebra that lacks a rib shaft distal to the costal plate of its associated rib. The lumbar transverse processes are anteroposteriorly broader and dorsoventrally deeper than in the thoracic series (Jenkins, 1971). Posteriorly, the centra of the lumbar vertebrae become increasingly wider. Anteriorly, the neural spines of the lumbar vertebrae are relatively thin, but each spine progressively broadens anteroposteriorly. Posteriorly, the neural spines are robust and more triangular than the thoracic series in dorsal view. The transverse processes of the lumbar vertebrae are directed posterolaterally and ventrally.

Sacral

The most prominent characteristic of the five sacral vertebrae in *Galesaurus* is the contact of ribs with the medial surface of the iliac blade. Jenkins (1971) noted that the articulation of the zygapophyseal facets is almost parallel to the parasagittal plane and that the zygapophyses and anapophyses are smaller than those of the lumbar vertebrae. Posterior to the first sacral vertebra, the transverse processes become progressively slender (RC 845). The neural spines of the sacral vertebrae, project further posteriorly than those of the lumbar series. The apex of each neural spine is more oval compared to the almost triangular form of those in the lumbar series.

Caudal

The 25 caudal vertebrae have been preserved in *Galesaurus* specimen SAM-PK-K10465. The terminal caudal vertebrae have been dislodged from their normal positions and are more poorly preserved than the rest of the skeleton and are therefore difficult to count. However, the caudal count of SAM-PK-K10465 is 25 (six attached to the skeleton and two detached articulated portions each containing eight and 11 vertebrae respectively), which differs from the 15 suggested by Broom (1932a) and Brink (1954). Transverse processes and ribs are present in the anterior six caudal vertebrae, but are absent in the posterior 19 vertebrae (SAM-PK-K10465). Not all the caudal vertebrae are preserved in BP/1/4506 as only 21 remain. The total caudal count for *Galesaurus* is thus 25.

As in *Thrinaxodon*, the anapophyses of the caudal vertebrae in *Galesaurus* are smaller than in the sacral and presacral series (Jenkins, 1971). The caudal vertebrae diminish in length and height posteriorly, and they are anteroposteriorly narrower and dorsoventrally shallower than those of the sacral and presacral vertebrae. Posteriorly, the neural spines are triangular in shape as seen in dorsal view and progressively decrease in length along the series. A characteristic of the caudal vertebrae is the short, robust transverse processes, which are directed laterally.

4.2.2 Ribs

Cynodonts possess ribs throughout the whole vertebral series i.e. cervical (including the atlas and axis), thoracic, lumbar, sacral and caudal. A unique feature of many cynodonts is the characteristic expansion of some of the rib shafts to form costal plates. These costal plates vary structurally in different vertebral regions and also among different cynodont families. Expanded costal plates are present in *Thrinaxodon* and *Galesaurus*.

Atlantal and Axial

Traditionally, the atlantal ribs were believed to be absent in cynodonts, but in 1934 Parrington described a *Galesaurus* rib associated with one of the first two cervical vertebrae, possibly the atlantal rib. The atlantal ribs in SAM-PK-K10465 and NMQR

3678 are relatively thin and spatulate at the proximal ends. The rib is shorter than the rest in the cervical series. Due to the articulated state and lack of preparation of the axial skeleton, the atlantal rib is described from the literature. Jenkins (1971) described the atlantal rib as thin and spatulate at the proximal end. The tuberculum process is short and rectangular in outline whereas the facet on the tuberculum is constricted in the middle and thus has an hourglass shape (Jenkins, 1971). The facet on the atlas transverse process is similar in outline, but slightly larger than the tuberculum facet, which may be attributed to the presence of cartilage or connective tissues during life. Ventral to the tuberculum is a small tubercle representing the capitulum. The diameter of the capitulum is almost half that of its parapophyseal facet on the atlantal intercentrum. The difference in size may be due to the presence of cartilage or connective tissues during life. The shape of the rib shaft is slightly medially concave and laterally convex (Jenkins, 1971).

Cervical

The anterior cervical ribs in *Galesaurus* (SAM-PK-K10465) are smaller and shorter than the posterior ones. In lateral view the cervical rib terminates proximally in a thin triangular plate. Jenkins (1971) noted that in *Thrinaxodon* the apex of the triangle represents the diverging tuberculum and capitulum, which are not separated as distinct processes and are continuous with the rib shaft. The cervical ribs are directed posterolaterally and ventrally (NMQR 3678).

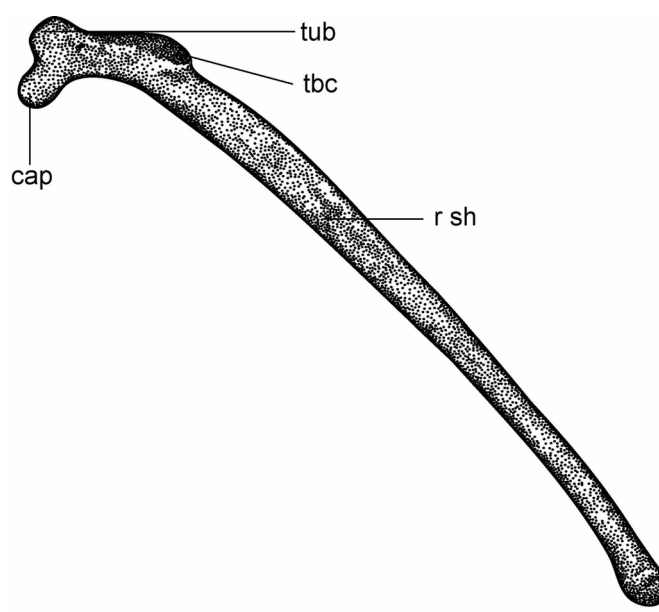


Figure 22. Posterior cervical rib of *Galesaurus planiceps*, NMQR 3542, in lateral view. Scale bar represents 1 cm. Abbreviations: **cap**, capitulum; **r sh**, rib shaft; **tbc**, costal tuberculum; **tub**, tuberculum.

In SAM-PK-K10465, the tuberculum (**tub**) of both the cervical and thoracic ribs is robust and continues with the distal shaft of the rib (**r sh**). Anteriorly, the capitulum (**cap**) and the tuberculum (**tub**) lie close together, with the capitulum lying ventral and somewhat anterior to the tuberculum (Fig. 22). The tuberculum is oriented medioventrally and slightly anteriorly. This orientation is comparable to that of the thoracic ribs (Jenkins, 1971). The cervical ribs are oriented mediolaterally and become progressively longer, tapering distally.

Thoracic

In SAM-PK-K10465, the rib shaft of the first 12 thoracic ribs is continuous between the capitulum and distal costal shafts via a distinct ventral ridge of the costal plate. In the anterior thoracic ribs, the thin blade-like edge of the tubercular process is laterally confluent with the rising dorsal edge of the costal plate. Differentiation of the costal plates occurs at the fourth thoracic rib whereas the development of a costal tubercle (**tbc**) becomes increasingly larger in the posterior thoracic (Fig. 23) and lumbar series. Posterior to the sixth thoracic rib, the costal tubercle is represented by a swelling on the dorsomedial edge of the costal plate, and the dorsal edge of all the tubercular

processes between the transverse process and the costal tubercle becomes anteroposteriorly broader and transversely wider. The costal plate (p) of the anterior thoracic rib is an almost vertical bone flange that descends from the dorsal edge of the rib shaft. The costal plates with the largest surfaces are those of the 11th to 13th thoracic ribs. The external surface of the anterior thoracic plate faces anterolaterally and is superficially concave. The posterior half of the costal plate expands posteriorly and lies on the anterior half of the next plate posteriorly (Jenkins, 1971).

Both *Galesaurus* and *Thrinaxodon* have expanded ribs in the thoracic and lumbar regions, although the details along the thorax differ. The thoracic rib expansion in *Galesaurus* is proximally wider than long (width 1.5X length) and consists of a small, pronounced anteriorly oriented protrusion and prominent posteriorly projecting flange. In *Thrinaxodon*, the thoracic rib expansion is proximally longer than wide (width 0.7X length) and consists of a less prominent posteriorly projecting flange and the anterior protrusion is absent.

According to Jenkins (1971), a characteristic of *Galesaurus*, and probably also *Thrinaxodon*, is that the ribs posterior to the fifth thoracic vertebra, including all lumbar and sacral ribs have an anteroposteriorly oriented groove across the dorsal edge of the tubercular process. Anteriorly, the groove is shallow, but it widens progressively as the tubercular processes become larger from the thoracic to the lumbar series. This groove is absent in the study specimens, but the possibility that this is due to poor preservation cannot be ruled out.

The capitular facet of a *Galesaurus* (SAM-PK-K1119) thoracic rib is tiny, rounded, and slightly convex, similar to the description of Jenkins (1971). The tubercular facet is a little narrower than the capitular facet and is straight, thin and extends from the transverse process almost to the capitular facet. The dorsal half of the capitular facet is flat and the ventral half is slightly concave. The orientation of the capitular facet varies depending on the ossification of the bone (Jenkins, 1971). Due to their articulated state and lack of preparation of the thoracic ribs of the study specimens, the rib morphology will be described from the description of Jenkins and specimen SAM-PK-K1119. The

transverse processes and the tuberculi of the thoracic vertebrae progressively broaden anteroposteriorly. Jenkins (1971) noted that the tuberculum and associated capitulum are separated by a thin, almost ventrally oriented bone lamina. In the anterior thoracic ribs, these laminae are flat, but become increasingly concave after the seventh thoracic rib.

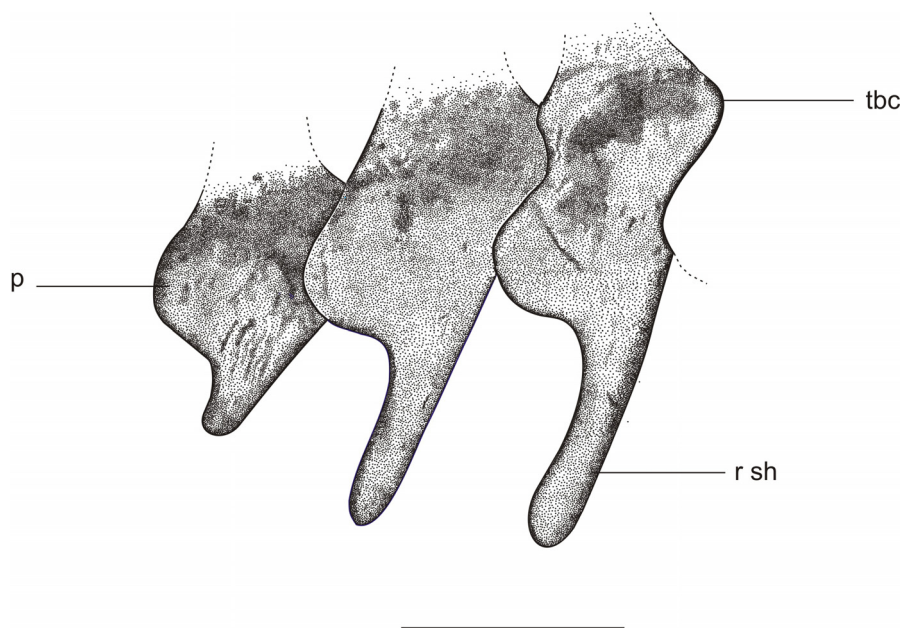


Figure 23. Three articulated posterior thoracic ribs of *Galesaurus planiceps*, SAM-PK-K10465, in lateral view. Scale bar represents 1 cm. Abbreviations: **p**, costal plate; **r sh**, rib shaft; **tbc**, costal tuberculum; dashed lines indicate the anterior portion of the rib and articulation with the following rib, which cannot be clearly distinguished due to preservation.

The anterior thoracic ribs have a gentle lateral curve and thus project more laterally (SAM-PK-K10465) than the cervical ribs. The anterior, thoracic ribs are relatively short, but they increase in length posteriorly with the fifth to eighth being the longest. The posterior portion of each rib is slender and projects posterolaterally. Anteriorly, the thoracic rib shaft comprises more than three-quarters of the rib length. The fourth thoracic rib has a prominent ridge on its proximodorsal surface and the shaft comprises a little more than half the rib length. On the right side of SAM-PK-K10465, the sixth rib is broken just distally to the costal plate. The seventh rib is absent. On the left side of the

skeleton, the sixth and seventh thoracic ribs are not preserved. The posterior six thoracic ribs have the characteristically expanded costal plates. The ribs are straighter and project slightly more laterally. The length of the ribs progressively shortens until the last thoracic rib is merely a spike.

Various authors (Brink, 1954, 1956, 1958; and Kemp, 1980) have suggested that this change in rib morphology from the eighth to the 13th thoracic rib indicates the presence of a mammal-like diaphragm, which bounds the pleural cavity to rib 13, and is thus involved with breathing.

Lumbar

Differences between the thoracic and lumbar rib morphology appear gradually, but the morphology of the posterior thoracic ribs differs from that of the posterior lumbar rib series. The lumbar ribs are fused to the transverse processes along a jagged sutures (Jenkins, 1971). In ventral view, lumbar ribs have an almost spatulate outline, is more robust anteriorly than posteriorly and is more laterally oriented than the thoracic.

In *Thrinaxodon*, adjacent centra share the connection of the first four lumbar ribs with the first four lumbar vertebrae, but posteriorly, Jenkins (1971) described the location of the ribs as being on each individual centrum. Ventrally, the following features exists in the articulated specimen RC 845: the connection of the slender first lumbar rib is shared by the 13th thoracic vertebra and the first lumbar; the second rib is present on the second lumbar vertebra; the third rib is present on the third lumbar vertebra; the fourth rib is shared by lumbar vertebrae four and five; the fifth is shared by lumbar vertebrae five and six; the sixth rib is absent; and the stout seventh lumbar rib is shared by lumbar vertebrae six and seven. Jenkins (1971) noted that the lumbar capitular articulation in *Thrinaxodon* shifts posteriorly up to the sixth lumbar vertebra, where the articulation is no longer intervertebral. This is in contrast to *Galesaurus* where the posterior tuberculum articulation is intervertebral. The first lumbar rib capitular process forms a 90° angle with the vertebral column (Jenkins, 1971). The capitular processes become increasingly shorter posteriorly towards the sacrum and they shift dorsally towards the broad tuberculi.

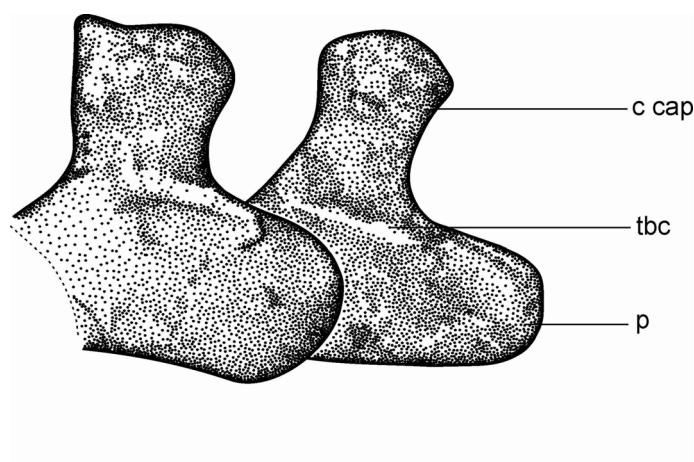


Figure 24. The first two anterior lumbar ribs of *Galesaurus planiceps*, RC 845, in lateral view. Scale bar represents 1 cm. Abbreviations: **c cap**, costal capitulum; **p**, costal plate; **tbc**, costal tuberculum. Dashed lines represent uncertain edges.

The lumbar ribs of both *Galesaurus* and *Thrinaxodon* are expanded. The lumbar ribs of *Galesaurus* are distally expanded, anteroposteriorly wider than long and oval in lateral view (Fig. 24). The lumbar ribs of *Thrinaxodon* are also distally expanded, are proximodistally wider than long and square in lateral view.

In *Galesaurus* the costal plates of the lumbar ribs become gradually less rectangular and the costal tubercle becomes anteroposteriorly longer and narrower. These tuberosities form a wavy bony bridge, which is parasagittally aligned with the iliac blade. Anteriorly, the costal plates are more expanded than posteriorly, and become progressively narrower (RC 845). The lumbar costal plates are a little shorter medially than laterally (NMQR 3542) and the medial surface projects posteriorly over the concave lateral surface of the posterior plate. This is in contrast to the anteriorly concave and medially convex costal plates that Jenkins (1971) described.

Sacral

The first sacral rib is the largest and its costal plate has a forked appearance (RC 845; SAM-PK-K10465; and NMQR 3678). The capitular and tubercular processes are fused and indistinguishable from one another (Jenkins, 1971). Jenkins (1971) found that in

Thrinaxodon the dorsal and ventral surfaces of the first sacral forked plate clasp the seventh lumbar plate. The larger ventral surface of the forked costal plate extends anteriorly and overlaps the lower medial surface whereas the dorsal portion overlaps the upper medial surface. The rest of the first sacral rib, posterior to the split of the fork, contacts the medial surface of the ilium and forms a bridge between the seventh lumbar vertebra and the pelvis (Jenkins, 1971). This does not appear to be the case in *Galesaurus*. The forked first sacral rib does not clasp the last lumbar vertebra dorsally; neither does it form a bridge between the pelvis and the last lumbar vertebra. The second to fifth ribs have a slightly expanded iliac contact. The sacral ribs decrease in size posteriorly, with the fifth rib being almost rectangular in shape (SAM-PK-K10465 and RC 845). The first four sacral ribs are directed laterally and their distal ends are slightly elongated anteroposteriorly.

In general the second to fourth sacral ribs are oriented laterally with their distal ends dorsoventrally flattened and anteroposteriorly elongated. The fifth sacral rib is roughly triangular in shape. Ventrally, the necks of the sacral ribs are slightly shorter than that of the lumbar ribs. The costal plates of the sacral ribs are narrower than those of the lumbar ribs (RC 845).

Caudal

The costal plates of the first four caudal ribs are relatively stout and have a forked appearance. Thereafter, the ribs are almost rectangular in shape but they vary in size. The caudal ribs are progressively smaller than the sacral and presacral ribs. The caudal vertebrae are in articulation and thus it is difficult to describe them in detail. Descriptions of the caudal ribs are therefore supplemented from the literature.

In SAM-PK-K10465, ribs are present on the anterior six caudal vertebrae and absent on the posterior 19. In BP/1/4506, the transverse processes of the last four caudal vertebrae are absent and they consist only of centra. Jenkins (1971) noted that the capitulum and tuberculum of the caudal ribs are fused and indistinguishable from one another. In all the study specimens the rib shaft is swollen where it contacts the transverse process on the first six caudal vertebrae. The ribs are posterolaterally and

somewhat ventrally oriented. Jenkins (1971) suggested that the first to fourth caudal ribs of *Galesaurus* may have been in contact with one another; but this is not the case in any of the *Galesaurus* specimens studied.

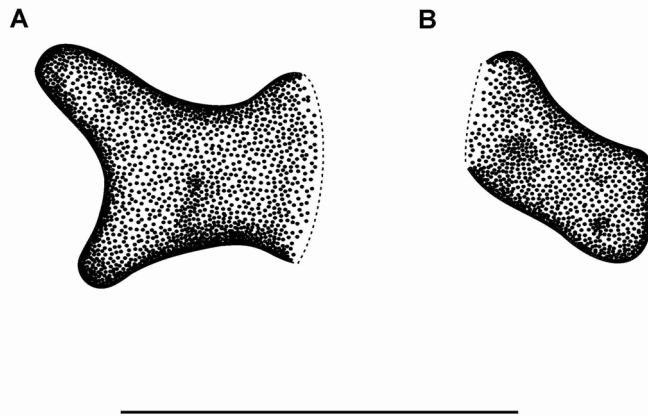


Figure 25. Caudal ribs of *Galesaurus planiceps*, RC 845, in lateral view A) the first right with forked distal end and B) fifth “rectangular” left caudal rib. Scale bar represents 1 cm. Dashed lines represent uncertain edges.

4.3 Appendicular Skeleton

4.3.1 Shoulder Girdle and Forelimb

Scapulocoracoid

The scapula of *Galesaurus* (Fig. 26) consists of a long, narrow blade that is bowed laterally and the dorsal border expands anteroposteriorly similar to that seen in *Thrinaxodon* (Jenkins, 1971). The scapula blade of the robust specimen NMQR 3542 (100% adult) is more expanded anteroposteriorly than that of the gracile specimen RC 845 (62% adult) and SAM-PK-K10465 (64% adult), as well as the *Thrinaxodon* specimens that Jenkins (1971) studied. The dorsal border of the scapula blade is nearly straight and has numerous striations (prominent in NMQR 3542) indicating the attachment of muscles. The anterior and posterior borders of the scapula blade are raised to form the supracoracoideus fossa (f spc) for the M. supracoracoideus (Jenkins, 1971). This fossa, deepest across the lateral section of the scapula blade, terminates as a narrow open groove (gr) ending on the supraglenoid buttress just anterior to the glenoid. Jenkins (1971) noted that the M. supracoracoideus would have extended across the scapula to insert on the greater tuberosity of the humerus, but it does not extend to the glenoid (g) ventrally.

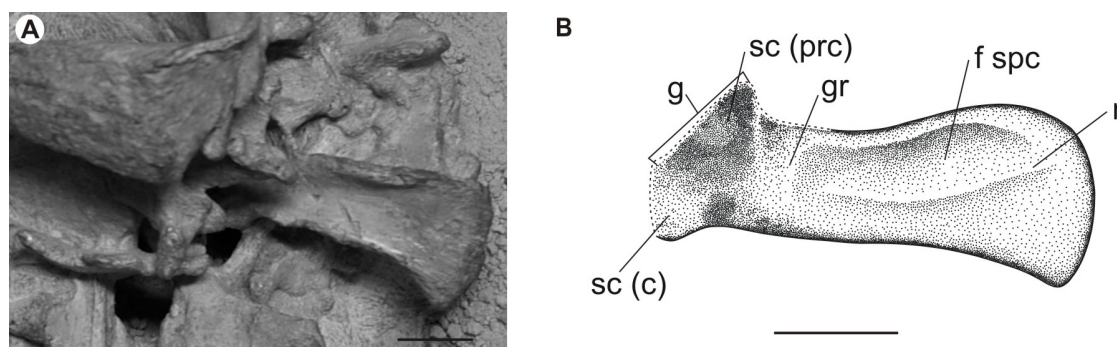


Figure 26. Left scapula of *Galesaurus planiceps*, in lateral view, A) photograph of specimen NMQR 3542 without lateral bony ridge and B) specimen RC 845, showing the lateral bony ridge. Scale bars represents 1 cm. Abbreviations: **f spc**, supracoracoideus fossa; **g**, glenoid; **gr**, groove marking ventral termination of supracoracoideus fossa; **r**, ridge; **sc (c)**, scapula articular surface for the coracoid; **sc (prc)**, scapula articular surface for the procoracoid. Dashed lines represent uncertain edges.

As in *Thrinaxodon* (Jenkins, 1971), the anterior border of the scapula is a distinct ridge that extends to the glenoid, and then becomes a low ridge at its base. This anterior border of the scapula is a free projection of a relatively thin sheet of bone, which is directed anteriorly at the scapulo-procoracoid contact instead of laterally as it is at the proximal end.

The posterior border of the scapula show a division between the attachment areas of the M. subcoracoscapularis and M. scapula triceps medially and the M. supracoracoideus and M. teres minor laterally (Jenkins, 1971). A shallow posteriorly oriented groove is observed on the medial surface of the scapula next to the posterior border and presumably represents the origin of the M. scapula triceps. Jenkins (1971) noted that the anterior and posterior borders of the scapula are thicker than the rest of the scapula in *Thrinaxodon* and this feature is also seen in *Galesaurus*.

The scapula blade is slightly curved. In medial view it is dorsoventrally concave, but is flat just below the dorsal border. In two of the small *Galesaurus* specimens (RC 845, but less pronounced in SAM-PK-K10465) a prominent lateral bony ridge (r) extends dorsoventrally on the middle of the lateral surface of the scapula blade. This bony ridge terminates just anterior to the groove of the supracoracoideus fossa (Fig. 26). The ridge probably provided an additional muscle attachment surface.

The acromion process (acr) is visible in specimen NMQR 135 where a fragment containing the scapula base, coracoid and procoracoid is preserved (Fig. 27). A thickening is present on the averted edge of the scapula, which terminates in a small protrusion anteriorly. This protrusion/tuberosity is not merely a fold in the anterior edge of the bone as Broom (1932a) noted. Jenkins (1971) suggested that the acromion process was not developed in *Thrinaxodon*, because in well-preserved specimens the averted edge is very thin and appears to be complete. However, he did describe a local thickening of the bone edge that could represent the point of acromioclavicular articulation (Jenkins, 1971).

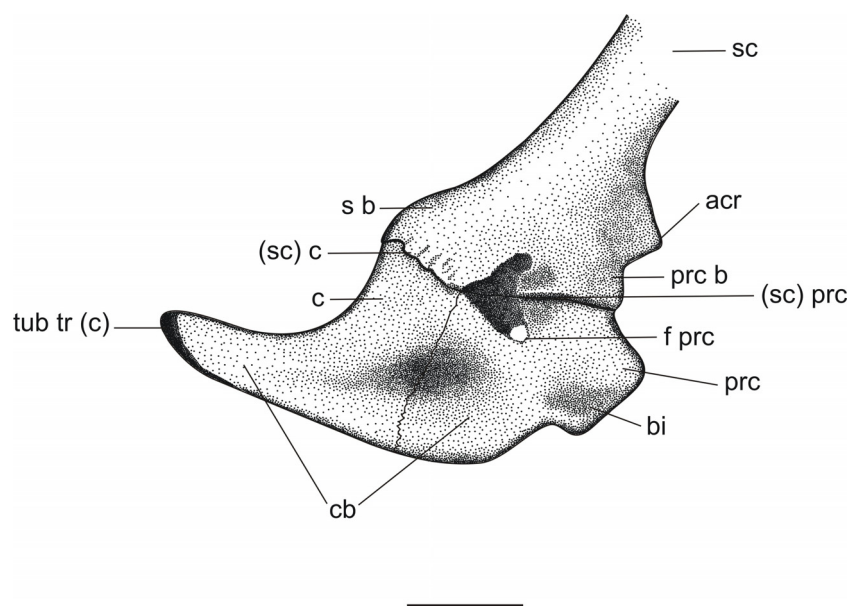


Figure 27. A reconstruction of the right scapulocoracoid of *Galesaurus planiceps*, in medial view. Reconstruction based on NMQR 3542 and NMQR 135. Scale bar represents 1 cm. Abbreviations: **acr**, acromion process; **bi**, fossa for the origin of the biceps muscle; **c**, coracoid; **cb**, fossa for the origin of coracobrachialis muscle; **f prc**, procoracoid foramen; **prc**, procoracoid; **prc b**, procoracoid buttress; **s b**, supraglenoid buttress; **sc**, scapula; **(sc) c**, scapula articular surface for the coracoid; **(sc) prc**, scapula articular surface for the procoracoid; **tub tr (c)**, tuberosity for the origin of the coracoid head of triceps muscle.

A linear depression is observed posterolaterally above the glenoid rim and adjacent to the anterior border of the scapula blade in the large specimen NMQR 3542 (100% adult) that may represent the *M. teres minor* attachment. Jenkins (1971) noticed this depression in larger specimens of *Diademodon* and *Cynognathus* where ossification was complete, but not in smaller specimens of these genera. This observation agrees with the findings here as the depression is present in the largest specimen known (NMQR 3542) but absent in gracile specimens.

In larger cynodonts, such as *Diademodon* and *Cynognathus*, Jenkins (1971) noticed a groove representing the origin of the *M. teres major* on the thickened dorsoposterior edge of the scapula. The medial wall of this groove expands posteriorly and serves as the origin of the serratus anterior musculature (Jenkins, 1971). This groove is also

present in the large specimen NMQR 3542, but is not observed in the poorly ossified smaller specimens. Specimen SAM-PK-K10468 (100% adult) is also notably robust, but both scapulae have been damaged in this area and thus, it cannot be determined if a groove was present. Although this groove has not been observed in *Thrinaxodon*, Jenkins (1971) believed that this was due to poor ossification.

The base of the scapula consists of a supraglenoid buttress (s b) that bears a semicircular articulation facet on the dorsal portion of the glenoid (Fig. 27), and a procoracoid buttress (prc b), both of which are located on the medial side of the scapula base. In *Galesaurus*, the procoracoid buttress meets the procoracoid, which is concave (NMQR 135 and NMQR 3542). This condition differs from *Thrinaxodon* where the contact is convex. As Jenkins (1971) noted in *Thrinaxodon*, the scapulocoracoid complex in *Galesaurus* has an uneven texture implying an extensive cartilaginous covering in life. The larger anterior procoracoid buttress (prc b) is partially separated from the smaller posterior supraglenoid buttress (s b) by a sulcus that leads into the procoracoid foramen (Fig. 27; prc) below, which probably accommodated a nerve. The sutural surface of the procoracoid buttress in *Galesaurus* is wider, straight and extends more posteroventrally (Figs. 26; 27; (sc) prc) than that in *Thrinaxodon* (Jenkins, 1971). However, the contact between the procoracoid buttress of the scapula and the dorsal border of the procoracoid is similar. The scapula surface of the glenoid is slightly convex in *Galesaurus*, and faces posterolaterally and ventrally as it does in *Thrinaxodon* (Jenkins, 1971).

As in *Thrinaxodon*, the triangular-shaped coracoid is fused to the procoracoid by a jagged, but fairly straight suture (Fig. 27) (Jenkins, 1971). The posterodorsal edge of the coracoid is a flat shelf and the ventral edge is thick and concave. This edge appears to be blunter than that in *Thrinaxodon*. The posterodorsal and ventral edges of the coracoid come together posteriorly to form a swollen tuberosity for the coracoid head of the M. triceps [tub tr(c)]. The ventral border of the procoracoid-coracoid complex of both *Galesaurus* and *Thrinaxodon* has a rugose texture indicating cartilaginous extensions (Jenkins, 1971).

Two fossae are present on the procoracoid-coracoid complex (Fig. 27). A depression on the coracoid appears where the posterior process begins to broaden and is deepest at the coracoid-procoracoid suture. It extends onto the lateral surface of the procoracoid and Jenkins (1971) suggested that it served as the origin of the coracobrachialis muscle (cb). A second oval fossa on the lateral surface of the procoracoid is oriented ventrally and represents the origin of the M. biceps (bi). In the robust specimen NMQR 3542, a ventral rim is present and separates the latter fossa from the M. coracobrachialis origin, whereas a more anteroventrally oriented edge separates the M. biceps origin from the remaining lateral surface of the procoracoid from where the M. supracoracoideus arises. These rims are not observed in the gracile specimens.

As in other cynodonts, the procoracoid in *Galesaurus* is large. A big foramen (f prc), oriented slightly posterodorsally, is present on the procoracoid for the transmission of the M. supracoracoideus and blood vessels (Jenkins, 1971). The thickest part of the procoracoid plate is where the scapula, coracoid and procoracoid contact to form the glenoid and from here the plate becomes thinner anteriorly.

Clavicle

In the clavicle of *Thrinaxodon*, described by Jenkins (1971), the lateral third is a slender rod, which is directed dorsally as well as laterally. The medial long axis constitutes two-thirds of the clavicle and meets the lateral third at an angle of approximately 145°. The long axis consists of a progressively expanding, spatulate plate directed medially and horizontally. In contrast, the clavicle of *Galesaurus* (SAM-PK-K10468) is a large relatively stout element (Fig. 28). It is slightly flattened and directed in a horizontal plane. The medial half of the clavicle consists of a slim rod, which gradually expands proximally to form an expanded spoon-like plate. The rod ends abruptly, curves distally and terminates at the articulation facet for the acromion (con acr). The articulation facet is a small concavity on the distal end of the clavicle that opens ventrally. The broad flange, present on the lateral third of the clavicle in *Thrinaxodon* (Jenkins, 1971), is absent in *Galesaurus*. The proximal spoon-like plate has numerous striations (st) on the dorsal surface, which extend parallel to the longitudinal axis of the clavicle. These

striations probably represent the attachments of ligamentous or connective tissue which connected the clavicle to the interclavicle during life (Jenkins, 1971).

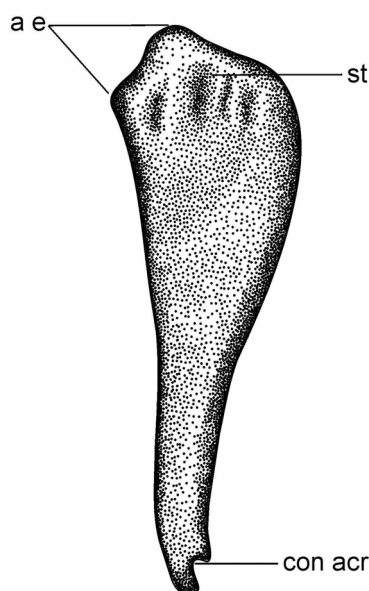


Figure 28. The left clavicle of *Galesaurus planiceps*, SAM-PK-K10468, in dorsal view. Scale bar represents 1 cm. Abbreviations: **ae**, anterior edge of the medial half of the clavicle; **con arc**, concavity for the reception of the acromion process; **st**, striations possibly indicating ligamentous or other connective tissue binding the interclavicle to the clavicle in life.

In the robust specimen NMQR 3542 the proximal clavicle plate lies almost in a horizontal plane with two small, but prominent, tuberosities on either side. In specimen SAM-PK-K10468 the flat appearance of the clavicle does not appear to be due to compression by the surrounding sediments because it would also have affected the rest of the specimen (the manus and skull which is in immediate proximity to the clavicles). This is not the case and thus, the flatness of the clavicle appears to be natural.

Parrington (1934) described the skull and postcranial material of *Galesaurus*, but some of the postcranial material was not positively identified as that of *Galesaurus*, because the skull was absent. He briefly described the clavicle, but this description does not

agree with the clavicle described here and appears to be more similar to that of *Thrinaxodon*.

Interclavicle

The interclavicle of *Galesaurus* is essentially the same as that of *Thrinaxodon* described by Jenkins (1971). The interclavicle is observed in ventral view SAM-PK-K10468 and the best preserved, RC 845 (Fig. 29). The interclavicle is a cruciate bone with a long posterior ramus. Four ridges extend from an anterior medial tuberosity; two pass laterally (l r), one anteriorly (a p) and the longer ridge extends posteriorly (p p).

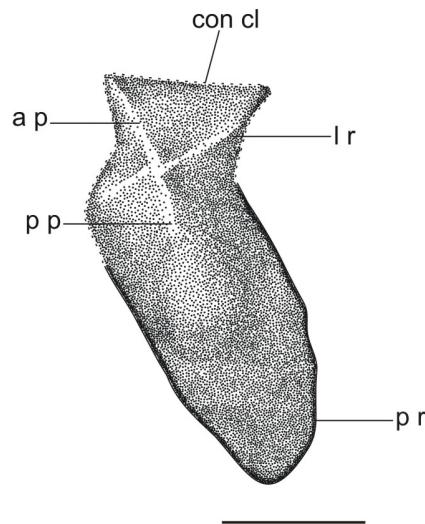


Figure 29. Interclavicle of *Galesaurus planiceps*, RC 845, in ventral view. Scale bar represents 1 cm. Abbreviations: **a p**, anterior ridge, possibly for the origin of parts of the pectoralis musculature; **con cl**, concavity for articulation of medial end of clavicle; **l r**, lateral ridge, delineating posterior border of concavity for the medial end of the clavicle; **p p**, posterior ridge, possibly for the origin of portions of the pectoralis musculature; **p r**, posterior ramus. Dashed lines represent uncertain edges.

The lateral and anterior ridges create a bilateral, triangular striated depression for the reception of the medial ends of the clavicles (con cl), indicating the connection of the clavicle and interclavicle by cartilaginous or ligamentous connective tissue in life. The anterior ridge (a p) consists of a thin bony lamina with vertical sides and divides the two triangular striated depressions. The posterior ridge (p p), which is probably the site of origin for the pectoral musculature, is clearly defined anteriorly and gradually fades

posteriorly. The long posterior ramus has fine striations indicating muscle attachment, and gradually narrows to form a thin oval-shaped distal end.

Humerus

The proximal end of the humeral head (h) in *Galesaurus* and *Thrinaxodon* has a smooth, convex shape whereas the articular surface has a rough texture, which can be attributed to the ends probably having been largely cartilaginous (Fig. 30A; B) (Jenkins, 1971). The articulation facet on the humeral head is strap-shaped and in both *Galesaurus* and *Thrinaxodon*, the lesser tuberosity (lt) is slightly thicker than the greater tuberosity (gt). A slight depression separates the greater from the lesser tuberosity and in the robust *Galesaurus* (NMQR 3542) a small protrusion is present adjacent to the slight depression, similar to that in *Thrinaxodon*. This protrusion is absent in the gracile specimens. The surface of the protrusion is rough and may have been a site for muscle attachment. The proximal edge of the humeral head is sharp and somewhat higher than the surface for the dorsal articulation facet, which slopes slightly ventrally. The articular surface is oriented dorsally and slightly anteromedially (Jenkins, 1971). As in *Thrinaxodon*, a dorsolateral lip raises the articulation facet above the dorsal surface of the shaft in *Galesaurus*.

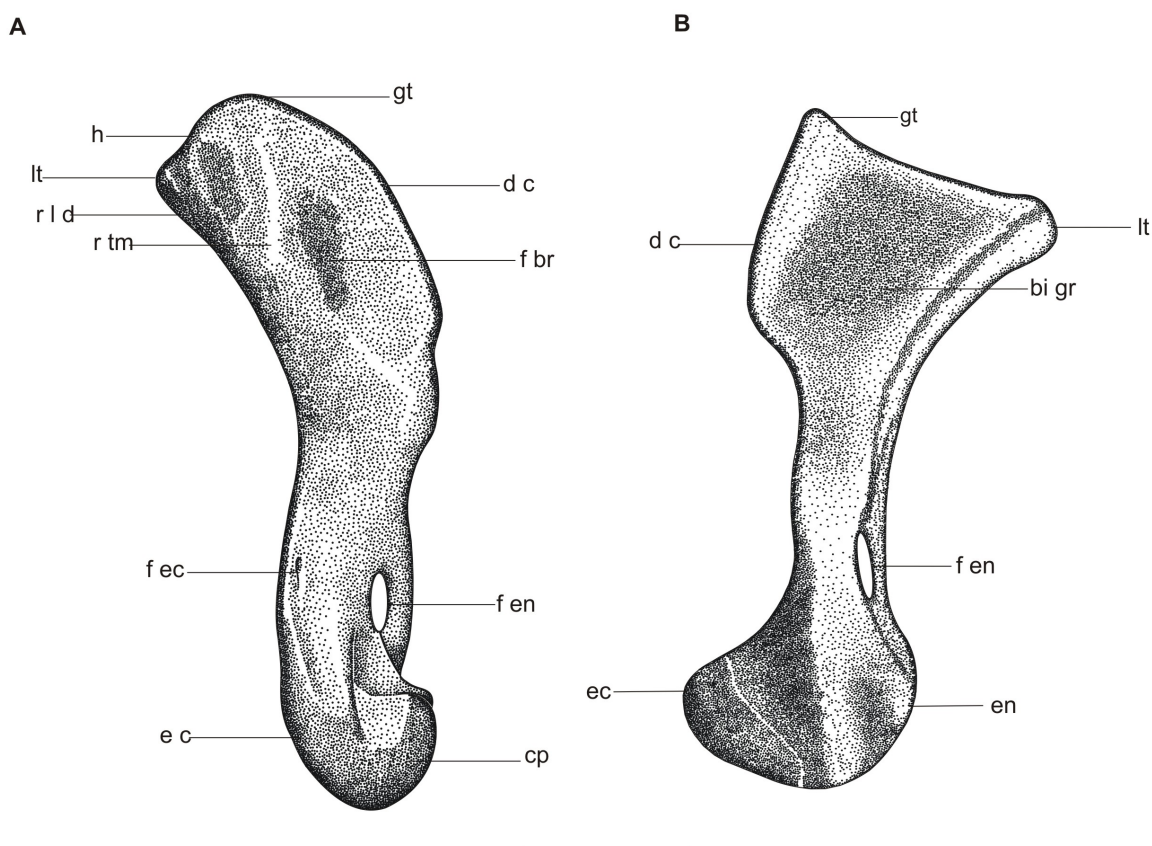


Figure 30. The right humerus of *Galesaurus planiceps*, A) NMQR 3542, in anterolateral view and B) SAM-PK-10468, in ventral view. Scale bar represents 1 cm. Abbreviations: **bi gr**, bicipital groove; **dc**, deltopectoral crest; **cp**, capitulum; **ec**, ectepicondyle; **en**, entepicondyle; **f br**, fossa probably related to *M. brachialis* origin; **f ec**, ectepicondylar foramen; **f en**, entepicondylar foramen; **gt**, greater tuberosity; **h**, head; **lt**, lesser tuberosity; **r l d**, ridge possibly representing the insertion of *M. latissimus dorsi*; **r tm**, ridge possibly representing the insertion of the *M. teres minor*.

On the highest proximal corner of the greater tuberosity a fairly thin, coarse ridge runs distally to thicken and form the deltopectoral crest (**dc**). As in *Thrinaxodon*, striations on the anterodistal margin of the deltopectoral crest probably indicate the *M. pectoralis* insertion (Jenkins, 1971). The deltopectoral crest constitutes approximately half the width of the proximal end and about one third the length of the humerus. The proximal half of the humerus can be divided into two planes (Fig. 30B), namely the deltopectoral crest and the adjoining shaft, which in ventral view, meet to form the broad bicipital groove (**bi gr**) (Jenkins, 1971). The proximolateral corner of the greater tuberosity is a distinctly broad, rounded surface that is more pronounced in *Galesaurus* than in

Thrinaxodon. The deltopectoral crest is an almost rectangular flange, which is thickest along its connection with the shaft, similar to *Thrinaxodon*. The deltopectoral crest terminates at a small tuberosity roughly midway along the shaft from where a low ridge runs posterodistally to bridge the entepicondylar foramen (Jenkins, 1971) (Fig. 30; f en). This robust bony ridge encloses the entepicondylar foramen, which is a distal extension of the deltopectoral flange. Striations on the ridge, dorsal and ventral to the entepicondylar foramen, probably represent muscle attachment for the M. pectoralis (Jenkins, 1971).

Striations, probably for the insertion of M. supracoracoideus, and a small terminal tuberosity are present on the deltopectoral crest (d c). A shallow, but broad fossa (f br) (Fig. 30A) is present on the anterolateral surface of the deltopectoral crest and probably indicates the origin of M. brachialis (Jenkins, 1971). A possible insertion for the M. teres minor is presented by a ridge (r tm) that separates the broad fossa from the humeral head. A second low and uneven ridge (r l d) extends across the dorsal surface of the humeral shaft and may have been the site for the insertion of the M. latissimus dorsi (Jenkins, 1971). In gracile *Galesaurus* specimens the above-mentioned ridges are not particularly obvious, but this may be due to poor ossification. The triangular distal end of the humerus of both *Galesaurus* and *Thrinaxodon* has an asymmetrical appearance due to the entepicondyle (en) being farther from the radio-ulnar process than the ectepicondyle (ec) (Jenkins, 1971). In *Galesaurus*, an oval entepicondylar (f en) and ectepicondylar (f ec) foramina are present. Each foramen inclines away from the shaft. The entepicondylar foramen is twice the size of the ectepicondylar foramen and is enclosed by a flange with a slightly swollen border, as seen in *Thrinaxodon* (Jenkins, 1971). The entepicondyle of *Galesaurus* is a heavy strap-shaped process with an uneven terminal border that indicates the possible presence of cartilage during life. It extends from the entepicondylar foramen to the trochlea. The ectepicondyle has a more rounded appearance compared to the entepicondyle. In contrast to *Thrinaxodon* (Jenkins, 1971), the ectepicondyle in *Galesaurus* (NMQR 3542) is notably thicker (35% thicker) than the entepicondyle. This condition differs from that in the gracile *Galesaurus* specimens, which instead agrees with the findings of Jenkins (1971) of a thicker entepicondyle than ectepicondyle.

Radius

As in *Thrinaxodon*, the radius is a simple cylindrical bone with expanded ends (Jenkins, 1971). The distal end is bowed slightly medially to assist with the passage of the radius over the anterior surface of the ulna (Fig. 31A; B). The proximal end is wider than the distal end and has a flat articulation surface (pr ar f), which is anteroposteriorly concave and slopes medially (Jenkins, 1971). The proximal end of the radius in specimen SAM-PK-K1119 (69% adult) is poorly ossified and only a shallow depression is present. Although ossification of the proximal end is poor, the outline and orientation of the articulation facet resembles that of larger cynodonts (Jenkins, 1971). Full ossification of the proximal end of the radius is observed in specimen NMQR 3542 (100% adult) and the facet is fully developed. Jenkins (1971) noted that in larger cynodonts, the proximal articulation facet is crescent shaped and this feature is also observed in the preserved radii of the robust *Galesaurus* specimen NMQR 3542.

A tuberosity with an articulation facet (fu) for the radial notch of the ulna is present posteromedially at the proximal end (Fig. 31B). A posterior ridge (r), visible only on the midshaft due to poor preservation of the posterior portion of the radius, passes from the ulna facet along the side of the shaft. Jenkins (1971) noted a prominent swelling on the shaft of larger cynodonts and this is also present in the preserved robust *Galesaurus* NMQR 3542. The swelling may represent a radial tuberosity for the insertion of the *M. biceps*. A vertically oriented fossa, medial to the radial tuberosity, may represent the insertion of a major antebrachial flexor muscle.

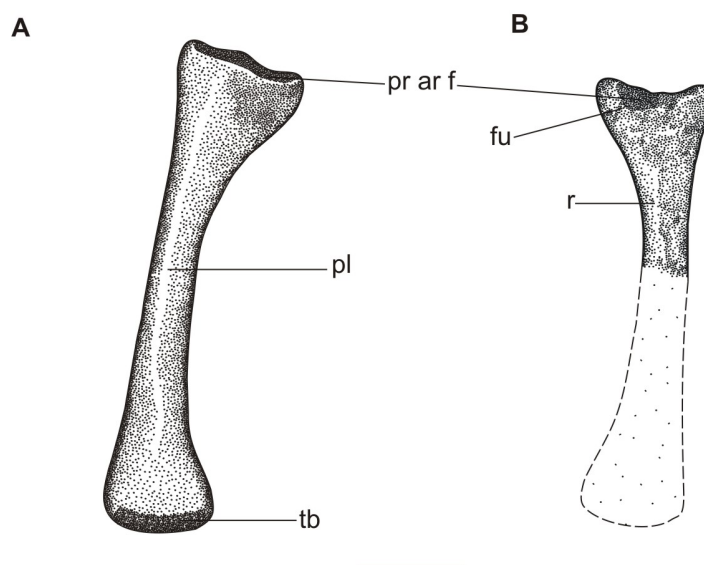


Figure 31. The left radius of *Galesaurus planiceps*, NMQR 3542, in A) lateral and B) posterior view. Scale bar represents 1 cm. Abbreviations: **fu**, facet for articulation with radial notch of ulna; **pl**, posterior lineation; **pr ar f**, proximal articular facet; **tb**, tuberosity for ulnar contact; **r**, ridge bearing a radial tuberosity. Dashed lines represent uncertain edges.

Ulna

The ulna is preserved in specimens SAM-PK-K10465, SAM-PK-K10468 and NMQR 3542. It is short and slender, but the presence of a high anteromedially oriented crest (*ul cr*) that extends down 90% of the entire shaft, results in the bone having a broad appearance in lateral view (Fig. 32). This crest is present in *Thrinaxodon* and was reported by Jenkins (1971). The ulnar crest probably served as an insertion for a radio-ulnar interosseous ligament Haines (1946; Jenkins 1971). The ulnar shaft is flattened medially and consists of a thin sheet of bone. The proximal end of the ulnar is slightly concave and the crest passes parallel to the shaft axis (Jenkins, 1971). The ulna shaft is also more distinct in *Thrinaxodon* in lateral view than it is in *Galesaurus*.

The crest widens just below the head of the ulna and then narrows again, approximately two-thirds down the bone shaft. *Galesaurus* SAM-PK-K1119 differs from this condition as the ulna crest ends almost at the base of the distal end, which Jenkins (1971) did not mention in his description. The preserved gracile SAM-PK-K10468 was not fully

prepared in this area and thus the length of the ulna crest cannot be confirmed. The distal end of the ulna slopes medially where it is slightly longer laterally than medially, allowing it to articulate with the ulnare. As in *Thrinaxodon* (Jenkins, 1971), the proximal end expands laterally and is wider than the distal end. Anteromedial ossification of the bone appears to be incomplete or cancellous (gracile specimens SAM-PK-K119; SAM-PK-K10465). An ossified olecranon is absent, whereas an osseous base from which a presumably cartilaginous olecranon process arose, is present (Jenkins, 1971). The proximal end has an oval facet (pr ar f) that slants slightly laterally towards the shaft axis anteriorly. As in *Thrinaxodon* (Jenkins, 1971), two articulation facets can be seen on the proximal end in lateral view; a spoon-shaped anterior fossa (f e), which suddenly attenuates distally and terminates between the middle and distal third of the ulna, and a smaller radial notch (rd nt) on the posterior surface. The posterior fossa is better developed than the radial notch.

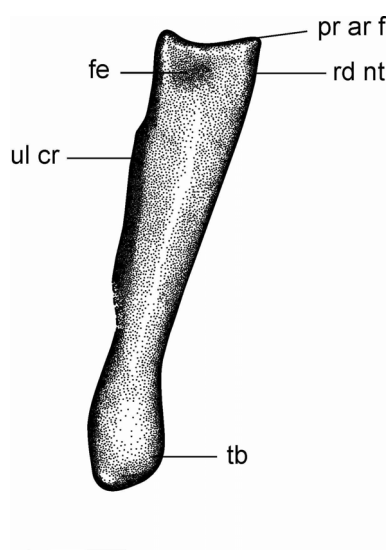


Figure 32. The left ulna of *Galesaurus planiceps*, SAM-PK-K10465, in lateral view. Scale bar represents 1 cm. Abbreviations: **fe**, fossa; **pr ar f**, proximal articulation facet; **rd nt**, radial notch; **tb**, tubercle possibly representing the attachment of an extensor muscle; **ul cr**, ulna crest. Dashed lines represent uncertain edges.

Manus

Previous descriptions of the cynodont manus are inadequate as only a few, incomplete specimens were studied. The degree of preparation was also insufficient, and thus information in the literature is limited.

There are ten bones in the carpus (Fig. 33A; B), including the pisiform (pi), in contrast to the suggested eleven in *Thrinaxodon* (Jenkins, 1971). The bones are arranged in three rows (SAM-PK-K10465). The proximal row includes the ulnare (ul), intermedium (i) and radiale (ra), the second row includes two centralia (C1 and C2) and, the third row contains four distal carpals (1-4). A well-developed pisiform (pi) lies adjacent and posterior to the ulnare. The radiale and ulnare are similar in size, but larger in comparison to the rest of the carpal bones.

The pisiform is relatively flat with a rounded posterior and a slightly pointed anterior edge, and it articulates with the ulnare.

The ulnare lies proximal of the ulna and is flat, stout (longer than wide) and almost rectangular in shape, as in *Thrinaxodon*. A dorsal facet in the centre of the ulnare is for articulation with the ulna. A small depression in the middle of the ulnare possibly served for the central positioning of the ulna on the ulnare. The ulnare is thicker on the lateral side and slopes gently towards the thinner medial side. This is in contrast to that seen in *Thrinaxodon* where the medial portion forms the thickest part of the bone (Jenkins, 1971). The dorsal surface of the ulnare is pitted and uneven, which is possibly due to poor ossification or fossilization. The ulnare articulates with the intermedium and medial centrale as well as with the fourth distal carpal (dc 4). The medial and distal articulation facets of the ulnare are almost vertical.

The intermedium is a small, roughly quadrangular bone and lies between the radius and ulna, articulating with the ulnare, the medial centrale (C2), and at its distal corner with the radiale. Its lateral side is convex and articulates with the ulnare, whereas its medial side is concave (Fig. 33A; B).

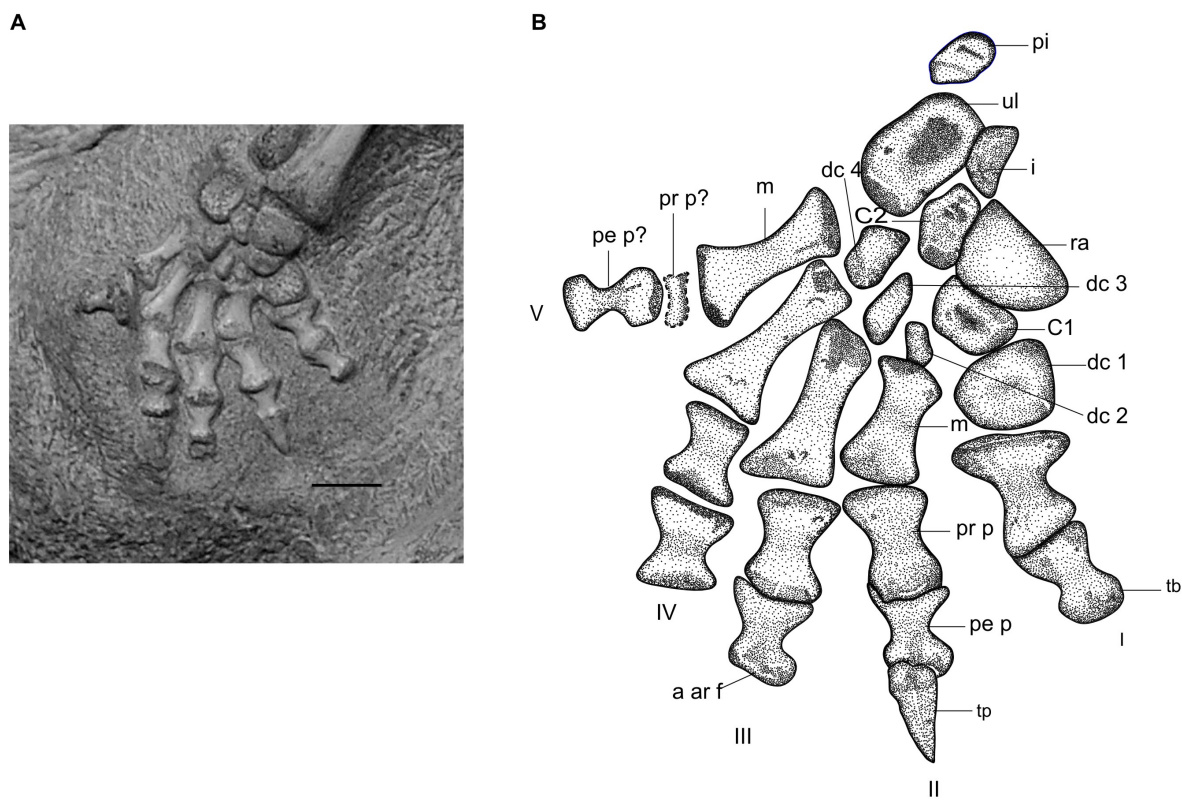


Figure 33. The right manus of *Galesaurus planiceps*, SAM-PK-K10465, in dorsal view. A) Photograph *in situ*, and B) drawing of right manus. Scale bars represents 1 cm. Abbreviations: **a ar f**, anterior articular facet; **C1**, radial centrale; **C2**, medial centrale; **i**, intermedium; **m**, metacarpals; **pe p**, penultimate phalanx; **pr p**, proximal phalanx; **ra**, radiale; **tb**, tubercle for ligamentous tendinous or capsular attachment; **ul**, ulnare; **pi**, pisiform; **tp**, terminal phalanx; **I-V**, digits; **dc, 1-4**, distal carpals. Dashed lines represent uncertain edges.

The radiale is a stout roughly oval-shaped thick bone, which tapers to a point proximolaterally. The dorsal surface of the radiale contains a rounded facet where it articulates with the radius; has almost vertical medial, proximal, and distal articulation facets, and articulates laterally with the medial centrale. There is a medial, semicircular articulation facet on the distolateral side of the radiale to which muscles or ligaments probably attached. This condition is in contrast to the radiale in *Thrinaxodon*, which Jenkins (1971) described as having a flat ventral surface with two slight depressions, separated by a low slanting ridge.

In contrast to *Thrinaxodon*, the radial centrale (C1) of *Galesaurus* is not cylindrical, but quadrangular. It has a straight anterior edge and is more robust than the medial centrale. Its surface is rounded and smooth with a distolateral facet on which the radiale articulated. According to Jenkins (1971), both centralia of *Thrinaxodon* have a cylindrical appearance and the small medial centrale is slightly dorsoventrally compressed with a depression on the anterior surface on which distal carpal 1 articulated. This depression is present on the distolateral surface of the medial centrale of *Galesaurus*. The medial centrale (C2) has unequal sides and lies between the ulnare and radiale, anterior to the intermedium and posterior to distal carpal 3. Laterally, the medial centrale articulates with the ulnare and with the rounded surface of the radiale medially. The distal surface of the medial centrale has a small central depression and a groove to which a muscle or ligament active in manus movement may have attached.

Distal carpal 1 is a large roughly quadrangular bone that articulates with the sloping distomedial end of the radial centrale (C1), the large flat posterior end of metacarpal I and the small medial articulation surface of metacarpal II in life. All the articulation surfaces are almost vertical. The dorsal surface of the carpal is flat and pitted, showing poor ossification or fossilization. In ventral view (SAM-PK-K10468; Fig. 34A; B), the bone has a articulation facet, and a posteromedial tuberosity is present to which muscles or ligaments probably attached.

Distal carpal 2 is a tiny, almost rectangular bone lying posterior to metacarpal II (Fig. 33A; B). The dorsal surface is somewhat rounded with a slight anterior depression. The bone thickens posteriorly. The posterior articulation surface of metacarpal II is slightly sloped towards distal carpal 2, whereas the proximal, lateral and medial articulation surfaces are more vertical. Distal carpal 3 has a cylindrical appearance and widens anteriorly. It articulates with the posterior end of metacarpal III.

Distal carpal 4 articulates with the posterior end of metacarpal IV. This carpal has an almost rectangular shape with a thick, long medial side and nearly vertical articulation surfaces. The dorsal surface is almost flat with a small depression in the centre.

Broom (1932b) assumed that distal carpals 4 and 5 in *Thrinaxodon* were fused, but Parrington (1939) described a *Thrinaxodon* specimen with a distinct distal carpal 5. Distal carpal 5 is not distinguishable in SAM-PK-K10465 or NMQR 3678 but distal carpal 4 is larger than the other distal carpals except for distal carpal 1. Hopson (1995) found the fifth distal carpal was absent in *Galesaurus* and this observation agrees with that found in the present study. The relative sizes of the carpals in SAM-PK-K10465 is similar to those of *Thrinaxodon* (Jenkins, 1971), and is in the order of I > IV > III > II.

The metacarpals are well developed. The various size of the metacarpals is almost identical to those of *Thrinaxodon* (Jenkins, 1971) namely IV > III > V > II > I. In dorsal view (Fig. 33A; B), all the metacarpals are nearly symmetrical and have an elongated hourglass shape. In ventral view (Fig 34A; B), the bones have an asymmetrical shape because the distal ends are thicker than the proximal ends. The distal articulation facets are slightly convex (Fig. 33A; B), and square in shape, whereas the proximal ends have flat, almost rectangular articulation facets similar to those of *Thrinaxodon* (Jenkins, 1971). Metacarpals II to V are notably slender in comparison to the shorter and stouter metacarpal I. The proximal end of each metacarpal flares laterally. The distal ends have uneven articulation surfaces that can be attributed to the presence of cartilage. The proximolateral surface of each metacarpal articulates with the adjacent metacarpal. The proximal end of metacarpal I has a broad end, articulates with distal carpal 1 and narrows towards the midshaft, widening again towards its distal end.

The proximal phalanx (pr p) of digits II and III appear to have moved a little over each of the penultimate phalanges, whereas articulation in digits I and IV appear to be natural (SAM-PK-K10465). The proximal phalanx of digit V is preserved, but has been dislodged and stands vertically. The penultimate phalanx and terminal phalanx of digit 1 is missing as are the terminal phalanges of all digits except II.

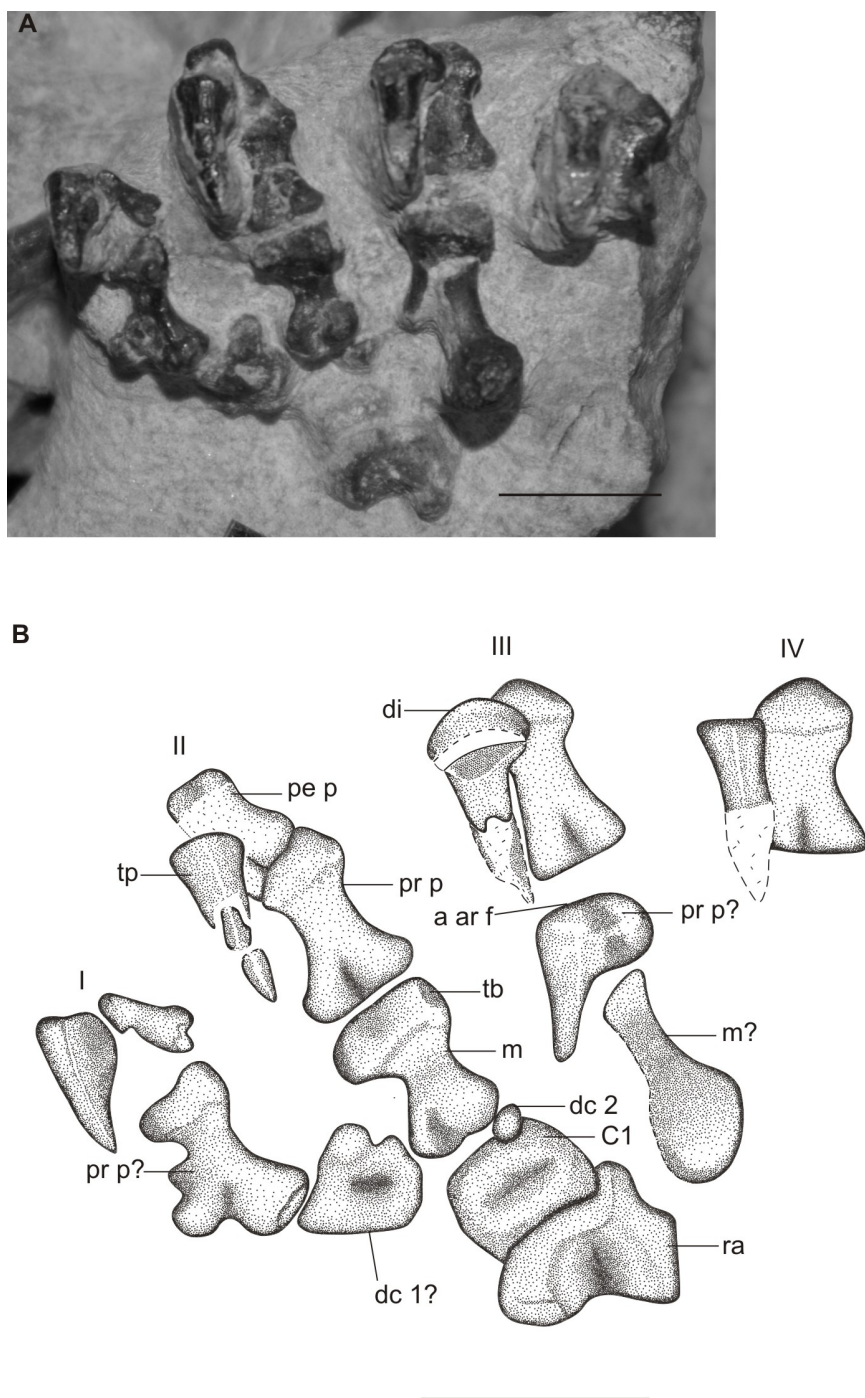


Figure 34. The left manus of *Galesaurus planiceps*, SAM-PK-K10468, in ventral view. C) Photograph *in situ* and D) drawing of left manus. Scale bars represents 1 cm. Abbreviations: **a ar f**, anterior articular facet; **C1**, radial centrale; **di**, plate-like disc; **m**, metacarpals; **pe p**, penultimate phalanx; **pr p**, proximal phalanx; **ra**, radiale; **tb**, tubercle for ligamentous tendinous or capsular attachment; **tp**, terminal phalanx; **I-V**, digits; **dc, 1-4**, distal carpals. Dashed lines represent uncertain edges.

The penultimate phalanges (pe p) are shaped like an hourglass similar to the metacarpals and proximal phalanges. Their proximal ends are slightly wider than the distal ends. As in *Thrinaxodon* (Jenkins, 1971), the proximal half of every penultimate phalanx expands gradually in dorsal view, from a fairly constricted waist to a posterior terminus with a vertical, oval facet. The distal half of every penultimate phalanx flares to form an almost spherical terminus where a concentric, convex articular facet is present. This facet (a ar f) has an anteroventral inclination of approximately 45° to the long axis of the bone and being this a prominent feature of a penultimate phalanx. Four tubercles (tb), similar in size, can be seen in ventral view at the four “corners” of the proximal phalanges. Striations on their proximal and distal ends mark the attachments for ligaments or digital flexors in a similar way as seen in *Thrinaxodon* (Jenkins, 1971). The anterior ends of the penultimate phalanges are cylindrical in shape. The two ends of the “cylinder” face slightly anterodorsally and in ventral view, the penultimate phalanx has a concave appearance.

The complete terminal phalanx II (tp) is preserved in SAM-PK-K10465 (Fig. 33A; B). The posterior end of the terminal phalanx overlaps with the anterodorsal surface of the penultimate phalanx (pe p). The terminal phalanx (tp) is approximately the same length as the penultimate phalanx and tapers to a sharp point

In two of the *Galesaurus* specimens (gracile NMQR 3678; robust SAM-PK-K10468) a plate-like disc (di) is present anterior to metacarpal III (Fig. 34A; B). In SAM-PK-K10465 the plate-like disc is not visible in digit III, as the digit is not fully preserved (Fig. 33A; B). The absence of the reduced plate-like discs in digit IV results in a digital formula of 2?-3-4-3?-3? for *Galesaurus*. Hopson (1995), indicated a digital formula 2-3-4?-4-3 for *Galesaurus*. Thus the correct digital formula of *Galesaurus* is probably 2-3-4-4-3. The digital formula for *Thrinaxodon* is also 2-3-4-4-3 (Parrington 1939; Jenkins, 1971).

4.3.2 Pelvic Girdle and Hind limb

Ilium

As in other cynodonts, the ilium of *Galesaurus* consists of a relatively slim, expanded blade separated from the base by a constricted neck (Fig. 35A; B) (Jenkins, 1971). Facets for contact with the pubis and ischium as well as a third of the acetabulum are present on the base. Anteriorly, Jenkins (1971) noted that the outline of the iliac blade in *Thrinaxodon*, *Cynognathus*, and *Diademodon* is broadly rounded and spoon-shaped, but varies with ossification. Broom (1932b) described the ilium of *Galesaurus*, as similar to *Thrinaxodon*, but more rounded with a significantly higher blade than *Thrinaxodon*. Jenkins (1971) doubted this description, but the present study has confirmed the observation of Broom (1932b) in the robust *Galesaurus* (Fig. 35A). The iliac blade has a slightly straighter posteroventral edge in the gracile morph compared to the robust morph. The latter edge intersects a moderately convex dorsal edge at roughly 80°. In *Thrinaxodon*, and in the gracile *Galesaurus* specimens, the dorsal edge of the iliac blade is less convex than the robust *Galesaurus*, and it narrows towards each end. A sharp rim is formed by the tapering of the anterior and dorsal edges of the iliac blade. Striations (st) on the rugose dorsal edge of the medial side indicate cartilaginous extensions (Fig. 35A). In smaller cynodonts, the texture of the lateral surface of the iliac blade is usually smooth without muscle markings, but in larger cynodonts this surface bears irregularly spaced striations radiating away from, but not reaching the neck (Jenkins, 1971). In the robust *Galesaurus* specimen NMQR 3542 the striations are prominent on the anterior and dorsal margins in medial view, whereas the medial surface of the iliac blade is uneven and represents the possible presence of connective tissue in the sacro-iliac fusion (Jenkins, 1971). Striations on the posterior surface of the iliac blade are not visible due to the position in which the ilium is preserved. The iliac blade of the gracile *Galesaurus* exhibits smaller and more or less evenly spaced striations on the medial and dorsal surfaces, whereas the posterior surface shows a few horizontal striations just above the posteroventral edge.

Jenkins (1971) described the cynodont iliac blade as relatively thin except for the presence of a thick supra-acetabular buttress (*s pa bu*) at the iliac base (Fig. 35B) and a swollen, straight posteroventral edge that is shaped like a rod-like buttress, expanding from the posterior end of the ilium to the supra-acetabular buttress.

The iliac blade in the robust *Galesaurus* differs from the usual cynodont condition in that dorsally, the anterior portion of the iliac bone rises gradually to a relatively rounded dorsomedial blade and then flattens gradually posteriorly (Fig. 35A). In medial view, the robust *Galesaurus* has a fossa dorsally in the middle of the iliac blade. In lateral view the iliac blade in the gracile *Galesaurus* is almost flat and a fossa is present anterodorsally (Fig. 35B). Jenkins (1971) noted a slight thickening of the cynodont iliac blade anterodorsal to the acetabulum and this is also observed in the *Galesaurus* specimens studied. In the cynodonts that Jenkins (1971) examined, the highest section of the blade lies directly above the acetabulum contrasting with the gracile and robust *Galesaurus* specimens in this study where the highest section is on the anterior part of the iliac blade (Fig. 35A; B).

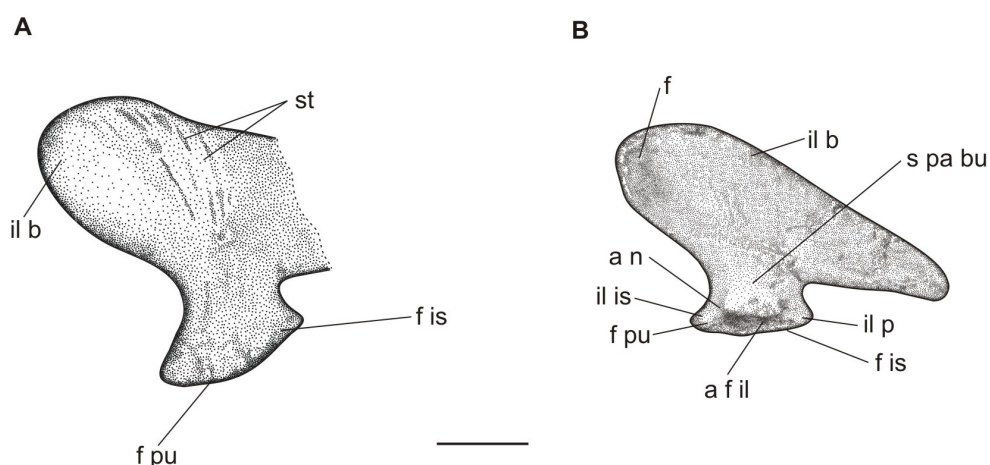


Figure 35. The right ilium of *Galesaurus planiceps*, A) reconstruction of NMQR 3542, in medial view and B) RC 845, in lateral view. Scale bar represents 1 cm. Abbreviations: **a f il**, acetabular facet of the ilium; **a n**, acetabular notch; **f**, fossa; **f is**, facet for articulation with the ischium; **f pu**, facet for articulation with the pubis; **il is**, ischial process of the ilium; **il b**, iliac blade; **il p**, ilium plate; **s pa bu**, supra-acetabular buttress; **st**, striations. Dashed lines represent uncertain edges.

A laterally projecting supra-acetabular buttress (s pa bu), an anteromedially directed process for the articulation with the pubis (il p) and a posteromedially directed process for the ischium (il is) are present on the mediolaterally broad base of the ilium. The lateral rim of the acetabular facet of the ilium (a f il) is round whereas the facet itself is concave and faces almost directly ventrally. A supra-acetabular notch (a n) lies posterior to the supra-acetabular buttress.

The articulation surfaces of the pubic and ischial processes are strap-shaped and widen at the anterior (pubic) (f pu) and posterior (ischial) (f is) ends. The pubic surface is approximately three-quarters the length of the ischial surface (Jenkins, 1971).

Pubis

The pubis in the gracile specimens RC 845 and BP/1/4506 is not preserved in articulation and may have been damaged because the pubic dorsal head is flattened. Jenkins (1971) described the pubis of the holotype of *Cynognathus crateronotus*, and this pubis appears similar to that of *Galesaurus* and thus, the pubic head will be described from the literature. The pubis consists of a ventromedially directed blade with an acetabular facet and articulation surfaces for the pubis and ilium on the dorsal head. The acetabular facet of the pubis faces both posterodorsally and laterally, and is oval in shape (a f pu) (Fig. 36). Jenkins (1971) suggested that the cartilaginous articulation surface in cynodonts was probably concave during life and this is probably also the case in *Galesaurus*.

The pubic facet is the smallest of the facets that encompass the acetabulum (Jenkins, 1971). A comparison between the pubic facet with the ischial and iliac facets reveals a less protruding lateral rim; this feature is more prominent in the robust *Galesaurus* than the gracile *Galesaurus*. An uneven articulation facet, present on the dorsomedial rim of the pubic head, articulates with the pubic process of the ilium. The posterior boundary of the facet faces posteriorly and contacts the ischium above the obturator foramen (Jenkins, 1971).

Just below the head, the pubis constricts to form a short neck. The pubic neck is more elongated in the robust *Galesaurus* (BP/1/4506) than the gracile *Galesaurus* (RC 845). The ventromedially oriented pubic plate (pu p) is laterally concave and originates from the neck. The anterior edge of the pubic plate arises from the anteromedial surface of the neck and the posterior edge arises from the posteromedial surface (Jenkins, 1971). The slightly curved anterodorsal edge of the pubic plate turns ventrolaterally and anteriorly. It is large and rod-like (r pu), but is more prominent in the gracile *Galesaurus* specimen RC 845. In this specimen the rod-like anterodorsal edge is notably shorter than in the robust specimens. The rod terminates in a rounded, rugosity.

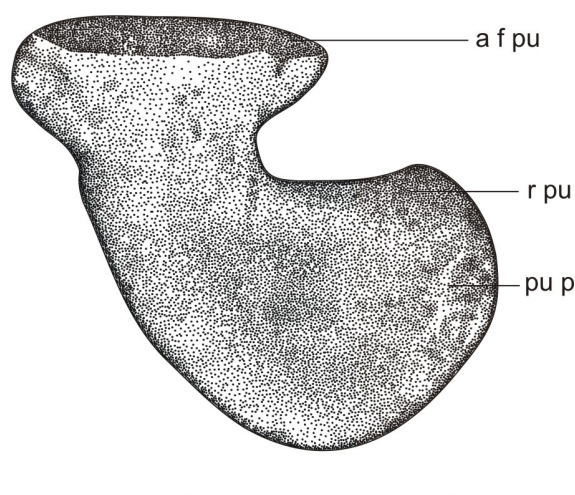


Figure 36. The right pubis of *Galesaurus planiceps*, RC 845, in lateral view. Scale bar represents 1 cm. Abbreviations: **a f pu**, acetabular facet of the pubis; **pu p**, pubic plate; **r pu**, rod-like anterodorsal edge of the pubis.

A broad U-shaped basin, deepest posteriorly along the pubo-ischial contact, is formed by the two opposing pubic plates, which meet along a thin symphysis in NMQR 3542. The anterior free edge of the pubis was incompletely preserved in all the material studied by Jenkins (1971). He thus concluded that it was particularly thin and was extended in life by cartilage. The anterior edge of the gracile *Galesaurus* appears to be complete and is relatively uneven indicating that cartilage may have been present. In

the robust specimens (NMQR 3542 and BP/1/4506), the surface of the anterior part of the pubis as well as part of the pubic blade is uneven, also implying a cartilage extension. Posteriorly, the pubic blade meets the ilium below the obturator foramen, which is only preserved in NMQR 3542. This part of the blade is relatively flat, but the surface is uneven and may indicate cartilage or muscle attachment.

Ischium

The pubis and ischium are similar in morphology in that they both consist of a head and a ventromedially directed plate (is p). Part of the acetabular surface for the femur and the symphyseal surfaces for the ilium and pubis are supported by the head (Fig. 37). Jenkins (1971) described the acetabular facet of the ischium in *Cynognathus*, as an oval surface with an almost straight medial border. This description agrees with the acetabular facet of the ischium in *Galesaurus*. The facet is orientated anterolaterally and slightly dorsally (a f is), which is also similar to *Cynognathus*. The ischial process of the ilium (f il) articulates with a strap-shaped articulation surface on the medial aspect of the ischial head, which expands dorsally (Jenkins, 1971). Jenkins (1971) noted that this articulation surface faces medially and anterodorsally, but turns more anteriorly near the cranial terminus to meet the pubis above the obturator foramen.

A constriction below the ischial head leads to a short neck. A fairly pronounced ridge extends from the middle of the lateral acetabular rim on the ischial head to three-quarters of the way towards the posterodorsal corner of the ischial plate (is r). This ridge is similar to that seen in *Thrinaxodon* (Jenkins, 1971). In contrast, the ridge in the more derived cynodonts, *Cynognathus* and *Diademodon*, gradually tapers posterodorsally and terminates near a prominent, but thin mediolaterally oriented ischial tuberosity (is tb) (Jenkins, 1971). This tuberosity in *Galesaurus* differs from that described by Jenkins (1971) in that it is a shorter articulation facet on a more rounded ischial plate (Fig. 37). This ischial tuberosity is a distinct lateral thickening of the mediolateral ischial plate. A posterolaterally oriented shallow groove (gr) is present between the ridge and the dorsal edge of the ischial plate. Jenkins (1971) found this groove to be well developed in *Cynognathus*, *Diademodon* and *Galesaurus*, but variable in *Thrinaxodon*. This groove is

well developed in all the *Galesaurus* specimens studied, but noticeably more prominent in the robust specimen, BP/1/4506 (79% adult), which would indicate its function as a muscle origin.

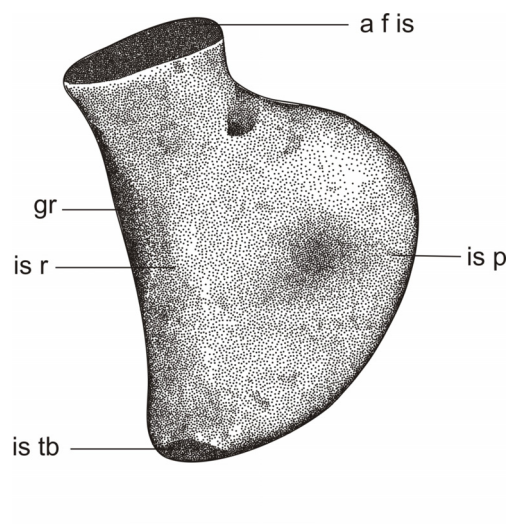


Figure 37. The right ischium of *Galesaurus planiceps*, RC 845, in lateral view. Scale bar represents 1 cm. Abbreviations: **a f is**, acetabular facet of the ischium; **gr**, groove in dorsal edge of ischium; **is p**, ischial plate; **is r**, ischial ridge; **is tb**, ischial tuberosity.

The ischial plate is relatively thin, anteroposteriorly elongated, almost round, and medially concave. Jenkins (1971) noted that the incomplete ischial plates he studied are straight posteriorly, and pass medially and ventrally to form a broad V-shaped notch with the corresponding edge of the other ischium. The ischial plate in these study specimens is slightly more rounded posteriorly than that described by Jenkins (1971). He described the ischial symphysis as long and narrow, with a thicker anterior articulation surface, and being approximately twice as long as the pubic symphysis. The anterior part of the ischial plate is thin and meets the posterior edge of the pubic plate below the obturator foramen (Jenkins, 1971).

Femur

The head (h) of the femur is slightly swollen and oval in outline (Fig. 38). The proximal articulation surface has a rough texture from the head to the greater trochanter. This can be attributed to the terminus probably having had a cartilaginous cap, which is not

preserved. The femoral head of the gracile *Galesaurus* (RC 845) exhibits a flat, strap-shaped edge from the head to the greater trochanter (gr tr), similar to that found in *Thrinaxodon* (Jenkins, 1971). The greater trochanter is slightly swollen and expanded in medial view (Fig 38A). The articulation surface of the proximal end of the femoral head is considerably thicker in the gracile specimens (RC 845; NMQR 3678). In *Thrinaxodon* and the gracile *Galesaurus*, the greater trochanter is slightly thicker than the connecting ridge (Jenkins, 1971). This is in contrast to the robust *Galesaurus* (NMQR 3542) where the greater trochanter expands dorsally and is as thick as the connecting ridge. Two surfaces can be distinguished on the greater trochanter; one facing posterodorsally, probably for the insertion of the M. ischio-trochantericus and one facing posteroventrally for the insertion of the M. ilio-femoralis (Jenkins, 1971).

An even, shallow concavity is present on the dorsal surface of the proximal end situated just below the femoral head and greater trochanter. It probably represents the origin for part of the M. femoro-tibialis. This concavity tapers gradually and ends ventral to the midshaft (NMQR3542; NMQR 3678).

As in all cynodont femora, both gracile and robust *Galesaurus* types have a round, deep intertrochanteric fossa (it f) between the femoral head and the greater trochanter when seen in ventral view (Fig. 38B). This fossa represents the insertion of the M. pubo-ischio-femoralis externus (Romer, 1922) and extends to the proximal end of the trochanteric crest and into the lesser trochanter with no evidence that the insertion extended distally along the crest (Jenkins, 1971).

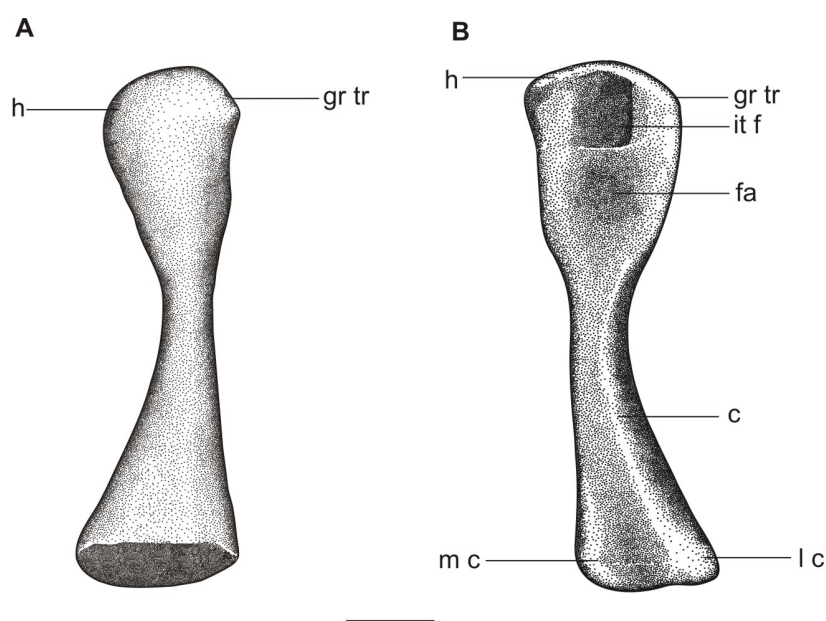


Figure 38. The right femur of *Galesaurus planiceps*, NMQR 3542 in A) dorsal and B) ventral view. Scale bar represents 1 cm. Abbreviations: **c**, crest between the ventral posterolateral surfaces of the femur; **fa**, fossa probably representing the adductor musculature insertion; **gr tr**, greater trochanter; **h**, femoral head; **it f**, intertrochanteric fossa; **l c**, lateral condyle; **m c**, medial condyle.

The lesser trochanter of the robust *Galesaurus* is a prominent bone extension that begins just below the femoral head and runs distally. The bone extension ends on the anterior surface. The trochanteric crest descends evenly and ends just above the midpoint of the shaft. Haughton (1924), Broom (1932a) and Jenkins (1971) noted that this trochanteric crest continues to the medial condyle in *Galesaurus* and *Thrinaxodon* as a sharp border, between the ventral and anterior surfaces of the shaft. This study agrees with their findings. As in *Thrinaxodon*, a fourth trochanter is absent in *Galesaurus*. In the more derived cynodonts, *Diademodon* and *Cynognathus*, the anterior and ventral surfaces distal to the lesser trochanter meet in a short thin groove (Jenkins, 1971). In the gracile *Galesaurus* specimen SAM-PK-K10465, this groove is more prominent than in the robust specimen NMQR 3542. A shallow groove is formed where the anterior surface of the lesser trochanter meets the femoral shaft and probably represents the insertion for the M. pubo-ischio-femoralis internus (Jenkins, 1971). In ventral view, a broad fossa on the lesser trochanter (**fa**) tapers gradually towards the

distal end. According to Romer (1922), this fossa and the posterior face of the trochanter probably represent the insertion for the adductor muscles.

This study confirms Broom's (1932a) initial observation that the posterior and ventral surfaces of the femoral shaft in *Galesaurus* are separated by a rounded crest (c) that runs from the greater trochanter to the midshaft. This is in contrast to the more derived cynodonts where the crest is more angular and runs from the greater trochanter to the side of the lateral condyle (Jenkins, 1971).

As in all cynodonts, the femoral shaft of *Galesaurus* is approximately square in cross-section through its centre, and expands distally to become more rectangular. Parts of the M. femoro-tibialis probably originated on the expanded dorsal surface as well as the medial and lateral parts of the shaft. The medial and lateral condyles on the distal end of the femur are approximately equal in size, but the medial condyle expands slightly more ventrally in the lateral one. This is in contrast to the larger cynodonts where a more robust lateral condyle (l c) and a narrower medial condyle (m c) are present. The distal condyles of the femur have a rough and uneven texture, which probably indicates a cartilaginous cap that articulated with the tibia before fossilization. Jenkins (1971) noted a slightly raised rugose area on the lateral condyle that might mark the site of femoro-fibular articulation and this is observed in *Galesaurus* NMQR 3542.

Tibia

As in all cynodonts, the tibial shaft of *Galesaurus* flattens anteroposteriorly and curves medially (Fig. 39). The proximal end of the tibia expands laterally and slightly anteriorly, resulting in the lateral edge being more concave than the medial edge, a concave anterior surface and a straight posterior surface. The expanded proximal end supports a large articular surface, which is approximately oval in outline with two oval facets for the articulation with the femoral condyles (pr ar s). A low anteromedially oriented ridge separates the slightly concave facets (Jenkins, 1971). The anteromedial facet of the tibia contacts the medial femoral condyle whereas the lateral facet contacts the large lateral femoral condyle. The posteromedial corner of the articulation surface is convex and unbroken with a ridge separating the femoral condyles. Jenkins (1971) mentions two tubercles on the proximal end of the tibia; one, which projects from the anteromedial edge of the articulation surface, is only present as a small protrusion in robust *Galesaurus* (NMQR 3542), and may represent the insertion of the quadriceps musculature; the other, smaller tubercle is not ossified or is absent in the gracile and robust *Galesaurus* (Jenkins, 1971).

Due to the anteroposterior flattening of the tibial shaft, distinct anterior and posterior surfaces can be distinguished. The anterior surface is relatively flat except for a ridge (r) dividing the shaft diagonally into medial and lateral surfaces. A superficial, but distinct fossa (f), is present proximomedial to the ridge on the anterior surface of the tibia, and possibly represents the origin of a pedal dorsiflexor muscle (Jenkins, 1971). The fossa and ridge disappear after reaching the medial edge. Jenkins (1971) suggested that both the ridge and fossa are related to extensor muscle attachment, but was not certain which muscles were involved. The distal half of the anterior surface is flat and Jenkins (1971) noted that in well-ossified cynodont specimens, a groove runs distally from the midpoint of the ridge to the distal end terminating at the swelling of the distal articular facet rim. This is not distinguishable or accessible in the gracile and robust specimens under study.

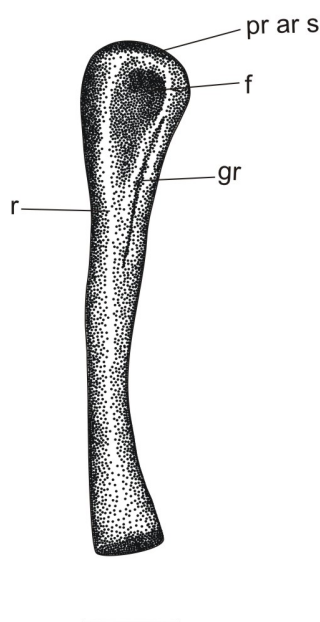


Figure 39. The left tibia of *Galesaurus planiceps*, NMQR 3542, in anterior view. Scale bar represents 1 cm. Abbreviations: **f**, fossa possibly representing the origin of a pedal dorsiflexor; **gr**, groove of uncertain origin; **pr ar s**, proximal articular facet; **r**, ridge possibly for muscle attachment.

Anterior and posterior surfaces of the tibia join medially along a sharply defined ridge. A tubercle is present on the proximal end of this ridge (Jenkins, 1971), but is more pronounced in *Thrinaxodon* than it is in *Galesaurus*. The anterior and posterior surfaces are separated laterally along their proximal half by a rounded part of the shaft, which becomes more defined distally. In medial view, the tibial head (proximal part of tibia) of *Galesaurus* is covered by extensive striations indicating muscle attachment (NMQR 3542).

The posterior surface is almost straight from proximal to distal end, and convex mediolaterally. On the lateral side of the tibia, a long and deep longitudinal groove (**gr**) can be distinguished (NMQR 3542). This groove, representing muscle attachment, extends farther proximally than distally. Jenkins (1971) noted that this groove is relatively longer and deeper in *Galesaurus* and *Thrinaxodon* than in larger cynodonts.

In *Thrinaxodon*, the tibia terminates distally in a flat, oval facet at right angles to the shaft axis, although the articular cartilage may have formed a different shape (Jenkins, 1971). However, in the robust *Galesaurus* (NMQR 3542) the articulation surface is almost square.

Fibula

The fibula has a slender shaft, which expands slightly at each end (Fig. 40). It is slightly broader proximally and sigmoidal elongated. The articulation surfaces face medially and slightly dorsally, with the proximal end being rounded and slightly convex. Due to the position of preservation, it appears that a prominent flange (fi fl) projects posteriorly. This may have been part of the femoro-tibial articulation, but perhaps served as a musculotendinous process (Jenkins, 1971). Proximally, the shaft is three-sided and thus appears triangular in cross-section.

The fibula of the robust *Galesaurus* (NMQR 3542) corresponds to fibular type II in *Thrinaxodon*, which Jenkins (1971) described as having a sharp ridge (m r) that descends from the proximal end along the medial side and continues with a second ridge (pm r) along the posteromedial side. As in *Thrinaxodon* (Jenkins, 1971), a longitudinal groove is present on the medial surface of the fibula in both the gracile (SAM-PK-K10465) and robust (NMQR 3542) specimens. However, the distal end of the fibula in *Galesaurus* is almost oval in cross-section, which is in contrast to the triangular cross-section described by Jenkins (1971) for *Thrinaxodon*.

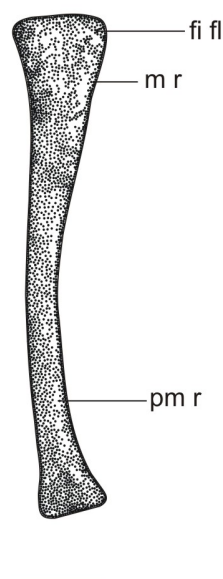


Figure 40. The left fibula of *Galesaurus planiceps*, NMQR 3542, in posterior view. Scale bar represents 1 cm. Abbreviations: **fi fl**, fibular flange; **m r**, medial ridge; **pm r**, posteromedial ridge.

Pes

There is more information on the manus than the pes in the literature, mainly with respect to digital morphology (Hopson, 1995). The available *Thrinaxodon* pes are usually poorly preserved and therefore Jenkins (1971) suggested that the pes was similar to that of the more derived cynodonts *Diademodon* and *Cynognathus*. However, with the new material in this study it can be shown that there are differences in pes morphology between *Galesaurus* and *Thrinaxodon*.

The *Galesaurus* pes is described using specimen BP/1/4506 (Fig. 41). This specimen has preserved most of the pes in articulation. The calcaneum (cal) of BP/1/4506 is anteroposteriorly extended, and in dorsal view, is convex in outline. Although the posterior region of the calcaneum is convex, the medial border is more dorsally oriented. The calcaneum is only slightly smaller than the astragalus (a) and differs from the large calcaneum and notably smaller astragalus of *Thrinaxodon* that Jenkins (1971) described.

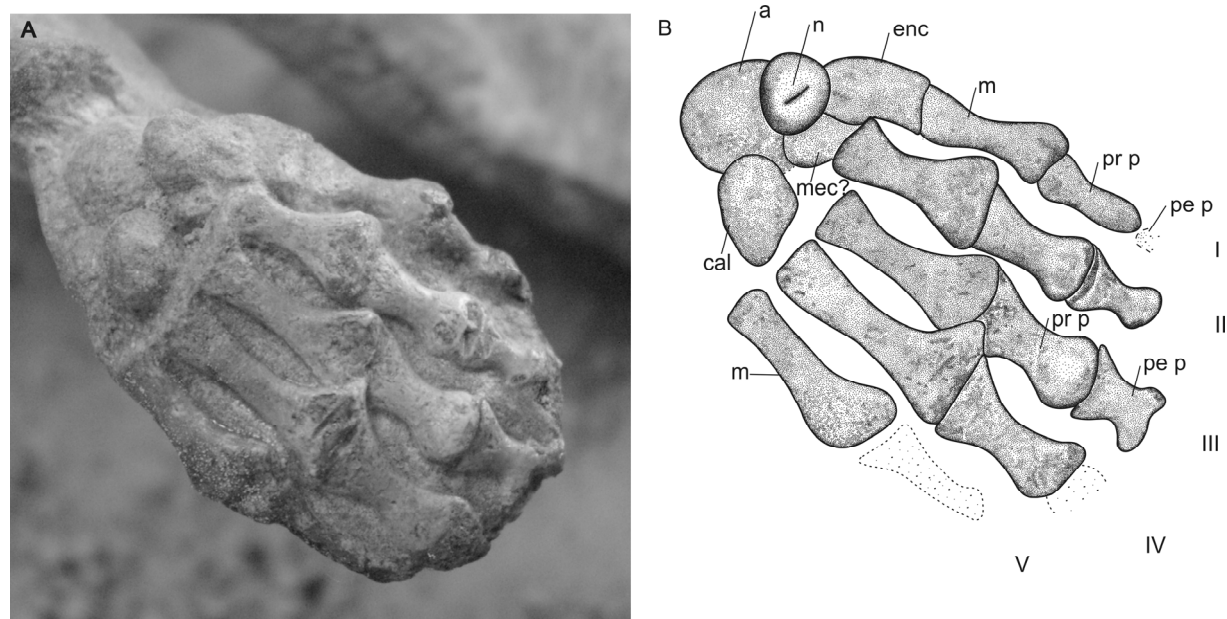


Figure 41. The right pes of *Galesaurus planiceps*, BP/1/4506, in dorsal view. A) Photograph *in situ* and B) drawing of right pes. Scale bar represents 1 cm. Abbreviations: **a**, astragalus; **cal**, calcaneum; **enc**, entocuneiform; **mec?**, mesocuneiform?; **m**, metatarsal; **n**, navicular; **pe p**, penultimate phalanges; **pr p**, proximal phalanges; **I-V**, digits. Dashed lines represent uncertain outlines.

The astragalus (**a**) is the largest bone in the pes and is a flat, almost round bone with a bulbously convex posterolateral region. This is in contrast to the hemispherical astragalus Jenkins (1971) described for *Thrinaxodon*. The dorsal surface of the astragalus in *Galesaurus* is pitted and uneven. Jenkins (1971) described a small bulbous facet on the posterolateral edge of the astragalar convexity in *Thrinaxodon* that may represent the fibular facet, but it is not visible in BP/1/4506 due to poor preservation. Posterior to this facet, a concavity leads in to the gently inclined posterior end of the astragalus. Jenkins (1971) suggested that, in the absence of a dorsal facet for the articulation with the tibia, the entire bulbous dorsal surface of the astragalus may represent the tibial contact. The posteromedial cleft that Jenkins (1971) described for *Thrinaxodon* is absent in *Galesaurus*.

The navicular (**n**) has an irregular elliptical form with a central dorsal fossa. It has been displaced and thus, its specific orientation and articulation with the ento-, meso- and

ectocuneiforms (first to third tarsalia) during life is unknown. It is not known if it articulated with the cuboid (fourth tarsal). Of the four distal tarsalia known, only the entocuneiform is definitely preserved. This bone is almost rectangular, similar to that described by Jenkins (1971) for *Thrinaxodon*. It articulates with metatarsal I and also with metatarsal II as Jenkins (1971) described. A small bone that lies behind metatarsal II could represent the mesocuneiform (mec?) or distal tarsal 2.

All five metatarsals are well-developed and preserved in undisturbed positions in BP/1/4506. Metatarsals I, III, IV and V are more slender than metatarsals II. The length of the metatarsals are $IV > III > V > I > II$. In dorsal view, the anterior end of each metatarsal flares laterally more than the posterior base. Metatarsals II and IV are more robust than the other metatarsals. All the metatarsals are almost symmetrical and have an elongated hourglass shape. Metatarsal V has a flat articulation facet on its lateral side, and probably served as muscle attachment, similar to the short flexor and peroneal musculature in mammals (Jenkins, 1971). The anterior articulation facets are slightly convex whereas the posterior ends have flat, almost rectangular articulation facets. The anterior and posterior ends of each metatarsal have uneven articulation surfaces that can be attributed to the former presence of cartilage.

The proximal phalanges are without exception longer than the penultimate phalanges. They are shorter than the metatarsals and are also almost symmetrical with an elongated hourglass shape. The proximal ends of the proximal phalanges are smooth and thus do not suggest extended cartilage coverage. The anterior and posterior ends of the proximal phalanges are almost equal in width whereas the anterior widths of the two penultimate phalanges are less than their posterior width. In dorsal view, the anterior half of a penultimate phalanx expands gradually from a fairly constricted waist to an anterior terminus with a vertical, oval facet. The terminal phalanges are not preserved in BP/1/4506.

In digit I, the proximal phalanx and a tiny portion of the penultimate phalanx are preserved. In digits II and III, both proximal and penultimate phalanges are completely preserved. The complete proximal and a small portion of the penultimate phalanges are

preserved in digit IV. The proximal phalanx of digit V is present, but poorly preserved. The reduced discs in digit III and IV, which Parrington (1933, 1939) described in the manus of *Thrinaxodon*, are not observed in the pes of *Galesaurus*. The single reduced disc of the manus seen in the robust (SAM-PK-K10465) and the gracile (NMQR 3678) *Galesaurus* specimens are also not observed in the available pes, if the identification of the fragmentary penultimate phalanges for digit I and IV is correct. Thus, the available material suggests the digital formula for the *Galesaurus* pes as 3-3-3-3-2? because the presence of a terminal phalanx for each digit can be assumed even though they are not preserved in available material. The pedal phalangeal formula for *Thrinaxodon* is 2-3-4-4-3 (Jenkins, 1971). Hopson (1995) found the pedal phalangeal formula for *Galesaurus* to be 2-3-4?-4-3. Thus, the pedal phalangeal formula for *Galesaurus* is still uncertain.

CHAPTER FIVE BONE HISTOLOGY

5.1 Ontogenetic status

A detailed bone histological analysis was conducted on *Galesaurus planiceps*. The bone microstructure of the tibia and fibula of RC 845 (62% adult), the femur of NMQR 3678 (71% adult) and the humerus, radius, ulna, femur and tibia of NMQR 3542 (100% adult) was examined.

5.2 Micro-analysis

5.2.1 RC 845

The relative bone wall thickness (RBT) of the tibia is approximately 24%. The overall bone tissue pattern of the tibia consists mostly of fibro-lamellar bone, which continues to the sub-periosteal surface (Fig. 42A). Prominent vascular canals radiate out from the medullary cavity and comprise 5.4% of the mid-cortical surface area (Fig. 42B). Vascularization decreases slightly towards the periphery.

Primary osteons are present throughout the mid-cortex. The haphazardly arranged osteocyte lacunae, which radiate branched canaliculi, are generally globular, although a few flattened osteocyte lacunae are also present in the mid-cortex. The osteocyte lacunae become more organized towards the periphery. Multiple, thin layers of circumferential endosteal lamellar tissue surround the medullary cavity and contain a mixture of globular and flattened osteocyte lacunae (Fig. 42B). Three annuli (Fig. 42B) are observed in the outer periphery.

The fibula has a relative bone wall thickness of approximately 19%. The element is characterized by a moderately vascularized (5.5%) arrangement of longitudinally oriented primary osteons oriented in radial rows within a fibro-lamellar bone matrix (Francillon-Vieillot et al., 1990) (Fig. 43A). Vascularization decreases slightly towards

the periphery. Fine trabeculae form an island in the medullary cavity. The globular osteocyte lacunae become fewer, more organised, and flattened towards the sub-periosteal surface (Fig. 43B). A large number of Sharpey's fibres are present in the mid-cortical and outer regions. Annuli are absent.

5.2.2 NMQR 3678

The femur is characterized by a relative bone wall thickness of approximately 19% (Fig. 44A), whereas *Thrinaxodon* varies between 22% to 27% (Botha, 2002). The overall bone tissue pattern consists of poor vascularized fibro-lamellar tissue (2.7%), which gradually becomes lamellar-zonal bone, towards the sub-periosteal surface (Fig. 44B). The fibro-lamellar tissue consists mostly of longitudinally and a few radially oriented primary osteons. A few longitudinally oriented primary osteons are observed in the lamellar-zonal bone tissue as well. The haphazardly arranged osteocyte lacunae are mostly globular in both the fibro-lamellar and lamellar-zonal bone tissue, but are more prominent in the mid-cortex. Branched canaliculi radiate from the osteocyte lacunae. A faint annulus is present in the mid-cortex. Widely spaced LAGs in the lamellar-zonal region become more closely spaced towards the sub-periosteal surface (Fig. 44B). Sharpey's fibres are absent.

5.2.3 NMQR 3542

The humerus of this specimen is poorly preserved and thus the RBT and vascularization could not be calculated. The cortex consists of fibro-lamellar bone with a thin lamellar-zonal region at the periphery (Fig. 45). The cortex is relatively poorly vascularized and exhibits an arrangement of longitudinally oriented primary osteons oriented in radial rows. A few, small secondary osteons are also present, mostly in the inner cortex (Francillon-Vieillot et al., 1990). The osteocyte lacunae are flattened and less abundant in the outer lamellar-zonal bone tissue.

The radius of NMQR 3542 is characterised by a notably thick cortex of 39% (Fig. 46A), compared to 25% in *Thrinaxodon* (Botha, 2002). The cortex consists of poorly

vascularized (2.7%) fibro-lamellar bone, which becomes lamellar-zonal towards the periphery. Primary osteons are present in the fibro-lamellar bone and a few are present in the lamellar-zonal bone tissue. The osteocyte lacunae are globular, becoming more organized towards the periphery (Fig. 46B). Branched canaliculi radiate from the osteocyte lacunae. Sharpey's fibres are present in the outer cortex. Multiple annuli and LAGs (Fig. 46B) are also observed in the peripheral lamellar-zonal region.

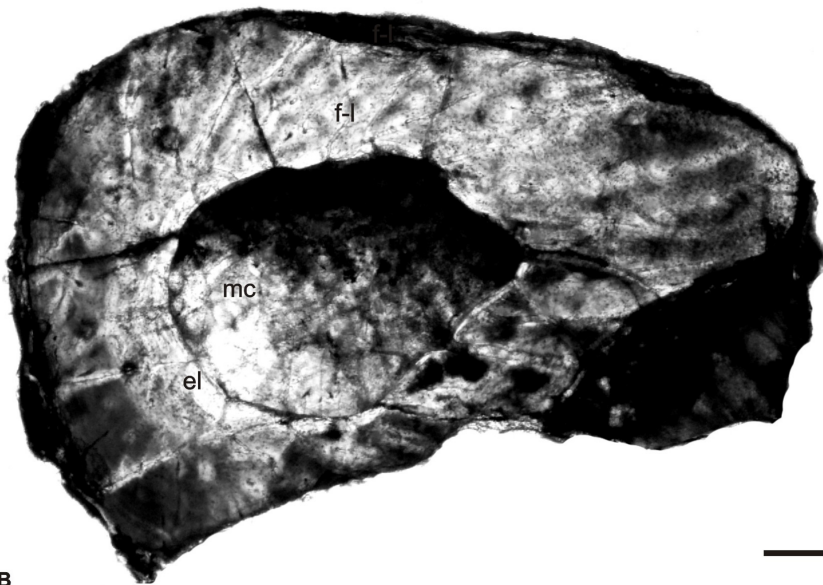
The ulna of NMQR 3542 is also characterised by a relatively thick bone wall of 36% (Fig. 47A) compared to 28% in *Thrinaxodon* (Botha, 2002). The cortex consists mostly of poorly vascularized (3.7%) fibro-lamellar bone with mostly globular osteocyte lacunae that radiate branched canaliculi. The bone tissue becomes lamellar-zonal towards the periphery. This region contains fewer primary osteons, and vascular canals, flattened osteocyte lacunae and two annuli. Longitudinal primary osteons are numerous in the inner- and mid-cortex. Thin layers of circumferential endosteal lamellar tissue surround the medullary cavity. Sharpey's fibres are observed in the mid- and outer cortex (Fig. 47B).

The thickness of the *Galesaurus* femoral bone wall is 20% (Fig. 48A) compared to the variation of between 22% and 25% in *Thrinaxodon* (Botha, 2002). The *Galesaurus* femur is poorly vascularized (3.8%) and becomes less vascularized towards the periphery. The cortex consists of fibro-lamellar bone that becomes a thick lamellar-zonal region towards the sub-periosteal surface (Fig. 48B). This lamellar-zonal region, which is the thickest of such regions in all the elements studied, contains multiple annuli and LAGs (Fig. 48C). The globular osteocyte lacunae become more organized towards the periphery. Sharpey's fibres are present in the mid-cortex and periphery (Fig. 48B).

The relative bone wall thickness of the tibia NMQR 3542 is approximately 21% (Fig. 49A). The tibial cortex consists of poorly vascularized (2.9%) fibro-lamellar bone that becomes lamellar-zonal bone towards the periphery. Vascularization decreases within the lamellar-zonal bone (Fig. 49B). The globular osteocyte lacunae are more abundant in the inner- and mid-cortex, but a few flattened osteocyte lacunae are present at the

periphery. Sharpey's fibres are present in the outer cortex (Fig. 49B). The fibro-lamellar bone is uninterrupted with annuli and LAGs only occurring in the lamellar-zonal region (Fig. 49B; C).

A



B

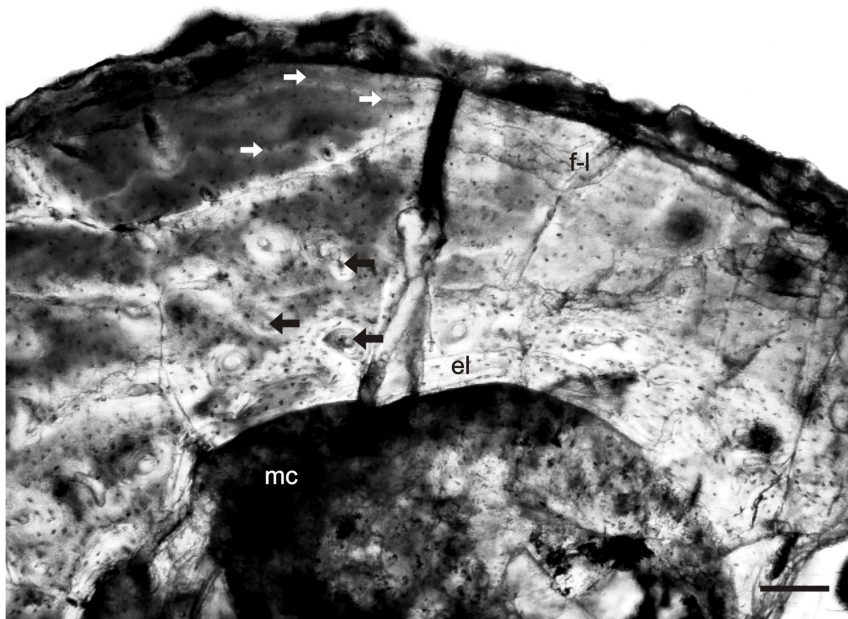


Figure 42. Transverse sections of *Galesaurus planiceps*, tibia RC 845. A) Low magnification view showing the overall bone tissue of the tibia with a fibro-lamellar cortex. Scale bar represents 413 μ m. B) Multiple layers of endosteal lamellar tissue surround the medullary cavity. Multiple annuli are present at the periphery (white arrows). A few sparse primary osteons are observed in the inner cortex (black arrows). Scale bar represents 1000 μ m. Abbreviations: **el**; endosteal lamellar bone; **f-l**, fibro-lamellar bone; **mc**, medullary cavity.

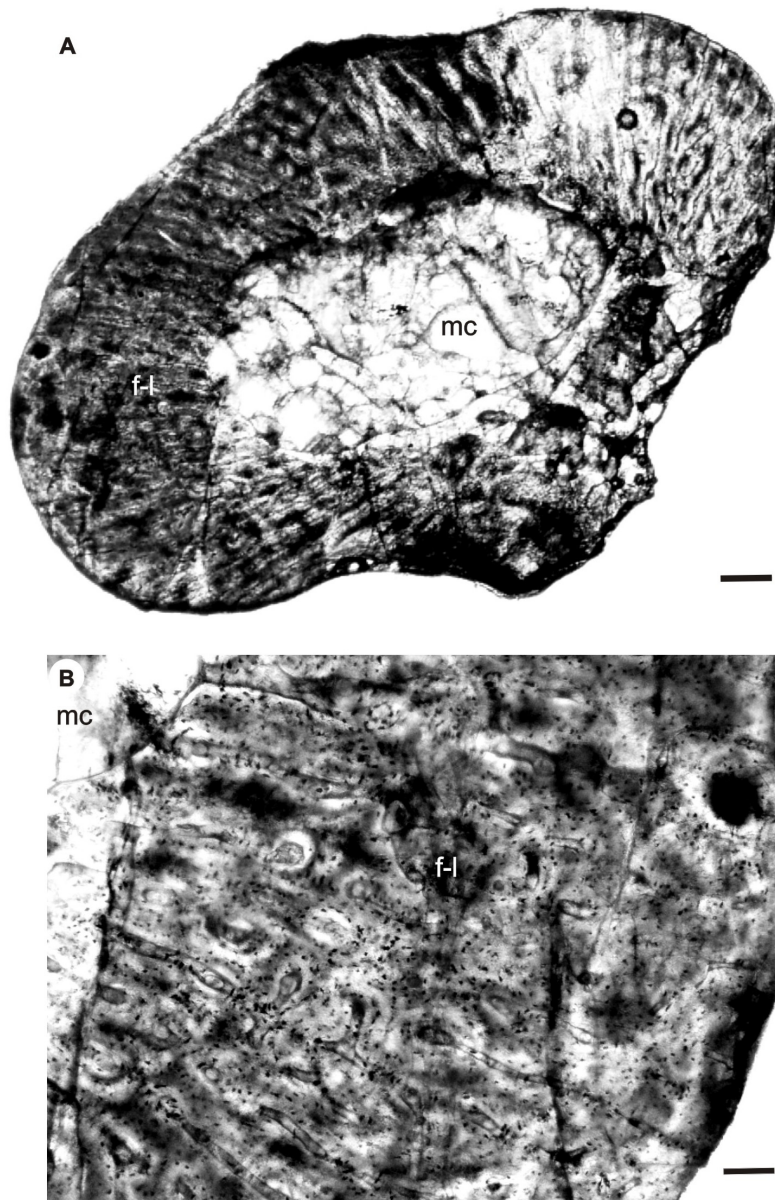
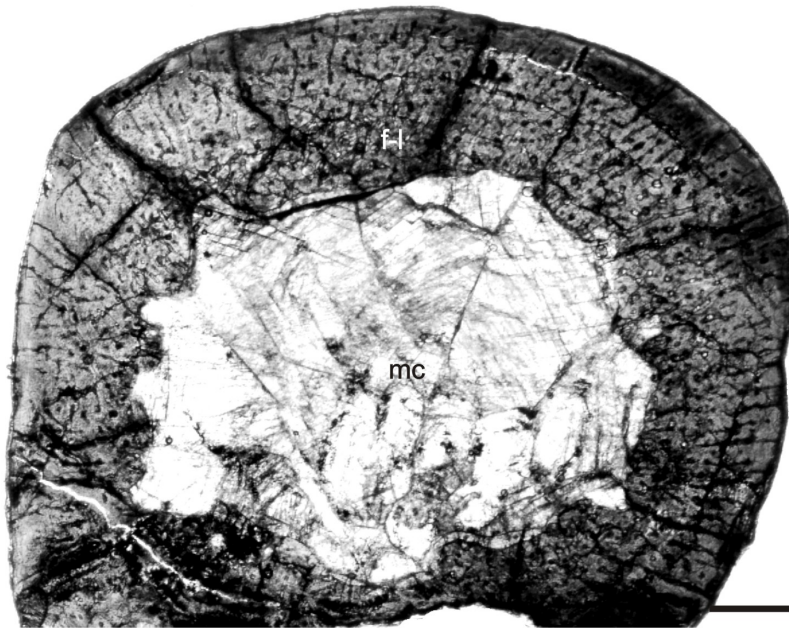


Figure 43. Transverse sections of *Galesaurus planiceps*, fibula RC 845. A) Low magnification view showing the overall bone histology of the fibula which contains a moderately vascularized fibro-lamellar cortex. Scale bar represents 413 μ m. B) High magnification of longitudinally oriented primary osteons in radial rows. Scale bar represents 1000 μ m. Abbreviations: **f-l**, fibro-lamellar bone; **mc**, medullary cavity.

A



B

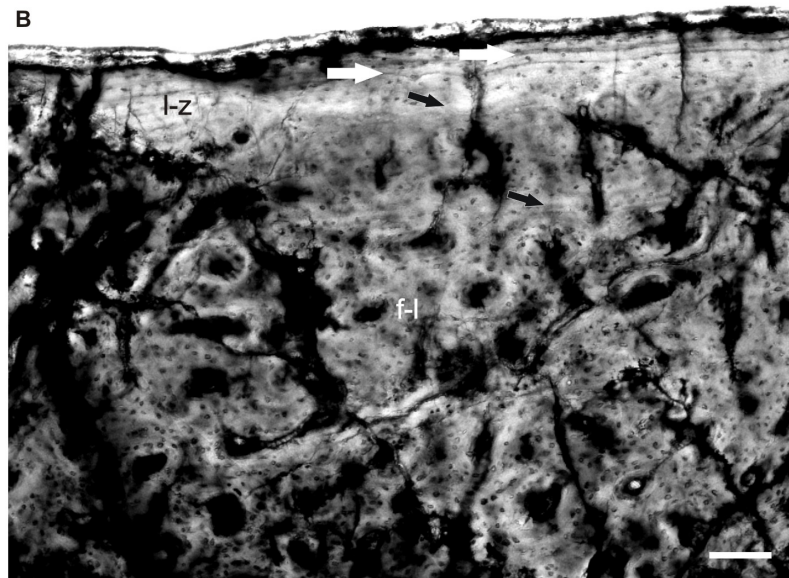


Figure 44. Transverse sections of *Galesaurus planiceps*, femur NMQR 3678. A) Low magnification showing relatively poorly vascularized fibro-lamellar bone. Scale bar represents 413 μ m. B) Lamellar-zonal bone at the periphery. Multiple LAGs (white arrows) are present in the lamellar-zonal region. Annuli (black arrows) are present in the outer fibro-lamellar cortex. Scale bars represent 1000 μ m. Abbreviations: **f-l**, fibro-lamellar bone; **l-z**, lamellar-zonal bone; **mc**, medullary cavity.

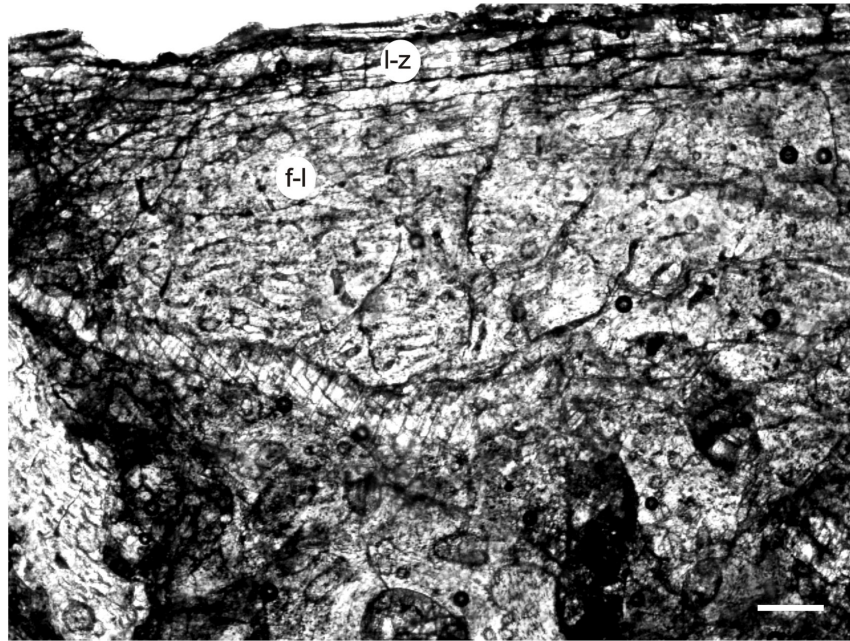


Figure 45. Transverse section of *Galesaurus planiceps*, humerus NMQR 3542. The bone tissue pattern consists of fibro-lamellar bone and a thin lamellar-zonal peripheral region. Scale bar represents 1000 μ m. Abbreviations: **f-l**, fibro-lamellar bone; **l-z**, lamellar-zonal bone.

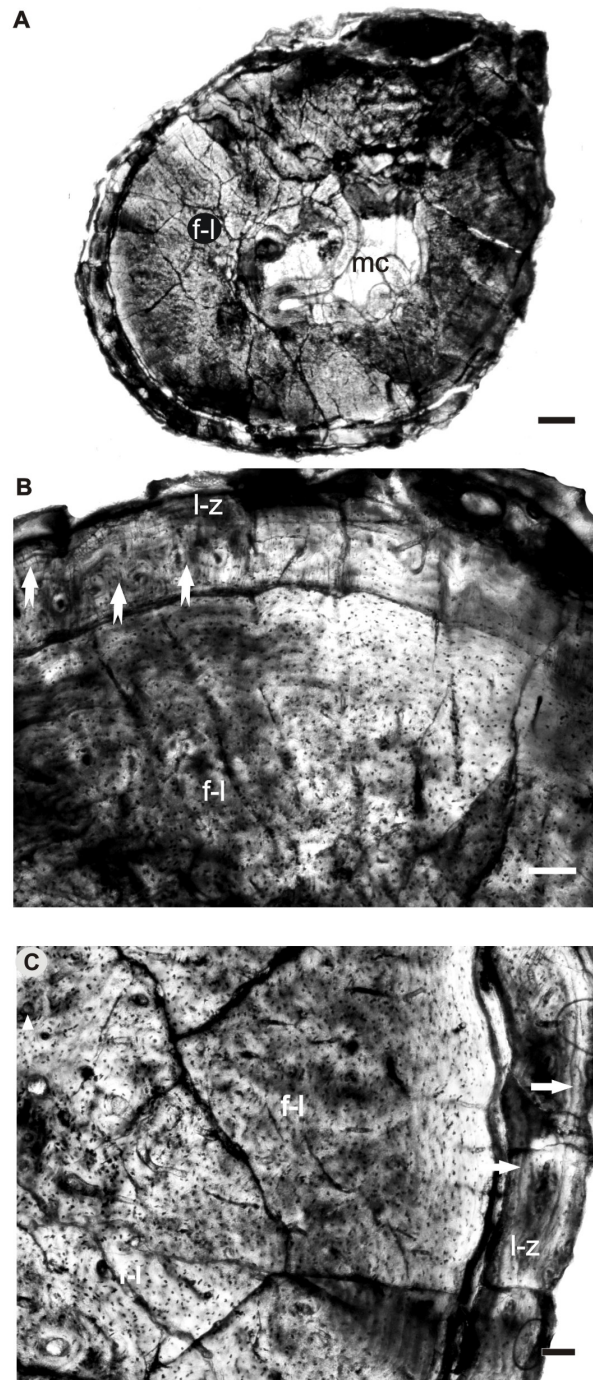


Figure 46. Transverse sections of *Galesaurus planiceps*, radius NMQR 3542. A) Low magnification of the radius showing the thick fibro-lamellar cortex. Scale bar represents 413 μ m. B) Sharpey's fibres (\rightleftharpoons) in the outer cortex. Scale bar represents 1000 μ m. C) Multiple annuli and LAGs (white arrows) are present in the peripheral lamellar-zonal region. Scale bar represents 1000 μ m. Abbreviations: **f-l**, fibro-lamellar bone; **l-z**, lamellar-zonal bone; **mc**, medullary cavity.

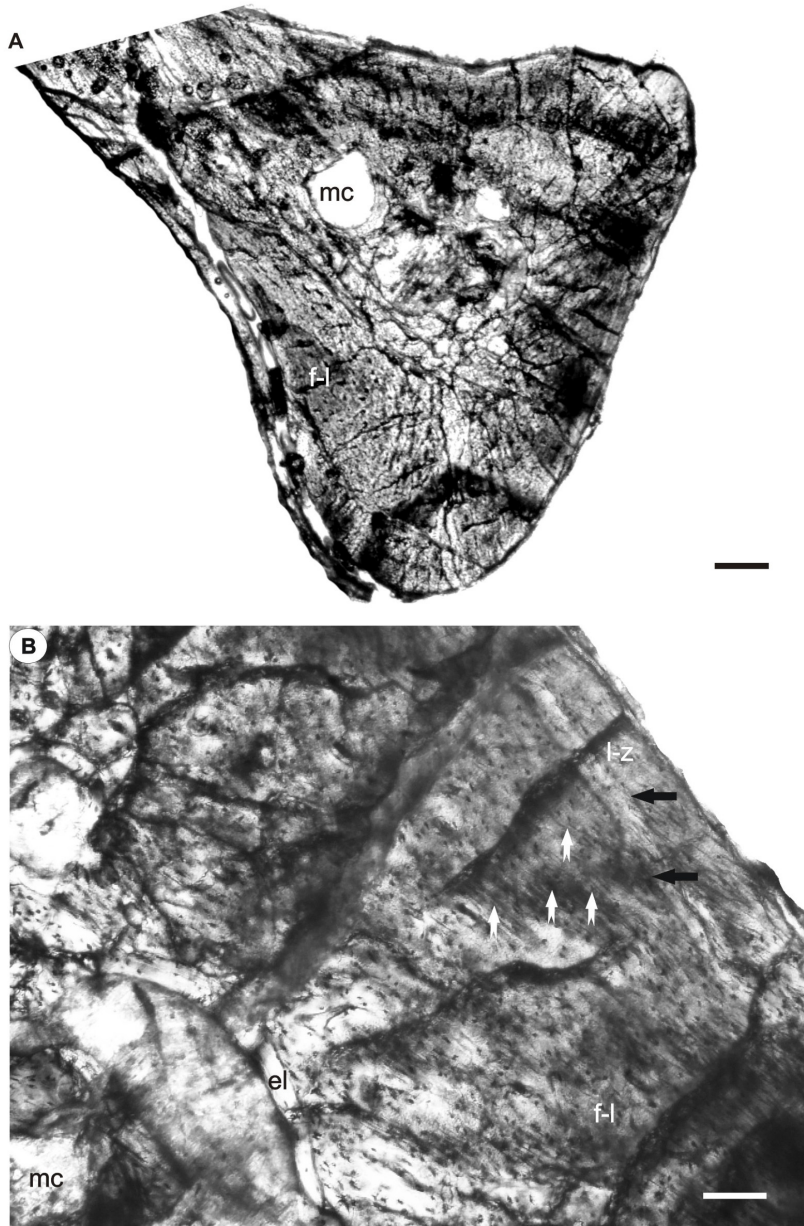


Figure 47. Transverse sections of *Galesaurus planiceps*, ulna NMQR 3542. A) Low magnification showing the general bone tissue consisting mainly of fibro-lamellar bone. Scale bar represents 413 μ m. B) A small lamellar-zonal region is present at the periphery. Sharpey's fibres (white arrows) are observed in the mid- and outer cortex. LAGs (black arrows) are present in the peripheral lamellar-zonal region. Scale bar represents 1000 μ m. Abbreviations: **el**, endosteal lamellar bone; **f-l**, fibro-lamellar bone; **l-z**, lamellar-zonal bone; **mc**, medullary cavity.

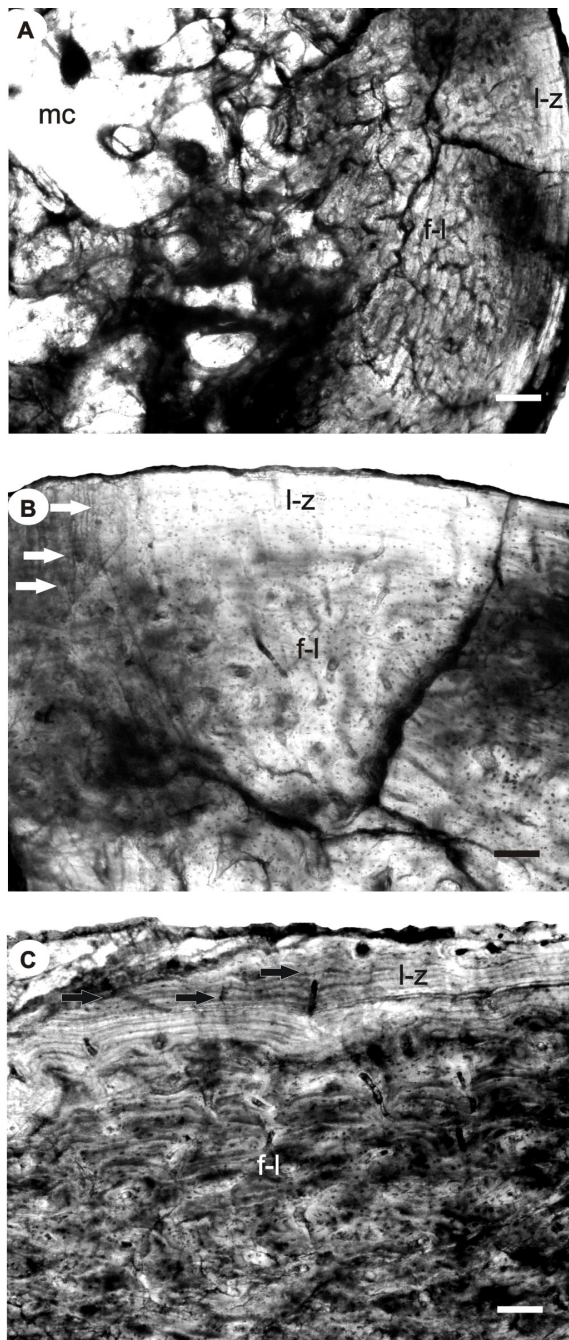


Figure 48. Transverse sections of *Galesaurus planiceps*, femur NMQR 3542. A) Poorly vascularized fibro-lamellar bone, becoming lamellar-zonal bone at the periphery. B) Sharpey's fibres (white arrows) are present in the mid- and outer cortex. C) Multiple annuli and LAGs (black arrows) are present in the peripheral lamellar-zonal region. Scale bars represent 1000µm. Abbreviations: **f-l**, fibro-lamellar bone; **l-z**, lamellar-zonal bone; **mc**, medullary cavity .

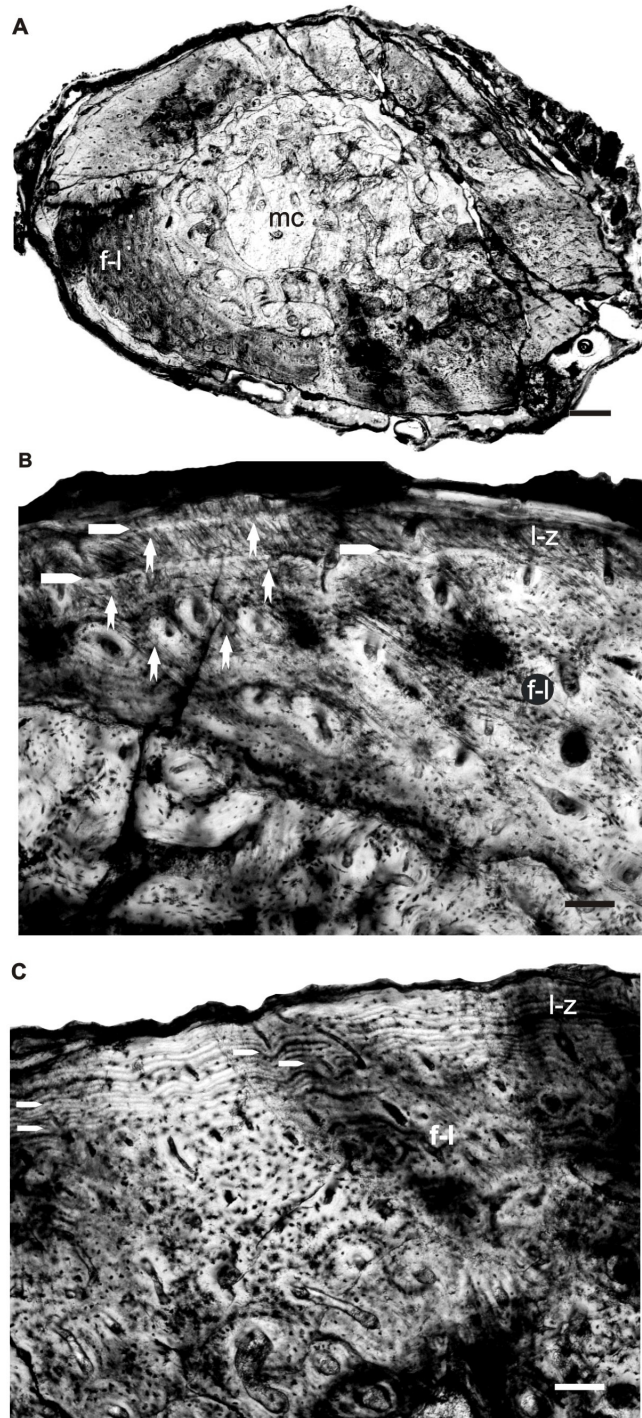


Figure 49. Transverse sections of *Galesaurus planiceps*, tibia NMQR 3542. A) Low magnification showing poorly vascularized fibro-lamellar bone, which becomes lamellar-zonal bone at the sub-periosteal surface. Scale bar represents 413 μ m. B) Sharpey's fibres (white arrows) are present at the periphery. Scale bar represents 1000 μ m. C) Multiple annuli and LAGs are indicated by arrows in the lamellar-zonal bone. Scale bar represents 1000 μ m. Abbreviations: **f-l**, fibro-lamellar bone; **l-z**, lamellar-zonal bone; **mc**, medullary cavity.

5.3 Interpretations

Postcranial material of *Galesaurus* is relatively rare and therefore only three specimens, two gracile (RC 845 and NMQR 3678) and one robust (NMQR 3542), were thin sectioned for bone histological analysis. Two elements of RC 845, one element of NMQR 3678 and five elements of NMQR 3542 were analysed.

Gracile specimens RC 845 and NMQR 3678 are 62% and 71% adult size respectively and are considered to be sub-adults (Table 3). The relative bone wall thickness (RBT) values of the tibia and fibula (RC 845) are 19% and 24% respectively, and the RBT of the tibia of NMQR 3678 is also 19%. The thickness of the compact bone wall of these two gracile specimens (RC 845 and NMQR 3678) is well below 30% and does not suggest an aquatic, semi-aquatic, or fossorial lifestyle (Wall, 1983; Magwene, 1993; Botha, 2003). The RBT of *Thrinaxodon* ranges from 22% to 28% (Botha, 2002), which is comparable to that of the gracile *Galesaurus* specimens. The overall bone tissue pattern of *Thrinaxodon* consists mostly of uninterrupted moderately vascularized (4.79%; Botha, 2002) fibro-lamellar bone compared to that of the gracile *Galesaurus* specimens, which consists mostly of uninterrupted moderate to poorly vascularized (5.4% for RC 845 and 2.7% for NMQR 3678) fibro-lamellar bone, which indicates that bone was deposited at a moderately fast rate in the two taxa (Francillon-Vieillot et al., 1990; Reid, 1996). The osteocyte lacunae in the two gracile specimens of *Galesaurus* become more organized and vascularization decreases towards the slowly forming lamellar-zonal periphery, indicating a decrease in growth rate, because vascular density correlates positively with growth rate in osseous tissues (Ricqlès, 1983). A lower overall vascularized density in specimen NMQR 3678 suggests that growth was slightly slower than that of RC 845.

Multiple thin layers of circumferential endosteal lamellar tissue surround both the medullary cavities of the long bones of RC 845 and NMQR 3678 suggesting that these individuals were not juveniles (Cormack, 1987; Reid, 1996). An annulus (observed in specimen NMQR 3678) in the fibro-lamellar cortex corresponds to a period of slow growth where after growth continued at a relatively rapid rate (Reid, 1996). Well-defined annuli are present in the periphery of RC 845, whereas annuli and LAGs are present in

the outer lamellar-zonal bone tissue of NMQR 3678. This pattern differs from that seen in *Thrinaxodon* where the outer region consists of parallel-fibred bone instead of lamellar-zonal bone, and growth rings are absent.

The shift to slowly forming lamellar-zonal tissue and appearance of LAGs and annuli in the outer periphery of both gracile *Galesaurus* specimens suggests that these specimens had probably achieved adulthood as overall growth had begun to slow down. Numerous Sharpey's fibres are present in the tibia of RC 845, which represent points of insertion of ligaments and tendons (Leeson and Leeson, 1981), suggesting that the muscles attached to the hind limb were used during strong muscle movement. Sharpey's fibres were not observed in the fibula and humerus.

The robust *Galesaurus*, NMQR 3542 is the largest specimen known. As in the gracile *Galesaurus* specimens, multiple thin layers of circumferential endosteal lamellar tissue surround the medullary cavity and suggest that this individual was not a juvenile (Cormack, 1987; Reid, 1996). The RBT values for the robust *Galesaurus* elements range from 39% in the radius; 36% in the ulna; 21% in the tibia, to 20% in the femur. The RBT values for the radius and ulna exceed 30% and therefore suggest modifications in lifestyle, which would require an increase in limb bone thickness such as an aquatic, semi-aquatic, or fossorial lifestyle (Wall, 1983; Magwene, 1993; Botha, 2003). Sharpey's fibres are also present in *Thrinaxodon*, but more obvious in both the gracile and robust *Galesaurus* specimens, thus indicating strong muscle attachment in *Galesaurus*.

All the robust *Galesaurus* limb bones exhibit a fibro-lamellar bone cortex, which becomes lamellar-zonal bone towards the periphery. The presence of fibro-lamellar bone indicates that this animal deposited bone at a relatively rapid rate early in ontogeny (Francillon-Vieillot et al., 1990; Reid, 1996). The transition to lamellar-zonal bone tissue indicates an overall decrease in growth rate (Francillon-Vieillot et al., 1990) and possible onset of sexual maturity (Reid, 1996). The transition from annuli to multiple successive LAGs that lie close together at the periphery indicates that growth decreased even further or ceased completely during the unfavourable growing season

and suggests that *Galesaurus* was susceptible to environmental fluctuations (Francillon-Vieillot et al., 1990; Reid, 1996).

The bone histology of *Thrinaxodon* is similar to that of *Galesaurus* suggesting a similar growth pattern early in ontogeny. Initially *Galesaurus* and *Thrinaxodon* grew relatively rapidly and continually. The appearance of parallel-fibred bone in *Thrinaxodon* indicates that the overall growth then decreased, possibly with the onset of sexual maturity (Botha and Chinsamy, 2005). However, the presence of lamellar-zonal bone with multiple annuli and LAGs in *Galesaurus* indicates that the overall growth was slower than *Thrinaxodon* or even ceased completely during the unfavourable growing season, suggesting that this taxon was more susceptible to environmental fluctuations than was *Thrinaxodon*.

CHAPTER SIX

DISCUSSION

***Galesaurus* Biology**

This study provides a redescription of the postcranial skeleton of the Early Triassic basal cynodont *Galesaurus planiceps*, based on new material. This cynodont was previously known from cranial material and partially postcranial elements, but recently discovered new material, comprising well-preserved and complete postcrania allowed a detailed redescription of the postcranial skeleton. The examination of the material of this taxa reveals the presence of two distinct morphs, namely a small, gracile form and a large, robust form.

The axial skeletons of the two morphs were found to be similar. However, all the well preserved axial skeletons of the study specimens are articulated, and thus small differences between them cannot be ruled out at this stage. Obvious differences between these morphs are present in the scapulae and ilia and more subtle differences in the humeri and femora.

One of the clearest differences, between these morphs, is the presence of a lateral bony ridge extending dorsoventrally along the middle of the lateral surface of the scapula in the gracile morph. This ridge, absent in the robust specimens studied, terminates, anterior to the groove of the supracoracoideus fossa, and probably provided additional muscle attachment on the scapula.

The robust *Galesaurus* humerus has a prominent low ridge extending across the dorsal surface of the humeral shaft, and possibly provided insertion for the *M. latissimus dorsi*. A second ridge providing insertion for the *M. teres minor* separates the broad fossa on the anterolateral surface of the deltopectoral crest from the humeral head. These articulation surfaces are less prominent in the gracile humeri. Jenkins (1971) reported that the entepicondyle on the humerus of *Thrinaxodon* is

thicker than the ectepicondyle, and in this study, the humerus of the gracile *Galesaurus* was found to be similar. However, the humerus of the robust *Galesaurus* exhibits an ectepicondyle which is thicker than the entepicondyle.

Another notable difference in the morphology of these morphs is the iliac blade. That of the robust *Galesaurus* is more elongated and rounded, with the blade set significantly higher than that of the gracile *Galesaurus* as previously indicated by Broom (1932b). The anterior portion of the iliac blade in the robust *Galesaurus* rises gradually to become a relatively rounded dorsomedial blade, which then gradually flattens posteriorly. In the robust *Galesaurus* only one fossa is visible dorsally (due to bone obstruction) on the middle of the iliac blade, whereas the gracile *Galesaurus* also has an anterodorsally oriented fossa on the almost flat iliac blade, similar to the more derived cynodonts *Cynognathus* and *Diademodon*. Jenkins (1971) described the highest section of the cynodont iliac blade as directly above the acetabulum, whereas in the robust *Galesaurus*, it is on the anterior part of the iliac blade and in the gracile *Galesaurus*, it is above the pubic process of the ilium.

The iliac blade of the gracile *Galesaurus* exhibits small and evenly spaced striations on the medial and dorsal surfaces, whereas the posterior surface is almost devoid of these except for a few just above the posteroventral edge. In the robust morph, the striations are more prominent on the anterior and dorsal margins whereas the medial surface of the iliac blade is uneven and may represent the former presence of connective tissue in the sacro-iliac articulation (Jenkins, 1971).

A comparison of the pubic facet with the ischial and iliac facets reveals a less protruding lateral rim in the gracile morph. This feature is more prominent in the robust morph than the gracile morph. The pubic neck of the robust *Galesaurus* is also more elongated than that of the gracile morph. In contrast the anterodorsal edge of the pubic plate, which is enlarged and rod-like, is more prominent and notably shorter in the gracile morph.

The femoral head of the gracile morph exhibits a flat, strap-shaped edge from the head to the greater trochanter, whereas the proximal edge of the greater trochanter is slightly swollen and expands towards the femoral head. This is in contrast to the robust *Galesaurus* where the femoral head has a steeper slope medially. The proximal articulation surface of the femoral head is notably thicker than that of the gracile morph. Furthermore, the greater trochanter of the femur in the gracile morph is slightly thicker than the connecting ridge. This differs from the robust *Galesaurus* where the greater trochanter expands dorsally and is as thick as the connecting ridge. In the more derived cynodonts, *Diademodon* and *Cynognathus*, the anterior and ventral surfaces distal to the lesser trochanter meet in a short thin groove (Jenkins, 1971). In the gracile morph, this groove is more prominent than in the robust morph.

The morphological differences between the two morphs may be attributed to 1) ontogeny 2) sexual dimorphism or 3) two subspecies.

1) Ontogeny

The gracile specimens are the smallest specimens in this study. This may indicate that the gracile specimens were juveniles. The smallest gracile specimen (RC 845) is 62% of the adult size (63 mm basal skull length), whereas specimen NMQR 3678 has a basal skull length of 72 mm and represents 71% of the adult size. Thus, based on size, both specimens are considered to be sub-adults (Table 3). The bone histology of the gracile morphs RC 845 and NMQR 3678 exhibit multiple layers of circumferential endosteal lamellar tissue around the medullary cavity (less prominent in 62% adult, RC 845). This suggests that these individuals were not juveniles (Cormack, 1987; Reid, 1996) and that medullary expansion was near completion (Reid, 1993). In these gracile specimens, a shift from rapidly growing fibro-lamellar bone to a thin region of peripheral lamellar-zonal bone is present (more prominent in 71% adult, NMQR 3678). This transition to an overall slowly forming tissue organization and the presence of LAGs and annuli in the outer periphery of both specimens suggests that sexual maturity had been reached (Klevezal, 1996). With age (in the larger specimen, NMQR

3678), the LAGs are more prominent and the tissue more organized. Enlow (1969) found that the growth patterns of rapidly growing juvenile crocodiles and turtles are occasionally uninterrupted, but as they age, growth becomes slower and interrupted. Vascularization is also influenced by age (Sander, 2000). Moderate vascularization (5.4%) is present in the gracile specimen RC 845 (62% adult), whereas NMQR 3678 (71% adult) exhibits a lower vascularisation of 2.7%.

In the robust specimen NMQR 3542 (100% adult), multiple thick layers of circumferential endosteal lamellar bone surround the medullary cavity. The lamellar-zonal tissue region is thicker than that of the gracile specimens and is highly organised and interrupted by prominent anulli and LAGs. The vascularisation of this individual is 2.7%, and thus similar to that of the gracile NMQR 3678 (71% adult)

Traditionally, the presence of open neurocentral sutures is an indication of immaturity. This study has revealed that even in the robust (presumably 100% adult as it is the largest specimen known) *Galesaurus* specimens the neurocentral sutures remain open. These open neurocentral sutures may be due to exceptional preservation or may indicate that these sutures only closed late in ontogeny, similar to those found in monotremes (Parker and Haswell, 1949). This feature may be a characteristic of the Epicynodontia. Sidor and Smith (2004) noted that in *Progalesaurus* the neural arches are also not syntosed with the centra.

In the morphological description of *Galesaurus* (chapter 4) several differences between the appendicular skeletons of the two morphs were found that may be attributed to ossification. Several characteristics were present in the robust morph and absent or less developed in the gracile morph e.g. depressions, grooves, ridges, and small protrusions (Table 4). It should be noted that according to skull size the gracile specimens (RC 845 and NMQR 3678) represent 62% and 71% adult whereas the robust specimen (NMQR 3542) is

also one of the largest specimens known and is considered to be 100% adult. These differences in ossification could thus be attributed to the gracile specimens representing a younger ontogenetic age (but not juvenile), resulting in less ossification.

2) Sexual dimorphism

The presence of a small and a large morph may instead be an example of sexual dimorphism. In extant animals, the differences in morphology and size between individuals of the same species indicate different sexes. Sullivan et. al. (2002) mentioned that among extant tetrapods either sex may be the larger one, but morphological armament structures are almost always more developed in males than in females. As the fossil record is incomplete, it is unclear whether differences in size and morphology only reflect different sexes (Klein and Sander, 2008). It is also difficult to distinguish between genders of extinct animals using bone histology as there are no conclusive quantifiable methods for identifying a particular gender (Chinsamy et al., 1997).

In older taxa, claims for sexual dimorphism have been based on minor morphological differences (Romer and Price, 1940). Sullivan et. al. (2002) criticized these morphological differences and recommended further sampling and study. This is also recommended here, as sexual dimorphism cannot be confirmed in this study.

3) Subspecies

Another possibility for the differences in morphology is the presence of two subspecies. As noted in Table 4, subtle differences are present in the morphology of the gracile and robust specimens. The presence of two morphs is confirmed by sutural differences in the skulls (personal observation, 2009) and thus, further study on the skull of *Galesaurus* is necessary.

Table 4. A summary of the morphological and histological differences between gracile and robust *Galesaurus* morphs, and *Thrinaxodon*.

Element	Gracile <i>Galesaurus</i> (n=6)	Robust <i>Galesaurus</i> (n=6)	<i>Thrinaxodon</i>
Vertebrae			
Atlas	Facet for occipital condyles anteroposteriorly longer than facet for atlas centrum (Jenkins, 1971)	As for gracile	Length of facets equal
	Prominent bone protrusion at junction of neck and base of transverse process	As for gracile	Bone protrusion absent
	Tapering transverse process	As for gracile	Rectangular transverse process
ProAtlas	Gracile and elongated	Not preserved	More gracile and slightly more elongated
Remaining cervicals	3 rd , 4 th and 5 th neural spines fusiform in cross-section (Jenkins, 1971)	As for gracile	3 rd , 4 th and 5 th neural spines elliptical in cross-section (Jenkins, 1971)
	Height of anterior neural spines progressively decreases posteriorly (Jenkins, 1971)	As for gracile	No differentiation (Jenkins, 1971)
			(continued...)

Table 4 continued

Element	Gracile <i>Galesaurus</i> (n=6)	Robust <i>Galesaurus</i> (n=6)	<i>Thrinaxodon</i>
Thoracic	Transverse process twice as wide as centrum	As for gracile	Notably shorter
Ribs			
Thoracic	Rib expansion: proximal expansion wider than long (width 1.5X length) consisting of small, pronounced anteriorly oriented protrusion and prominent posteriorly projecting flange	As for gracile	Rib expansion: proximal expansion longer than wide (width 0.7X length) consisting of less prominent posteriorly projecting flange. Anterior protrusion absent
Lumbar	Rib articulation of posterior series intervertebral	Not preserved	Rib articulation of posterior series vertebral
	Distally anteroposteriorly expanded, wider than long, oval in lateral view	As for gracile	Distally proximodistally expanded, square in lateral view
Sacral	No contact between sacral and lumbar rib-plates or with ilium	Not preserved	Contact between 1 st sacral and 7 th lumbar rib plates. Sacral rib contacts ilium

(continued...)

Table 4 continued

Element	Gracile <i>Galesaurus</i> (n=6)	Robust <i>Galesaurus</i> (n=6)	<i>Thrinaxodon</i>
Appendicular Skeleton			
Pectoral girdle			
Scapula	Blade less expanded	Blade more anteroposteriorly expanded	As for gracile
	Bony ridge on scapula	Absent	Absent
	Coracoid edge not preserved	Distinct rounded posterodorsal coracoid edge	Coracoid edge more angular
Procoracoid	Not preserved	Procoracoid meets procoracoid buttress in concave angle	As for robust
Clavicle	Not preserved	Stout and directed in horizontal plane	Fragile and directed in two planes L-shaped (Jenkins, 1971)
Forelimb			
Humerus	Proximolateral corner of greater tuberosity pronounced	As for gracile	Proximolateral corner of greater tuberosity less pronounced
	Entepicondyle thicker than ectepicondyle	Ectepicondyle thicker than entepicondyle	As for gracile
Ulna	Shaft appears angular in lateral view, round in cross-section	As for gracile	Shaft appears smooth in lateral view, elliptical in cross-section (continued...)

Table 4 continued

Element	Gracile <i>Galesaurus</i> (n=6)	Robust <i>Galesaurus</i> (n=6)	<i>Thrinaxodon</i>
Manus			
Ulnare	Ulnare thicker on lateral side and slopes towards thinner medial side	Not preserved	Medial portion of ulnare forms thickest part of bone (Jenkins, 1971)
Centrale	Medial centrale has unequal sides and radial centrale is rectangular	Not preserved	Medial and radial centrale cylindrical
	Medial centrale has depression on posterior surface	Not preserved	Medial central has depression on anterior surface (Jenkins, 1971)
Pelvic girdle			
Ilium	Iliac blade curved with a low profile	Iliac blade curved with a higher profile	As for gracile
	Blade highest above pubic process of ilium	Blade highest on anterior part of iliac blade	As for gracile
Ischium	Not preserved	Ischial plate curved posteriorly	Ischial plate straight posteriorly
Hind limb			
Femur	Greater trochanter slightly thicker than connecting ridge	Greater trochanter expands dorsally and as thick as connecting ridge	As for gracile
			(continued...)

Table 4 continued

Element	<i>Gracile Galesaurus</i> (n=6)	<i>Robust Galesaurus</i> (n=6)	<i>Thrinaxodon</i>
Tibia	Not preserved	Terminates distally in almost square articulation facet	Articulation surface is a flat, oval facet (Jenkins, 1971)
Fibula	Not preserved	Distal end almost oval in cross-section	Distal end almost triangular in cross-section (Jenkins, 1971)
Pes			
Calcaneum	Not preserved	Astragalalar larger than calcaneum	Calcaneum larger than astralagar
Astralagalar	Not preserved	Flattish almost rectangular bone with bulbously convex posterolateral region	Hemispherical (Jenkins, 1971)
	Posteromedial cleft absent	Not preserved	Posteromedial cleft in astalagar

(continued...)

Table 4 continued

Element	<i>Gracile Galesaurus</i> (n=6)	<i>Robust Galesaurus</i> (n=6)	<i>Thrinaxodon</i>
Bone histology:			
RBT	19%	20% to 39%	22% to 27%
Bone tissue patterns	Fibro-lamellar cortex with peripheral lamellar-zonal bone Annuli and LAGs	Fibro-lamellar cortex with thicker peripheral lamellar-zonal bone Annuli and multiple LAGs	Fibro-lamellar cortex with peripheral parallel-fibred bone. Lamellar-zonal bone absent Annuli and LAGs generally absent [one LAG noted in one element (Botha and Chinsamy, 2005)]

The presence of uninterrupted fast growing fibro-lamellar bone suggests that the gracile *Galesaurus* morph grew quickly and continually early in ontogeny (Amprino, 1967; Reid, 1990). The overall vascularization of the gracile morph is higher than that of the robust morph further suggesting that the growth rate of the gracile *Galesaurus* was more rapid than the robust *Galesaurus*. The transition to lamellar-zonal bone tissue in both morphs and in all specimens analysed suggests the onset of sexual maturity (Reid, 1996) and an overall decrease in growth rate (Francillon-Vieillot et al. 1990). The shift from annuli to a decrease in the distance between successive peripheral LAGs (in both morphs) indicates that growth decreased even further or ceased completely during the unfavourable growing season and suggests that *Galesaurus* was susceptible to environmental fluctuations (Francillon-Vieillot et al., 1990; Reid, 1996).

It should be noted that different elements of each individual were thin sectioned and that it is difficult to draw final conclusions due to interelemental histovariability. Analysing a larger sample size of this genus would allow confirmation of these suggestions.

The bone microstructure of *Thrinaxodon* consists of moderately vascularized fibro-lamellar bone that becomes poorly vascularized parallel-fibred bone in older individuals (Botha and Chinsamy, 2005). The overall bone tissue pattern of *Thrinaxodon* is thus similar to that of *Galesaurus* and therefore suggests a similar growth pattern, at least initially. The presence of fibro-lamellar bone indicates that both taxa grew relatively rapidly and continually early in ontogeny. Growth then decreased as seen by the change in overall growth pattern, possibly with the onset of sexual maturity (Reid, 1996; Sander, 2000). However, there are slight differences in the growth patterns between the two taxa. The peripheral bone tissue in *Thrinaxodon* adults is parallel-fibred; lamellar-zonal bone with peripheral annuli and LAGs is absent. This differs from *Galesaurus*, which exhibits peripheral lamellar-zonal bone tissue with annuli and sometimes multiple LAGs. The appearance of these features in *Galesaurus* indicates that although overall growth decreased, it decreased further and even ceased periodically during an unfavourable growing season unlike

Thrinaxodon. This suggests that *Galesaurus* was more susceptible to environmental fluctuations than was *Thrinaxodon*.

The overall RBT values of the gracile *Galesaurus* range from 19% to 24%, which agrees with the morphological findings that the pectoral girdle of this morph is relatively slender (Chapter 4). The RBT values in the robust *Galesaurus* exceed 30%, in the forelimb, but there are no morphological specializations to suggest that *Galesaurus* was either aquatic or semi-aquatic. The general morphology of the appendicular girdle of the robust *Galesaurus* also indicates that this animal had a notably robust pectoral girdle and forelimbs, with distinct adaptations for muscle attachments suggesting strong forelimb movements. This includes a well developed deltopectoral crest, a more pronounced proximolateral greater tuberosity and a thicker ectepicondyle than entepicondyle in the humerus. Furthermore, the large number of Sharpey's fibres present in the bone histology of this robust morph implies strong muscle attachments and thus powerful limb movements. Thus, the morphology and bone microstructure of the robust *Galesaurus* indicates that this morph was more robust than *Thrinaxodon* and was capable of being an active burrower. It is possible that *Galesaurus* used burrows to escape the harsh environmental conditions of the Early Triassic. *Galesaurus* RC 845 was found in aggregation with the procolophonoid, *Owenetta kitchingorum* and a diplopod millipede (Abdala et al., 2006), implying that gracile *Galesaurus* was a burrower. It is thus evident that *Galesaurus* may have provided shelter for various other animals in its burrows.

An exceptionally well-preserved *Thrinaxodon* specimen, in a characteristic curled-up position, was described by Brink (1958). He speculated that *Thrinaxodon* was

fossorial or may have occupied existing burrows for shelter. Damiani et al. (2003) later also described a burrow cast containing an articulated *Thrinaxodon* skeleton and suggested that *Thrinaxodon* was the burrower. The evidence includes the design of the shaft and terminal chamber as well as scratch marks found on the burrow sides. By analyzing the bone microstructure of *Thrinaxodon* Botha (2002) found that the RBT values range from 22% to 27%. These relatively low RBT values and associated slender morphology do not indicate any modifications for a specialized lifestyle patterns such as aquatic, arboreal or fossorial. Brink (1958) and Damiani et al. (2003) specimens may instead indicate that *Thrinaxodon* utilized the burrows of other specimens and that it was not itself an active burrow maker.

The vascularisation value of the gracile *Galesaurus* NMQR 3678 (71% adult) is 2.7% and that of the *Thrinaxodon* (73% adult) varies from 2.64% to 2.78% (Botha, 2002). It thus appears that these animals grew at approximately the same rate (Ricqlès, 1983) and were also similar in age. The bone microstructure of *Thrinaxodon* consists of fibro-lamellar bone that becomes a thick poorly vascularized parallel-fibred region at the periphery. The transition to parallel-fibred bone tissue indicates the possible onset of sexual maturity (Reid, 1996) and the thick poorly vascularized parallel-fibred bone indicates continued slow growth thereafter (Francillon-Vieillot et al., 1990). In *Galesaurus* the transition from fibro-lamellar bone to lamellar zonal bone tissue also indicates the possible onset of sexual maturity (Reid, 1996). As the slow growing region in *Thrinaxodon* is thicker than that of *Galesaurus* at the same age, it appears that *Thrinaxodon* reached sexual maturity earlier in ontogeny. *Galesaurus* may have begun to reproduce later in ontogeny than *Thrinaxodon*. The latter genus may have produced offspring earlier in life allowing it to become relatively more abundant and successful.

Availability in Collections

In a country wide survey of all the major palaeontological collections, and on the assumption that all the *Galesaurus* and *Thrinaxodon* material was correctly identified, *Thrinaxodon* were found to be more abundant than *Galesaurus*. This suggestion is supported by the observation that *Thrinaxodon* is 6 times more abundant than

Galesaurus in the Karoo Basin (Table 5). It appears that *Galesaurus* is more abundantly represented in the central Karoo and *Thrinaxodon* in the Northern Karoo Basin (division of Karoo Basin according to Rubidge, 1995). Due to this distribution it is unlikely that these two taxa directly competed with one another for prey, and the competition for food was probably not a reason for the limited biostratigraphic distribution of *Galesaurus*.

Table 5. Spatial distribution of *Galesaurus planiceps* and *Thrinaxodon liorhinus* in the *Lystrosaurus* AZ of the Karoo Basin. Specimens are represented in the collections of the following Institutions: Albany Museum, Bernard Price Institute, Council for Geosciences, Iziko South African Museum, and National Museum.

	Northern Karoo Basin (%)	Central Karoo Basin (%)	Total occurrence percentage (%)
<i>Galesaurus</i> (n=18)	2	12	14
<i>Thrinaxodon</i> (n=112)	58	28	86
Sum	60	40	100

Biostratigraphic Implications

Galesaurus is a relatively rare, basal cynodont with a limited biostratigraphic range that extends from the Lower Triassic Palingkloof Member, Balfour Formation to the lowermost Katberg Formation of the *Lystrosaurus* Assemblage Zone in South Africa (Botha and Smith, 2006). Jenkins (1971) considered the postcrania of *Galesaurus* to be indistinguishable from the more common, closely related sister taxon, *Thrinaxodon*. The biostratigraphic range of *Thrinaxodon* extends the entire *Lystrosaurus* Assemblage Zone and thus the lowermost range of this genus overlaps with that of *Galesaurus*. This poses difficulty in distinguishing these taxa on the basis of postcranial material when skull material is absent. However, this study has shown that although there are similarities, there are distinct differences between the postcrania of these genera. These differences may now be used to distinguish the postcrania of *Thrinaxodon* and *Galesaurus* when cranial material is absent.

CHAPTER SEVEN

CONCLUSIONS

1. A detailed morphological description of *Galesaurus planiceps* revealed the presence of two distinct morphs, namely a small, gracile form and a large, robust form. The morphological distinctions between the two morphs may be attributed to ontogeny, sexual dimorphism or the occurrence of two subspecies.
2. The postcranial morphology of *Galesaurus* can also be distinguished from *Thrinaxodon*, even in the absence of cranial material. The obvious differences between *Galesaurus* and *Thrinaxodon* include: a variation in the height of the cervical neural spines in *Galesaurus* (constant in *Thrinaxodon*); the presence of an anterior extension in the thoracic ribs in *Galesaurus* (absent in *Thrinaxodon*); and a difference in the highest point and shape of the iliac blade. A summary of the differences between the gracile and robust *Galesaurus* morphs, as well as *Thrinaxodon*, is presented in Table 4.
3. The RBT of the gracile *Galesaurus* varies between 19% and 24%, whereas a distinct characteristic of the robust *Galesaurus* is a notably higher RBT of more than 30% in the forelimb, which suggests a fossorial lifestyle. The RBT of *Thrinaxodon* ranges from 22% to 27%. Together with the overall morphology the thicker bone wall in *Galesaurus* indicates that it was a more robust animal compared to *Thrinaxodon*, and suggests that the former taxon was a more active burrower.
4. The bone microstructure of *Galesaurus* consists of rapidly forming uninterrupted fibro-lamellar that becomes slowly forming lamellar-zonal bone towards the periphery. This bone tissue pattern indicates that *Galesaurus* grew quickly and continually early in ontogeny, and then more slowly and intermittently with age. The transition to lamellar-zonal bone tissue suggests

the onset of sexual maturity as the appearance of this bone tissue indicates an overall decrease in growth rate. The presence of annuli and sometimes multiple LAGs in the lamellar-zonal bone indicates that growth decreased even further or ceased completely during the unfavourable growing season and that the growth of *Galesaurus* was seasonal and susceptible to environmental fluctuations.

5. The presence of fibro-lamellar bone in both *Thrinaxodon* and *Galesaurus* suggests that the initial growth of these taxa was similar. However, *Thrinaxodon* exhibits peripheral parallel-fibred bone, and lamellar-zonal bone with annuli and/or LAGs is absent. The absence of these features in *Thrinaxodon* suggests that although the growth rate decreased with age, it did not slow down or ceases periodically as did *Galesaurus*. This suggests that *Galesaurus* was more susceptible to environmental fluctuations than was *Thrinaxodon*.
6. The short biostratigraphic range of *Galesaurus* can now be tested by examining postcranial material previously identified as *Thrinaxodon* (in the absence of cranial material). If any of this material from the middle to upper Katberg Formation can be re-identified as *Galesaurus*, the biostratigraphic range of this taxon may be extended.

REFERENCES

- Abdala, F. 2007. Redescription of *Platycraniellus elegans* (Therapsida, Cynodontia) from the Lower Triassic of South Africa, and the cladistic relationships of Eutheriodonts. *Palaeontology* 50(3):591-618.
- Abdala, F., and R. Damiani. 2004. Early development of the mammalian superficial masseter muscle in cynodonts. *Palaeontologia Africana* 40:23-29.
- Abdala, A., J. C. Cisneros, and R. M. H. Smith. 2006. Faunal aggregation in the early Triassic Karoo Basin: Earliest evidence of shelter-sharing behaviour among Tetrapods? *Palaios* 21:507-512.
- Amprino, R. 1967. Bone histophysiology. *Guy's Hospital Report* 116(2):51-69.
- Benton, M. J. 1990. *Vertebrate Palaeontology*. Chapman and Hall, London, 377 pp.
- Boonstra, L. D. 1935. A note on the cynodont *Glochinodontoides gracilis* Haughton. *American Museum Novitates* 782:1-6.
- Botha, J. 2002. The palaeobiology of the non-mammalian cynodonts deduced from bone microstructure and stable isotopes. Ph. D. dissertation, University of Cape Town, South Africa, 217 pp.

References

- Botha, J. 2003. Biological aspects of the Permian dicynodont *Oudenodon* (Therapsida: Dicynodontia) deduced from bone histology and cross-sectional geometry. *Palaeontologia Africana* 39:37-44.
- Botha, J., and A. Chinsamy, 2000. Growth patterns from the bone histology of the cynodonts *Diademodon* and *Cynognathus*. *Journal of Vertebrate Paleontology* 20:705-711.
- Botha, J., and A. Chinsamy, 2005. Growth patterns of *Thrinaxodon liorhinus*, a non-mammalian cynodont from the Lower Triassic of South Africa. *Palaeontology* 48: 385-394.
- Botha, J., and R. M. H. Smith. 2006. Rapid vertebrate recuperation in the Karoo Basin of South Africa following the End-Permian extinction. *Journal of African Earth Sciences* 45:502-514.
- Botha, J., F. Abdala, and R. Smith. 2007. The oldest cynodont: new clues on the origin and early diversification of the Cynodontia. *Zoological Journal of the Linnean Society* 149:477-492.
- Botha-Brink, J., and F. Abdala. 2008. A new cynodont record from the *Tropidostoma* Assemblage Zone of the Beaufort Group: implications for the early evolution of cynodonts in South Africa. *Palaeontologia Africana* 43:1-6.
- Brink, A. S. 1954. *Thrinaxodon* and some other *Lystrosaurus* Zone cynodonts in the collection of the National Museum, Bloemfontein. *Navorsing van die Nasionale Museum Bloemfontein* 1(5):115-126.
- Brink, A. S. 1956. Speculations on some advanced characteristics in the higher mammal-like reptiles. *Palaeontologia Africana* 4:77-96.

References

- Brink, A. S. 1958. Note on a new skeleton of *Thrinaxodon*. *Palaeontologia Africana* 6:15-22.
- Brink, A. S., and J. W. Kitching. 1951. Some theriodonts in the collection of the Bernard Price Institute. *Annals and Magazine of Natural History* 12(4):1218-1235.
- Broom, R. 1903. On the classification of the Theriodonts and their allies. Report of the South African Association for the Advancement of Science 1:286-294.
- Broom, R. 1905. Notes on the localities of some type specimens of the Karroo Fossil Reptiles. *Albany Museum Records* 1:275-278.
- Broom, R. 1911. On the structure of the skull in cynodont reptiles. *Proceedings of the Zoological Society of London* 11:900-905.
- Broom, R. 1932a. The cynodont genus *Galesaurus*. *Annals of the Natal Museum* 7: 61-66.
- Broom, 1932b. The mammal-like reptiles of South Africa and the origin of mammals. H. F. and G. Witherby, London, 376 pp.
- Broom, R. 1936. Review of some recent work on South African fossil reptiles. *Annals of the Transvaal Museum* 18(4):197-413.
- Broom, R. 1938. On the structure of the skull of the cynodont *Thrinaxodon liorhinus* Seeley. *Annals of the Transvaal Museum* 19(2):263-269.

References

- Broom, R. 1948. A contribution to our knowledge of the vertebrates of the Karroo Beds of South Africa. Transactions of the Royal Society of Edinburgh 61:577-629.
- Buffrènil, V., and E. Buffetaut. 1981. Skeletal growth lines in an Eocene crocodylian skull from Wyoming as an indicator of ontogenic age and paleoclimatic conditions. Journal of Vertebrate Paleontology 1:57-66.
- Carroll, R. L. 1988. Vertebrate paleontology and evolution. W. H. Freeman, New York, 698 pp.
- Casinos, A., F. L. S. C. Quintana, and C. Viladiu. 1993. Allometry and adaptation in the long bones of a digging group of rodents (Ctenomyinae). Zoological Journal of the Linnean Society 107:107-115.
- Castanet, J., and E. Smirina. 1990. Introduction to the skeletochronological method in amphibians and reptiles. Annales des Sciences Naturelles, Zoologie 11:191-196.
- Catuneanu, O., H. Wopfner, P. G. Ericksson, B. Cairncross, B. S. Rubidge, R. M. H. Smith, and P. J. Hancox. 2005. The Karoo basins of south-central Africa. Journal of African Earth Sciences 43:211-253.
- Chinsamy, A. 1991. The osteohistology of femoral growth within a clade: a comparison of the crocodile *Crocodylus*, the dinosaurs *Massospondylus* and *Syntarsus*, and the birds *Struthio* and *Sagittarius*. Ph. D. dissertation, University of Witwatersrand, Johannesburg, 200 pp.
- Chinsamy, A. 1993. Bone histology and growth trajectory of the prosauropod dinosaur *Massospondylus carinatus* Owen. Modern Geology 18:319-329.

References

- Chinsamy, A. 1997. Assessing the biology of fossil vertebrates through bone histology. *Palaeontologica Africana* 33:29-35.
- Chinsamy, A., and P. M. Barrett. 1997. Sex and old bones. *Journal of Vertebrate Paleontology* 17(2):450.
- Chinsamy, A., and P. Dodson. 1995. Inside a dinosaur bone. *American Scientist* 83:174-180.
- Colbert, E. H., and J. W. Kitching. 1977. Triassic cynodont reptiles from Antarctica. *American Museum Novitates* 2611:1-30.
- Cormack, D. H. 1987. *Ham's histology*. J. B. Lippincott Company, London, 866 pp.
- Crompton, A. W. 1972. Postcanine occlusion in cynodonts and tritylodontids. *Bulletin of the British Museum of Natural History (Geology)* 21:30-71.
- Crompton, A. W., and F. A. Jenkins. 1973. Mammals from reptiles: a review of mammalian origins. *Annual Review of Earth and Planetary Sciences* 1:131-155.
- Damiani, R., S. Modesto, A. Yates, and J. Neveling. 2003. Earliest evidence of cynodont burrowing. *Proceedings of the Royal Society of London, B270*:1747-1751.
- Enlow, D. H. 1969. The bone of reptiles; pp. 45-80 in C. Gans, (ed.), *Biology of the Reptilia. Morphology A.*, 1:45-47 Academic Press, London.
- Fourie, S. 1974. The cranial morphology of *Thrinaxodon liorhinus* Seeley. *Annals of the South African Museum* 65(10):337-400.

References

- Francillion-Vieillot, H., V. de Buffrénil, J. Castanet, J. Geraudie, F. J. Meunier, J. Y. Sire, L. Zylberberg, and A. de Ricqlès. 1990. Microstructure and mineralization of vertebrate skeletal tissues; pp. 471-548 in J. G. Carter, (ed.), *Skeletal biomineralization: patterns, processes and evolutionary trends*, Van Nostrand Reinhold, New York.
- Gradstein, F. M., and J. G. Ogg. 2004. Geological time scale 2004 - why, how, and where next! *Lethaia* 37:175-181.
- Haines, R. W., 1946. A revision of the movements of the forearm in tetrapods. *Journal of Anatomy* 80(1):1-11.
- Haughton, S. H. 1924. On Cynodontia from the Middle Beaufort beds of Harrismith, Orange Free State. *Annals of the Transvaal Museum* 11:74-92.
- Hopson, J. A., 1994. Synapsid evolution and the radiation of non-eutherian mammals; pp. 190–219 in D. R. P. Prothero and R. M. Schoch (ed.), *Major features of vertebrate evolution*, Paleontology Society, University of Tennessee Publications, Knoxville.
- Hopson, J. A., 1995. Patterns of evolution in the manus and pes of non-mammalian therapsids. *Journal of Vertebrate Paleontology* 15(3):615-639.
- Hopson, J. A., and A. W. Crompton. 1969. Origin of mammals. *Evolutionary Biology* 3:15-72.
- Hopson, J. A., and J. W. Kitching. 1972. A revised classification of cynodonts (Reptilia: Therapsida). *Palaeontologia Africana* 14:71-85.

- Hopson, J. A., and J. W. Kitching. 2001. A probainognathian cynodonts from South Africa and the phylogeny of nonmammalian cynodonts. *Bulletin Museum of Comparative Zoology* 154(1): 5-35.
- Jenkins, F. A. 1971. The postcranial skeleton of African cynodonts. *Bulletin of the Peabody Museum of Natural History* 36:1-216.
- Kemp, T. S. 1969. The atlas-axis complex of the mammal-like reptiles. *Journal of the Zoological Society of London* 159: 223-248.
- Kemp, T. S. 1979. The primitive cynodont *Procynosuchus*: functional anatomy of the skull and relationships. *Philosophical Transactions of the Royal Society* B285:73-122.
- Kemp, T. S. 1980. The primitive cynodont *Procynosuchus*: structure, function and evolution of the postcranial skeleton. *Philosophical Transactions of the Royal Society* B288:217-258.
- Kemp, T. S. 1982. *Mammal-like reptiles and the origin of mammals*. Academic Press, London, 363 pp.
- Kemp, T. S. 1988. Interrelationships of the Synapsida; in M. J. Benton (ed.), *The phylogeny and classification of the tetrapods, Volume 2. Mammals*. Oxford University Press, Oxford, 23-29 pp.
- Kemp, T. S. 2005. *The origin and evolution of mammals*. Oxford University Press, New York, 331 pp.
- Kielan-Jaworowska, Z., R. L. Cifelli, and Z-X. Luo. 2004. *Mammals from the age of dinosaurs: origins, evolution, and structure*. Columbia University Press: New York.

References

- Klevezal, G. A. 1996. Recording structures of mammals. Determination of age and reconstruction of life history. A. A. Balkema, Rotterdam, 274 pp.
- Klein, N., and M. Sander. 2008. Ontogenetic stages in the long bone histology of sauropod dinosaurs. *Paleobiology* 4(2):247-263.
- Laurin, M., and R. R. Reisz. 1995. A reevaluation of early amniote phylogeny. *Zoological Journal of the Linnean Society* 113:165-223.
- Laurin, M., and R. R. Reisz. 1996. The osteology and relationships of *Tetraceratops insignis*, the oldest known therapsid. *Journal of Vertebrate Paleontology* 16(10):95-102.
- Leeson, T. S., and C. R. Leeson. 1981. *Histology*. W. B. Saunders, London, 600 pp.
- Magwene, P. M. 1993. What's bred in the bone: histology and cross-sectional geometry of mammal-like reptile long bones-evidence of changing physiological and biomechanical demands. MSc dissertation, Harvard University, Cambridge, 54 pp.
- Modesto, S. P., and J. S. Anderson. 2004. The phylogenetic definition of reptilia. *Systematic Biology* 53(5):815-821.
- Modesto, S. P., and N. Rybczynski. 2000. The amniote faunas of the Russian Permian: implications for Late Permian terrestrial vertebrate biogeography. 17-34; in M. J. Benton, E. N. Kurochkin, M. A. Shishkin, and D. M. Unwin (eds.). *The age of dinosaurs in Russia and Mongolia*. Cambridge University Press, Cambridge, 696 pp.

References

- Mundil, R., K. R. Ludwig, I. Metcalfe, and P. R. Renne. 2004. Age and timing of the Permian mass extinctions: U/Pb dating of closed-system zircons. *Science* 305:1760-1763.
- Owen, R. 1859. On some reptilian remains from South Africa. *New Philosophical Journal* 10:289.
- Owen, R. 1861. *Palaeontology, or a systematic summary of extinct animals and their geological relations*. 2nd edition, Adam and Charles Black, Edinburgh, 463 pp.
- Owen, R. 1876. *Descriptive and illustrated catalogue of the Reptilia of South Africa in the collection of the British Museum*. Taylor and Francis, London, 88 pp.
- Parker, T. J., and W. A. Haswell. 1949. *A textbook of Zoology*. 6th edition, C. Forster-Cooper (ed.), Macmillan and Company, 758 pp.
- Parrington, F. R. 1934. On the cynodont genus *Galesaurus*, with a note on the functional significance of the changes in the evolution of the theriodont skull. *Annals and Magazine of Natural History* 10(13):38-67.
- Parrington, F. R. 1939. On the digital formulae of Theriodont reptiles. *Annals and Magazine of Natural History* 11(3):209-214.
- Parrington, F. R. 1967. The vertebrae of early tetrapods. *Colloques internationaux du Centre national de la recherche Scientifique* 163:369-379.
- Parrington, F. R. 1977. Intercentra: a possible functional interpretation; in *Problems in vertebrate evolution*: S. M. Andrews, R. S. Miles, and A. D. Walker (eds.). *Linnean Society Symposium* 4:397-401.

References

- Reid, R. E. H. 1990. Zonal "growth rings" in dinosaurs. *Modern Geology* 15:19-48.
- Reid, R. E. H. 1993. Apparent zonation and slowed late growth in a small Cretaceous theropod. *Modern Geology* 18:39-406.
- Reid, R. E. H. 1996. Bone histology of the Cleveland-Lloyd dinosaurs and of dinosaurs in general, Part I: Introduction: Introduction to bone tissues. *Geology Studies* 41:25-71.
- Ricqlès, A de. 1983. Cyclical growth in the long limb bones of a sauropod dinosaur. *Acta Palaeontologica Polonica* 28:225-232.
- Ricqlès, A de., J. Meunier, J. Castanet, and H. Francillon-Vieillot. 1991. Comparative microstructure of bone; 1-77; in B. K. Hall, (ed.), *Bone 3: Bone matrix and bone specific products*. CRS Press, Boca Raton
- Rigney, H. W. 1938. The morphology of the skull of the young *Galesaurus planiceps* and related forms. *Journal of Morphology* 63:491-523.
- Romer, A. S. 1922. The locomotor apparatus of certain primitive and mammal-like reptiles. *Bulletin of the American Museum of Natural History* 46:517-606.
- Romer, A. S. 1966. *Vertebrate Paleontology*, 3rd edition, University of Chicago Press, Chicago. 468 pp.
- Romer, A. S., and L. W. Price. 1940. Review of the Pelycosauria. *Special Papers of the Geological Society of America* 28:1-538.

References

- Rubidge, B. S. 1995. (ed.), Biostratigraphy of the Beaufort Group (Karoo Supergroup). South African Committee for Stratigraphy, Biostratigraphic series No. 1. Council for Geosciences, Pretoria, 45 pp.
- Rubidge, B. S., and C. A. Sidor. 2001. Evolutionary patterns among Permo-Triassic therapsids. *Annual Review of Ecology and Systematics* 32:449-480.
- Sander, M. A. 2000. Longbone histology of the Tendaguru sauropods: implications for growth and biology. *Paleobiology* 26(3):466-488.
- Seeley, H. G. 1894. On the Therosuchia. *Philosophical Transactions of Royal Society B* 185:987-1018.
- Sidor, C. A., and R. M. H. Smith. 2004. A new galesaurid (Therapsida: Cynodontia) from the Lower Triassic of South Africa. *Palaeontology* 47(3): 535-556.
- Smith, R. M. H. 1995. Changing fluvial environments across the Permo-Triassic boundary in the Karoo Basin, South Africa and possible causes of tetrapod extinctions. *Palaeogeography, Palaeoclimatology, Palaeoecology* 117:81-104.
- Smith, R. M. H., and P. D. Ward. 2001. Pattern of vertebrate extinctions across an event bed at the Permian-Triassic boundary in the Karoo basin of South Africa. *Geology* 29:1147-1150.
- Stark, J. M., and A. Chinsamy. 2002. Bone microstructure and developmental plasticity and birds and other dinosaurs. *Journal of Morphology* 254:232-246.
- Sullivan, C., R. R. Reisz, and R. M. H. Smith. (2003). The Permian mammal-like herbivore *Diictodon*, the oldest known example of sexually dimorphic armament. *Philosophical Transactions of the Royal Society B* 270:173-178.

- Tatarinov, L. P. 1968. Morphology and systematics of the Northern *Dvinia* cynodonts (Reptilia, Therapsida; Upper Permian). *Postilla* 125:1-51.
- Van Heerden, J. 1972. Intraspecific variations and growth changes in the cynodont reptile *Thrinaxodon liorhinus*. *Navorsing van die Nasionale Museum Bloemfontein* 2(10):307-347.
- Van Heerden, J. 1976. The cranial anatomy of *Nanictosaurus rubidgei* Broom and the classification of the Cynodontia (Reptilia: Therapsida). *Navorsing van die Nasionale Museum Bloemfontein* 3(7):141-163.
- Van Heerden, J., and B. S. Rubidge. 1990. The affinities of the early cynodont reptile *Nanictosaurus*. *Palaeontologia Africana* 27:41-44.
- Van Hoepen, E. C. C. 1916. Preliminary notice of new reptiles of the Karroo Formation. *Annals of the Transvaal Museum* 5(3) (Supplement 2):2.
- Wall, W. P. 1983. The correlation between limb-bone density and aquatic habits in recent mammals. *Journal of Vertebrate Palaeontology* 57(2):197-207.
- Watson, D. M. S. 1920. On the Cynodontia. *Annals and Magazine of Natural History* 9(6):506-524.

Appendix 1: Skeletal measurements (mm)

Skeletal measurements (mm)

Individuals	SAM-PK-K10468	NMQR 3542	BP/1/5064	NMQR 3340	NMQR 135	BP/1/4506	BP/1/4714	NMQR 3678
% adult	100	100	99	99	90	79	78	71
Cranial elements								
Maximum length (snout tip to paroccipital process)	103	103	101	-	93.53	79	79	72
Snout tip to anterior border of postorbital	55.77	59.47	-	-	-	49.76	67.54	-
Supraoccipital to anterior border of orbit	56.64	54.15	-	-	-	-	-	-
Posterior border of orbit to occipital shelf	-	-	-	-	-	-	-	-
Length of pineal foramen	-	-	-	-	5.31	3.29	-	-
Width of pineal foramen	-	-	-	-	2.59	2.15	-	-
Length of orbit (left)	11.84	12.71	-	-	-	11.78	15.48	-
Length of orbit (right)	10.2	16.11	-	-	-	14.31	13.7	-
Height of orbit (left)	18.11	17.61	-	-	-	5.54	13.97	-
Height of orbit (right)	approx 18.53	13.58	-	-	-	7.48	11.34	-
Width of snout (just anterior to orbits)	approx 7.83	27.94	-	-	-	28.3	30	30.17
Interorbital width	23.59	23.78	-	-	23.25	20.73	16.11	-
Maximum width of skull (level with pineal foramen)	-	73.8	-	-	-	49.99	52.2	50.52
Width of lateral temporal fenestra (left)	35.98	31.36	-	-	-	18.84	23.45	-
Width of lateral temporal fenestra (right)	approx 23.25	30.51	-	-	-	22.99	21.86	-
Postcranial elements								
Clavicle								
Clavicle length (left)	32.07	-	-	-	-	39.13	-	-
Clavicle length (right)	approx 24.72	-	-	-	-	-	-	-
Clavicle width (left)	11.82	-	-	-	-	10.36	-	-
Clavicle width (right)	11.29	-	-	-	-	-	-	-
Scapulocoracoid								
Scapulocoracoid length (left)	-	38.85	-	-	-	41.99	-	-
Scapulocoracoid length (right)	-	-	-	-	-	51.33	-	-
Scapulocoracoid width (left)	18.08	14.17	-	-	-	19.7	-	-
Scapulocoracoid width (right)	15.9	-	-	-	-	18.71	-	-

Appendix 1 continue

Individuals

SAM-PK-K10468 NMQR 3542 BP/1/5064 NMQR 3340 NMQR 135 BP/1/4506 BP/1/4714 NMQR 3678

Elements

Left Humerus

Total length	46.46 -	-	-	-	53.46 -	-
Proximal width	19.31 -	-	-	-	15.71 -	-
Midshaft width	5.76 -	-	-	-	7.32 -	-
Distal width	approx 15.95 -	-	-	-	24.55 -	-

Right Humerus

Total length	-	58.14 -	-	-	-	-	41.72
Proximal width	21.2	13.92 -	-	-	-	-	12.79
Midshaft width	-	9.3 -	-	-	-	-	5.02
Distal width	-	25.82 -	-	-	-	-	-

Left Radius

Total length	35.68 -	-	-	-	38.52 -	-
Proximal width	5.28 -	-	-	-	7.58 -	-
Midshaft width	approx 2.83	6.89 -	-	-	4.84 -	-
Distal width	7.03	27.19 -	-	-	-	-

Left Ulna

Total length	-	53.03 -	-	-	40.73 -	-
Proximal width	7.18	12.95 -	-	-	8.36 -	-
Midshaft width	3.4	7.46 -	-	-	5.18 -	-
Distal width	-	9.15 -	-	-	10.78 -	-

Appendix 1 continue

Individuals

SAM-PK-K10468 NMQR 3542 BP/1/5064 NMQR 3340 NMQR 135 BP/1/4506 BP/1/4714 NMQR 3678

Elements

Right Ulna

Total length	-	51.66	-	-	-	-	-	-
Proximal width	-	8.35	-	-	-	-	-	-
Midshaft width	-	3.74	-	-	-	-	-	-
Distal width	-	9.28	-	-	-	-	-	-

Pelvis

Length of pelvis	- -	-	-	-	-	-	-	-
Length of ilium(right)	- -	-	-	-	-	44.3	-	38.48
Length of ilium(left)	- -	-	-	-	-	41.35	-	39.03
Length of pubis(right)	- -	-	-	-	-	23.84	-	-
Length of pubis(left)	- -	-	-	-	-	-	-	-

Left Femur

Total length	-	61.46	-	-	-	58.19	-	46.42
Proximal width	-	15.01	-	-	-	18.25	-	16.61
Midshaft width	-	7.14	-	-	-	8.15	-	5.32
Distal width	-	17.42	-	-	-	14.96	-	12.37

Right Femur

Total length	-	61.53	-	-	-	62.51	-	45.41
Proximal width	- -	-	-	-	-	19.93	-	-
Midshaft width	- -	-	-	-	-	8.48	-	-
Distal width	-	18.44	-	-	-	16.04	-	9.91

Left Tibia

Total length	-	52.51	-	-	-	approx 40.11	-	-
Proximal width	-	9.53	-	-	-	5.15	-	-
Midshaft width	-	3.82	-	-	-	4.29	-	-
Distal width	-	8.91	-	-	-	11.28	-	-

Appendix 1 continue

Individuals

SAM-PK-K10468 NMQR 3542 BP/1/5064 NMQR 3340 NMQR 135 BP/1/4506 BP/1/4714 NMQR 3678

Elements

Right Tibia

Total length	-	-	-	-	-	44.24	-	-
Proximal width	-	-	-	-	-	-	-	-
Midshaft width	-	-	-	-	-	4.31	-	-
Distal width	-	-	-	-	-	9.73	-	-

Left Fibula

Total length	-	-	-	-	-	39.75	-	-
Proximal width	-	-	11.23	-	-	16.01	-	-
Midshaft width	-	-	4.8	-	-	4.97	-	-
Distal width	-	-	-	-	-	7.33	-	-

Right Fibula

Total length	-	-	-	-	-	39.69	-	-
Proximal width	-	-	-	-	-	7.27	-	-
Midshaft width	-	-	-	-	-	4.07	-	-
Distal width	-	-	-	-	-	7.34	-	-

Appendix 1 continue**Skeletal measurements (mm)**

Individuals	RC 845	SAM-PK-K1119	SAM-PK-K10465	SAM-PK-K1388
% adult	63	69	65	-
<i>Cranial elements</i>				
Maximum length (snout tip to paroccipital process)	59.7	70.99	67	-
Snout tip to anterior border of postorbital	30.69	44.99	32.1	-
Supraoccipital to anterior border of orbit	-	32.51	28.09	-
Posterior border of orbit to occipital shelf	-	-	-	-
Length of pineal foramen	3.03	2.08	-	-
Width of pineal foramen	2.05	1.41	-	-
Length of orbit (left)	13.49	-	13.29	-
Length of orbit (right)	13.53	11.69	12.56	-
Height of orbit (left)	11.69	12.54	12.29	-
Height of orbit (right)	12.2	11.91	13.85	-
Width of snout (just anterior of orbits)	29.51	39.85	41.15	-
Interorbital with	16.41	17.68	16.02	-
Maximum width of skull (level with pineal foramen)	44.26	42.7	46.58	-
Width of lateral temporal fenestra (left)	20.58	18.56	-	-
Width of lateral temporal fenestra (right)	21.44	19.38	-	-
<i>Postcranial elements</i>				
<i>Scapulocoracoid</i>				
Scapulocoracoid length (left)	-	-	34.15	-
Scapulocoracoid length (right)	-	approx 38.44	27.32	-
Scapulocoracoid width (left)	-	-	16.1	-
Scapulocoracoid width (right)	-	approx 8.49	8.95	-

Appendix 1 continue

Individuals	RC 845	SAM-PK-K1119	SAM-PK-K10465	SAM-PK-K1388
<i>Elements</i>				
<i>Left Humerus</i>				
Maximum length	39.81	-	42.45	-
Proximal width	13.94	-	18.32	-
Midshaft width	8.48	4.6	4.84	-
Distal width	-	17.82	12.04	-
<i>Right Humerus</i>				
Maximum length	-	-	40.19	45.66
Proximal width	17.81	-	18.82	-
Midshaft width	5.82	-	12.92	-
Distal width	-	-	19.72	22.99
<i>Left Radius</i>				
Maximum length	-	27.56	34.32	46.96
Proximal width	-	6.08	9.85	16.98
Midshaft width	-	2.99	3.78	6.63
Distal width	-	6.29	8.99	23.84
<i>Right Radius</i>				
Maximum length	-	32.98	-	-
Proximal width	-	7.88	10.08	-
Midshaft width	-	3.19	4.06	-
Distal width	-	7.27	9.09	-
<i>Left Ulna</i>				
Maximum length	-	26.57	35.69	-
Proximal width	-	8.66	7	-
Midshaft width	-	4.5	5.02	-
Distal width	-	4.52	6.51	-

Appendix 1 continue

Individuals	RC 845	SAM-PK-K1119	SAM-PK-K10465	SAM-PK-K1388
<i>Elements</i>				
<i>Right Ulna</i>				
Maximum length	-	26.89	32.24	-
Proximal width	-	7.31	9.11	-
Midshaft width	-	5.23	5.09	-
Distal width	-	4.82	4.84	-
<i>Pelvis</i>				
Length of ilium(right)	40.4	-	-	-
Length of ilium(left)	36.64	-	39.02	-
Length of pubis(right)	-	-	-	-
Length of pubis(left)	-	-	-	-
<i>Left Femur</i>				
Maximum length	-	-	37.59	-
Proximal width	-	-	13.91	-
Midshaft width	-	-	5.25	-
Distal width	-	-	14.04	-
<i>Right Femur</i>				
Maximum length	-	-	45.99	-
Proximal width	-	-	12.42	-
Midshaft width	-	-	6.48	-
Distal width	-	-	14.34	-
<i>Left Tibia</i>				
Maximum length	-	-	44.86	-
Proximal width	-	-	8.51	-
Midshaft width	-	-	5.91	-

Distal width	-	-	-	-
--------------	---	---	---	---

Appendix 1 continue

Individuals

RC 845

SAM-PK-K1119

SAM-PK-K10465

SAM-PK-K1388

Elements

Right Tibia

Maximum length	-	-	39.39	-
Proximal width	-	-	9.49	-
Midshaft width	-	-	5.15	-
Distal width	-	-	-	-

Left Fibula

Maximum length	-	-	38.8	-
Proximal width	-	-	6.63	-
Midshaft width	-	-	2.94	-
Distal width	-	-	6.92	-

Right Fibula

Maximum length	-	-	36.25	-
Proximal width	-	-	7.92	-
Midshaft width	-	-	2.78	-
Distal width	-	-	4.82	-